Metal ion equilibria in biofluids-
Copper and rheumatoid arthritis

A thesis submitted to the

UNIVERSITY OF CAPE TOWN

in fulfilment of the requirements for the degree of

DOCTOR OF PHILOSOPHY

by

Mark Kelly

Department of Chemistry
University of Cape Town
Rondebosch
7700
South Africa

July 1998

ACKNOWLEDGEMENTS

I would like to extend my sincere thanks to the following:

My supervisor, Professor Graham Jackson, for his invaluable guidance and support throughout the course of this work.

My colleagues in the Department of Chemistry for their many useful discussions.

Professor Meyers of the Department of Rheumatology, University of CapeTown, for his comments on rheumatoid arthritis and for providing the figures in Chapter 1.

Drs Keraan and Wainright and the animal unit of the University of CapeTown Medical School, for their assistance with the animal screens.

To the University of Cape Town and the CSIR for financial support.

To my wife, Cheryl, and my Mother for their continued support and encouragement.

PUBLICATIONS

Parts of this thesis have been published in the following papers or presented at the following conferences:

PAPERS

Copper Rheumatoid Arthritis anti-inflammatory drugs. Part 1. Computer aided drug design, G E Jackson and M J Kelly, *Inorg. Chim. Acta,* 152(b23)(4) 215-217, 1988.

Copper Rheumatoid Arthritis anti-inflammatory drugs. Part 2. A Potentiometric and Spectroscopic Study of Copper(II) Polyaminodicarboxylate Complexes, G E Jackson and M J Kelly, *J. Chem. Soc. Dalton Trans.,* 2429, 1989.

Copper Rheumatoid Arthritis anti-inflammatory drugs. Part 3. A Potentiometric and Spectroscopic Study of Zinc(II), Calcium(II) and Magnesium(II) Polyaminodicarboxylate Complexes, G E Jackson and M J Kelly, *J. Chem. Soc. Dalton Trans.,* 1889, 1990.

CONFERENCE PROCEEDINGS

Novel Copper Antiarthritic Drugs, G E Jackson and M J Kelly, Inorganic '85, Rustenburg, South Africa, July 1985.

Copper Anti-inflammatory Drugs, G E Jackson and M J Kelly, South African Chemical Institute 75th Jubilee Convention, Durban, July 1987.

Complex Structures from N.m.r., G E Jackson and M J Kelly, Inorganic '88, Gordons Bay, South Africa, April 1988.

ABSTRACT

A computer model of blood plasma has been used to evaluate the factors affecting the ability of a ligand to increase the low molecular weight copper pool *in vivo*. The justification for using this speciation approach is based on the assumption that the low molecular weight copper complexes are important in the reduction of the inflammation associated with rheumatoid arthritis.

Based on the results of the simulation, two novel ligands, 3,6,9,12-tetra-azatetradecanedioic acid (ttda) and 3,6,9,-triazaundecanedioic acid (dtda) have been synthesised using a three step route. Multiple carboxylation was prevented by using the tosylate protecting group. The compounds were obtained in an overall yield of 14.7 and 29.0 %, respectively, and characterised using n.m.r, I.R. and mass spectrometry.

The stability constants of the complexes formed by these ligands with several metal-ions were determined using glass electrode potentiometry at 25°C and an ionic strength of 0.15 mol dm^{-3}. The metals used were the divalent ions of magnesium, calcium, manganese, cobalt, nickel, copper and zinc. The values determined followed the Irvine-Williams order of stability.

The stability constants determined were added to the blood model database and the expected mobilisation of copper calculated. The two ligands were found to be close in mobilising ability, in spite of the higher stability of the ttda complex. This result has been rationalised in terms of the relative effect of the competition from the calcium and zinc ions for the ligands. The computed values were compared with experimental results obtained from ultrafiltration studies. Broad agreement was obtained between the two sets of results.

For passive transport across a cell membrane, the complex is required to be electronically neutral. Evidence for metal-carboxylate complexation in the copper-ttda system was obtained from UV/VIS spectroscopy, and in the calcium-ttda system from n.m.r. spectroscopy.

A plausible theory advanced to explain the anti-inflammatory action of copper complexes is that of superoxide dismutase like activity. The potential activity of the copper-ttda

complex was assessed using a simple laboratory procedure. A low activity was determined for this complex.

The evidence obtained from the investigations undertaken during the work suggested that the copper-ttda complex had potential as an anti-inflammatory agent. Animal screens using rats in which the adjuvant arthritis model of rheumatoid arthritis had been developed were conducted. As the inflammation model was not successfully developed in the animals, no conclusions could be drawn as to the possibility of anti-inflammatory activity, but it was found that the administered copper was excreted very rapidly via the kidneys. The evidence indicates that while the copper-ttda complex remains intact in the blood stream, it is too polar to effectively pass out of the blood into the tissue.

STRUCTURAL FORMULAE OF LIGANDS USED IN THIS WORK

ttda

dtda

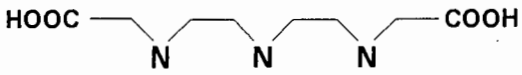

trienda

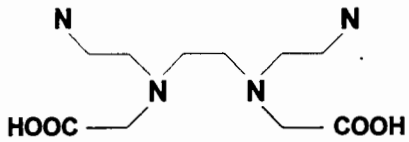

dtpa

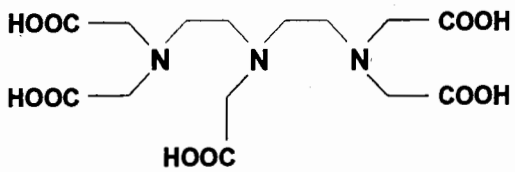

trien

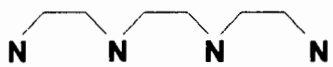

edda

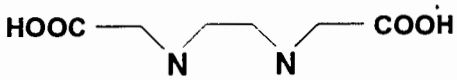

edta

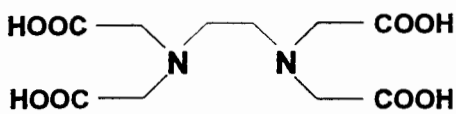

GLOSSARY OF SYMBOLS

$E°$	standard electrode potential.
T_L	total ligand.
E_{cell}	the measured emf of the cell.
R	universal gas constant.
T	absolute temperature.
F	Faraday constant.
T_{H^+}	calculated total proton concentration required for observed pH in the absence of complexation.
$\bar{n}$	average number of protons bound to a ligand in the absence of complexation.
β_{pqr}	overall stability constant, p = metal; q = ligand; r = proton.
σ	standard deviation of the stability constants.
R	crystallographic R-factor.
pK_w	ionisation constant of water.
A^λ	Absorption at wavelength λ.
ϵ_i	molar adsorption coefficient at wavelength λ of the *i* th species.
c_i	concentration at wavelength λ of the *i* th species.
$\varepsilon_{max.}$	molar adsorption coefficient at maximum absorption.
λ_{max}	wavelength of maximum absorption.
v	number of moles of ligand bound per mole of protein.
pD	negative log of the deuterium concentration.
K_0	equilibrium constant before ultrafiltration.
K_1	equilibrium constant after ultrafiltration.
δ	chemical shift.
p_i	fractional population of the i^{th} atom in the various species.
δ_i	chemical shifts of the i^{th} atom in the various species.

CONTENTS

CHAPTER 1

Introduction

1.1 Rheumatoid Arthritis

Rheumatoid arthritis is a chronic, debilitating disease of the connective tissue, and is the most severe of all the rheumatic diseases. It affects about 5% of the population of the western world and is particularly prevalent among the elderly. It is more prevalent in woman than in men. A cure has not yet been found. It often occurs first in the knuckle joints, appearing as a slight swelling, as shown in Figure 1.1, and is accompanied by stiffness.

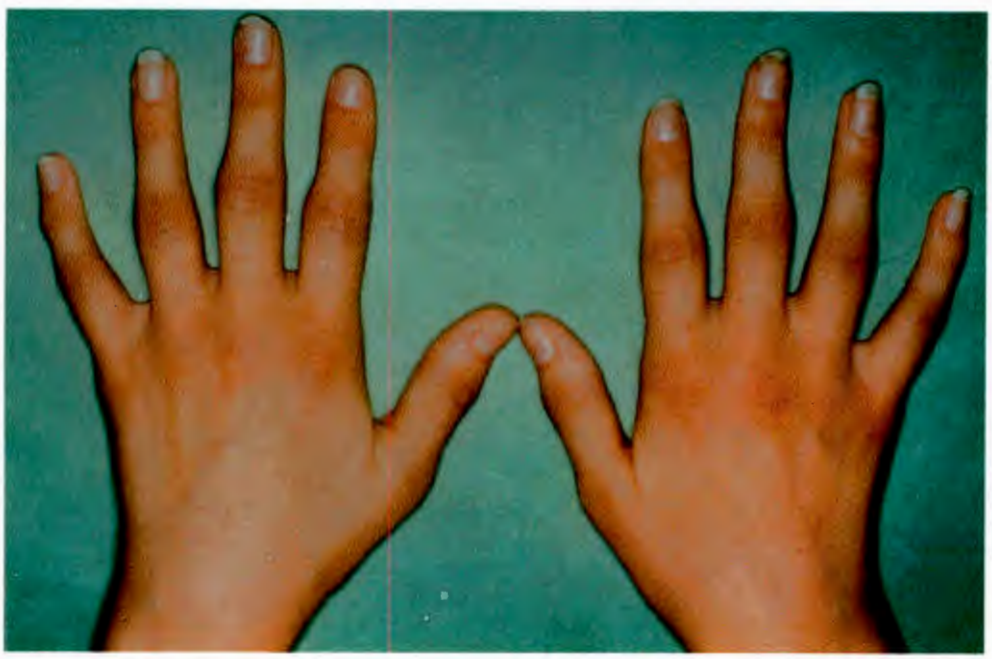

Figure 1.1: Early stages of Rheumatoid Arthritis.

As the disease progresses the inflammation increases, Figure 1.2, and can be accompanied by the progressive degeneration of the joint, caused by the unrestrained inflammation, until it is crippled, Figure 1.3.

A comparison of a normal joint and one damaged by rheumatoid arthritis is given schematically in Figure 1.4.

It may be restricted to the hands, but can spread to other joints, as well as tissue such as lungs, skin, blood vessels, muscles and heart. The course of the disease is unpredictable and can proceed through periods of activity and remission.

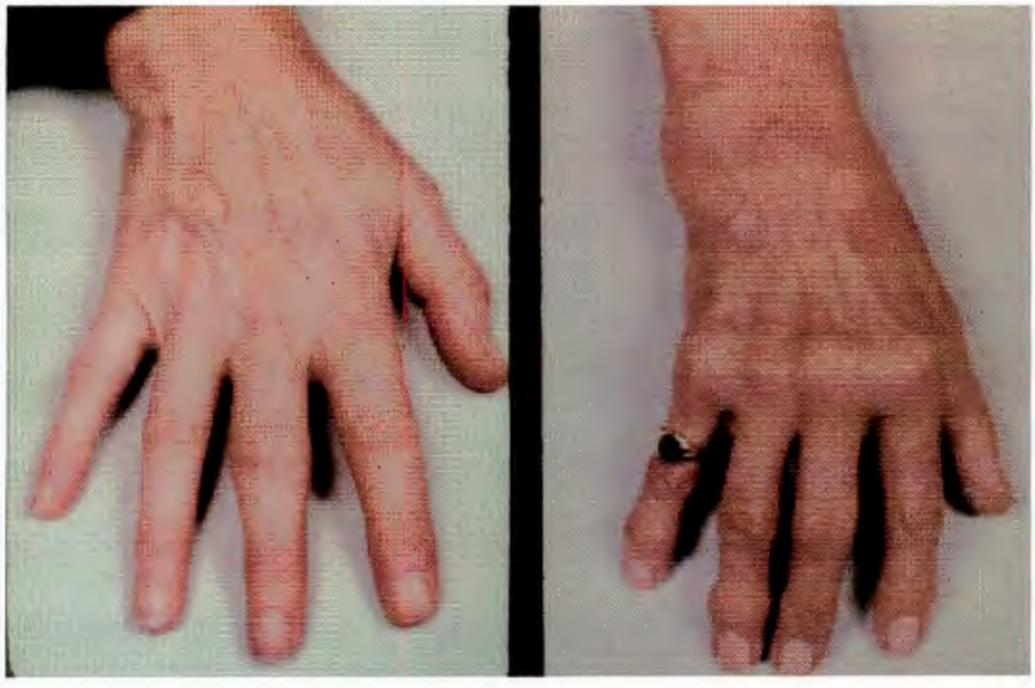

Figure 1.2: Later stages of Rheumatoid Arthritis.

Figure 1.3 Chronic Rheumatoid Arthritis.

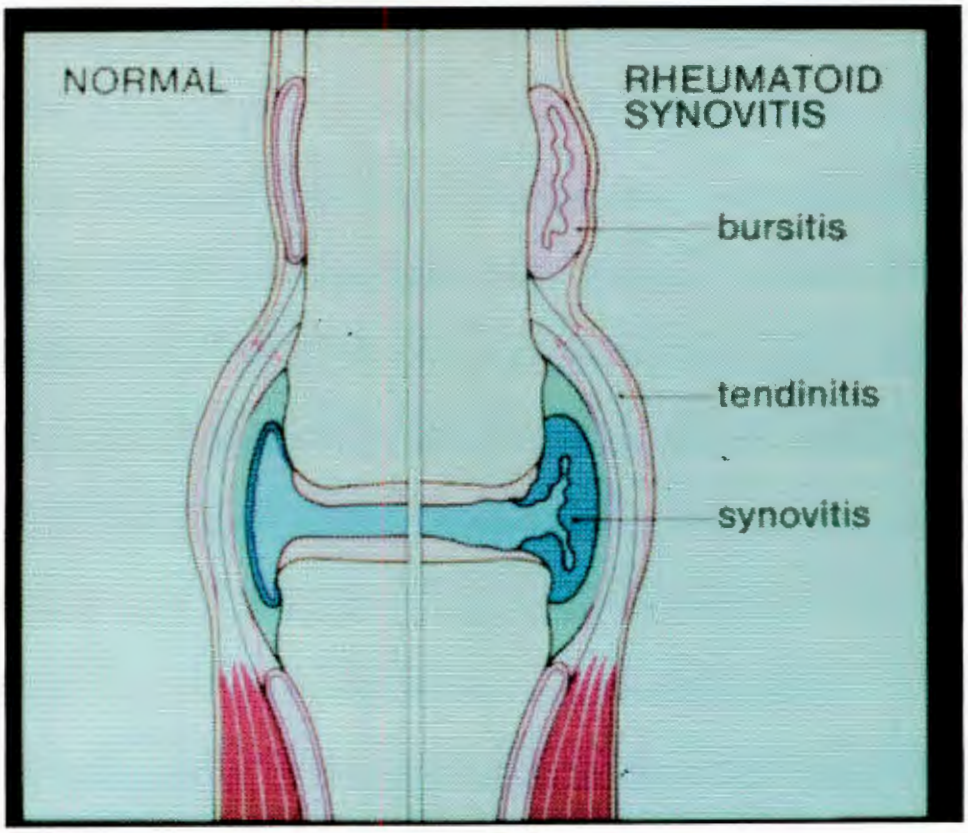

Figure 1.4: Schematic representation of the degeneration of a joint affected by Rheumatoid Arthritis.

The etiology of rheumatoid arthritis is not well understood (Rafter, 1982). Clinical evidence suggests that several factors together result in the onset of RA, rather then one single defect. There is little evidence to suggest that the disease is hereditary. Many theories centre on the breakdown of the auto-immune system (Walker, 1977; Reynolds, 1976). It is possible that an anti-inflammatory response to some physical, emotional or hormonal stress is not properly regulated by the usual feedback mechanisms, and the irritation continues to stimulate itself.

In Rheumatoid arthritis extensive infiltration of activated polymorphonuclear leucocytes into the joint space occurs (Bury et al., 1988). Activated leucocytes produce superoxide radicals, O_2^-, which aid in the destruction of ingested microorganisms. A significant fraction of these radicals escapes from the surface of the leucocytes, and in normal circumstances intracellular tissue damage is controlled by the superoxide dismutases, a group of enzymes that are able to disproportionate superoxide radicals. However the extracellular concentration of the enzymes is low and it has been suggested that superoxide radicals may be involved in the depolymerisation of hyaluronic acid and general tissue damage that can accompany the inflammatory process. It has also been suggested that release of lysosomal proteinases to the extracellular fluid causes degradation of collagen and proteoglycan (Barrett and Saklatvala, 1981).

There is a suggestion (Weber, 1984) that a potassium deficiency disrupts the copper metabolism of the body, which leads to an inappropriate requirement for copper. In people with marginal copper reserves, this demand may be met at the expense of other copper dependent enzymes, such as lysyl oxidase and superoxide dismutase. The absence of these enzymes can result in the tissue damage which accompanies rheumatoid arthritis.

The condition is usually treated with drugs initially. These include non-steroidal anti-inflammatory drugs (NSAIDs), eg aspirin or d-penicillamine. Anti-rheumatoid preparations, slow-acting anti-inflammatory drugs (SAARDs) eg gold and immuno-suppressive drugs. Cortisone and derivatives are used extensively, and when first used were extremely effective. The deleterious side effects of cortisone have, however, limited its use. Gold based drugs prevent further degradation, but will not repair damage that has already occurred in the joints. They can be toxic to skin, kidney, liver and bone marrow. They affect the inflammatory cells and reduce the inflammation, and reduce the rheumatoid factor.

In patients with advanced disease, surgery has been successfully used. Knee and hip replacement procedures have restored mobility to many sufferers, but these methods of treatment are costly.

1.2 Physiology of copper

1.2.1 Normal Physiology

Copper is an essential element in human physiology, and occurs throughout the body. It has been established that copper is required for haemoglobin synthesis, growth, keratinisation, pigmentation, bone formation, reproduction, fertility, development and function of the central and peripheral nervous systems, cardiac function extracellular connective tissue formation and regulation of monoamine concentrations (Underwood, 1977) Copper is deeply involved in a number of biochemical pathways associated with inflammation, for example prostaglandin biosynthesis, as well as connective tissue metabolism. It is stored in the liver, and released homoeostatically to meet the normal requirements of body tissues. Increased copper release occurs in response to many disease states (Sass-Kortsak, 1967).

1.2.2 Altered physiology of copper in disease

Altered copper levels have been reported in rheumatoid arthritis (Sorenson, 1978), cancers (Hrgovicic *et al*, 1973) and seizures (Brunia and Buyze, 1972). Rheumatoid arthritis patients have higher mean serum or plasma copper concentrations. Concentrations return to normal with disease remission. It has been suggested that the increased concentration of copper-containing compounds indicates a 'putative modulator' role of these compounds in inflammation (Bonta, 1977). Normal or low serum copper concentrations found in some patients could be due to failure of this mechanism as a result of depleted liver copper stores.

1.3 Copper and Rheumatoid arthritis

Several folklore remedies for the treatment of arthritis are associated with copper. These include foodstuffs rich in copper, such as shellfish and nuts. Copper jewellery, including the copper bangle, are also believed to have beneficial effects in the control of arthritis (Whitehouse, 1976). It has been shown that l.m.w. copper complexes liberated from albumin by penicillamine are pharmacoactive (Whitehouse *et al*, 1975).

1.4 Clinical Anti-inflammatory activity of copper

Several reviews have been published on the anti-inflammatory activity of copper complexes (Sorenson, 1979 ; Bonta, *et al* 1980; Sorenson, 1981). It has been suggested that copper complexes of clinically used antiarthritic drugs were formed *in vivo* and that they were responsible for the beneficial effects of these drugs (Sorenson,1976; Sorenson, 1976; Sorenson,1981). This suggestion was supported by observations that copper complexes of many non anti-inflammatory complexing agents had anti-inflammatory activity in animal models of inflammation. In a comparison of the effectiveness of copper, gold and silver thiomalate and thiosulphate in models of inflammation, the copper complexes were effective, while the activity of the gold and silver complexes was much lower.

Clinical studies conducted from 1940 to 1950 showed various copper complexes to be effective in treating a variety of arthritic diseases (Sorenson and Hangarter, 1979). The

advent of hydrocortisone as an apparent cure for arthritis led to the disuse of the copper agents.

There are several possible mechanisms to account for the anti-inflammatory activity of copper complexes.

a) Induction of Lysyl oxidase

The repair of damaged tissue requires cross-linking and extracellular maturation of the tissue components collagen and elastin. The copper dependent enzyme lysyl oxidase is responsible for this process. It has been shown in animal studies that lysyloxidase activity can be induced with copper(II) sulphate (Harris, 1976).

b) Modulation of Prostaglandin synthesis.

Copper complexes have been shown to decrease the synthesis of pro-inflammatory prostaglandin, PGE_2, and increase the synthesis of anti-inflammatory prostaglandin, $PGF_{2\alpha}$, (Boyle *et al*, 1976; Vargaftig *et al*, 1975). Modulation of the biosynthesis by copper complexes is an attractive mechanism for the action of copper.

c) Induction of Superoxide Dismutase and Superoxide Dismutase-Mimic Activity

Rheumatoid arthritis has been associated with decreased superoxide dismutase activity (McCord, 1974). Superoxide dismutase is known to have anti-inflammatory and antiarthritic activity (Huber and Menander-Huber, 1980). Many of the copper complexes studied have SOD like activity.

d) Stabilisation of Lysosomal Membrane

Copper is reported to decrease the permeability of human synovial lysosomes, thus decreasing the release of free lysosomal enzymes (Chayen *et al*, 1969).

e) Modulation of histamine

The modulation of the physiological effects of histamine may also be an important biochemical role for copper. There is evidence to support the suggestion that a copper-histamine complex is the active form of histamine (Sorenson, 1978).

The evidence presented in the literature suggests that there is a localised deficiency of copper, which is associated with the disease (May and Williams, 1978). As most of the serum copper is non-reversibly bound to ceruloplasmin, the fraction of copper which will be concerned with a localised deficiency is the labile component comprising the albumin and low molecular weight (l.m.w.) bound copper and the free metal ions. The l.m.w. fraction is thought to be important in the transport of metal ions across cell membranes and between biological sites (May and Williams, 1978). Their role in biological systems is not easy to investigate, as the concentration of these complexes is generally below the detection limits of available analytical techniques, and the equilibria would be disturbed by attempts to concentrate and extract the components for analysis. The concentration of ionic copper in plasma has been estimated to be approximately 10^{-20} mol dm^{-3} (May, Linder, and Williams, 1977). Copper thus occurs primarily in complex form.

A reliable way to overcome this analytical limitation is to use computer simulation to model the distribution of the metal ions in the plasma, and to determine the important complexes present under plasma conditions. A blood plasma model developed by May *et al* (May, Linder, and Williams, 1977), has been successfully used to account for several processes in drug therapy. The model requires the thermodynamic formation constants for the complexes present in plasma, as well as the overall component concentrations. Although the metal ion - protein interactions have not been fully characterised, it is possible to use these calculations to investigate aspects of the copper equilibria in the low molecular weight fraction.

The design of a therapeutic generally requires knowledge of the difference between the health and diseased state at a molecular level. Although there is no clear understanding of this in the case of rheumatoid arthritis, the observed effect of copper on the inflammation associated with the disease provides a basis for drug design. This approach is based on two assumptions. Firstly, the therapeutic effect of copper arise from an increase in the total labile copper concentration in body compartments such as the synovial fluid, and secondly, this increase is aided by the formation of complexes in plasma that can diffuse through the separating membrane into the synovial fluid. This can be achieved by simply increasing the labile copper concentration in the plasma. The most straight-forward way of administering the copper is by injection, but this is unfortunately associated with several undesirable side effects. The increase in the local concentration of copper complexes may be achieved by two general routes, as illustrated in Figure 1.5.

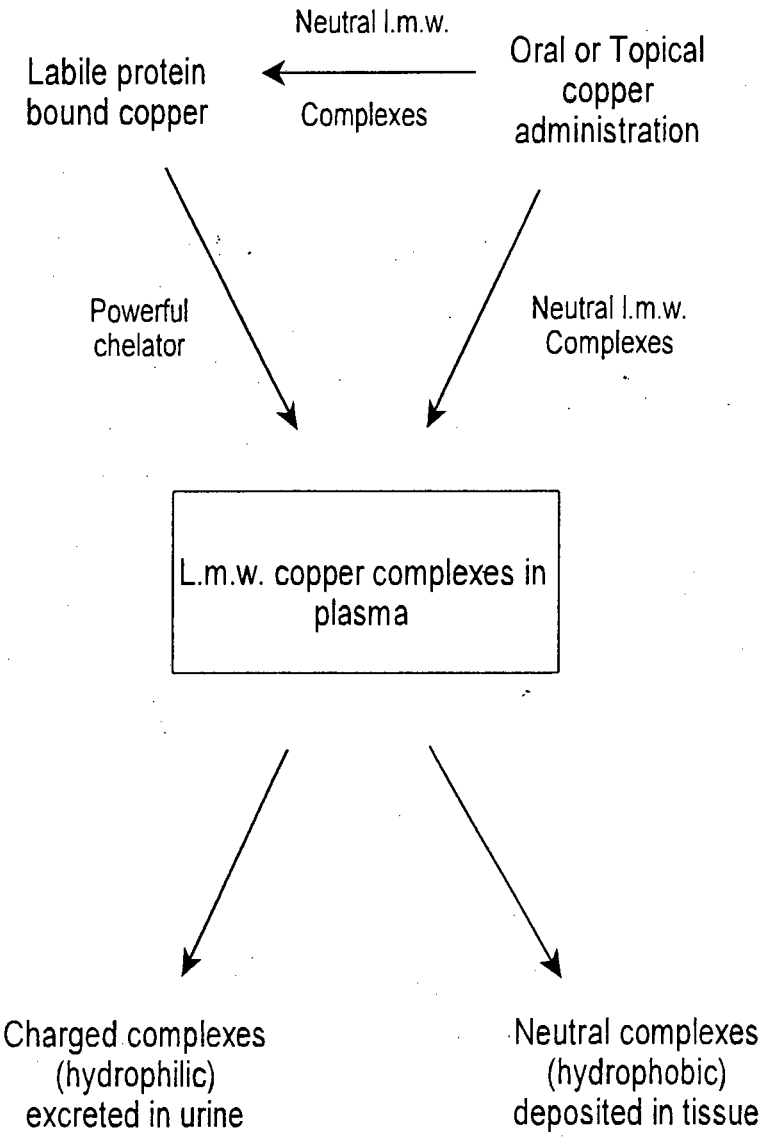

Figure 1.5: Routes for increasing the concentration of l.m.w. copper complexes in blood plasma

The one is based on the liberation of endogenous reserves, the other on copper supplementation by oral or topical administration.

For short term therapy endogenous rather than exogenous sources seem appropriate. There are three ways of achieving this aim.

- By equilibrium competition for the labile protein-bound copper.
- By decreasing the affinity of serum albumin for copper by allosteric effects
- By extracting copper from inert metalloproteins

1.5 Objectives of the research

The research presented above indicates that increasing the local concentration of l.m.w. copper complexes (May and Williams, 1978) by means of an externally administered ligand could be effective in relieving the symptoms of rheumatoid arthritis by stimulating anti-inflammatory activity. It is also possible that the copper complex of this ligand may act in some way against rheumatoid arthritis. The broad objectives of this research were to develop and investigate such a ligand, using the following methodology.

- To use computer simulation techniques to design a ligand that would facilitate the exogenous administration of copper(II). The ligand would have to be highly selective for copper(II) so that it did not disturb the *in vivo* distribution of other metal ions. It would also need to form a neutral complex with copper under in blood plasma conditions, in order to enable passage across the cell membrane.

- Synthesise representative ligands which were designed in stage one.

- Measure the formation constants of these ligands with copper(II) and the two most common blood plasma metal ions, zinc(II) and calcium(II).

- Use a computer model of blood plasma, together with the measured equilibrium constants, to evaluated the plasma mobilising ability of the studied ligands.

- Substantiate the computer simulation results using ultra-filtration.

- Study the structure of the copper complexes with the selected ligands in solution using UV/VIS spectroscopy.

- Measure the SOD activity of the copper complexes with the selected ligands using a simple *in vitro* assay.

- Finally, study the anti-inflammatory activity and toxicity of the most promising complex using the adjuvant model of arthritis in rats.

References

Barrett, A.J. and Saklatvala, J. (1981). in *Protinases in joint disease, Textbook of Rheumatology.*

Kelley, W.N., Harris, E.D., Ruddy, S. and Sledge, C.B. (eds), pp195-209, WA Saunders, Philadelphia).

Bonta, I.L., Parnham, M. , Vincent, J.E. and Bragt, P.C. (1980). *Progr. Med. Chem.*, **17**, 185.

Bonta, I.L. (1977). In *Inflammation: mechanisms and their Impact on Therapy, Agents and Actions, Suppl. 3.* Bonta, I.L., Thompson, J. and Brune, K. (eds.), Birkhäuser, Basel, pp 121ff.

Boyle, E. , Freeman, P.C., Goudie, A.C., Magan, F.R. and Thomson, M. (1976). *J. Pharm. Pharacol.*, **28**, 865.

Brunia, C.H.M. and Buyze, B. (1972). *Epilepsia*, **13**, 621.

Bury, A., Underhill, A.E., Burke, K., Fleming, R.P.E., Davies, J.R., and Gomm, P.S. (1988). *Inorg Chim Acta*, **152**, 171.

Chayen, J., Bitensky, L., Butcher, R.G., and Poulter, L.W. (1969). *Nature*, **222**, 281.

Harris, E.D. (1976). *Proc. Nat. Acad. Sci. U.S.,* **73**, 371.

Hrgovicic, M., Tessmer, C.F., Brown, B.W., Wilbur, J.R. Mumford, D.M., Thomas, F.B., Shullenberger, C.C. and Taylor, G. (1973). *Prog. Clin. Cancer,* **5**, 121.

Huber, W. and Menander-Huber, K.B. (1980) *Clinics in Rheumatic Diseases: Anti-Rheumatic Drugs*, Vol 2, (ed. Huskisson, E.) Saunders, London, pp 465 ff.

McCord, M. (1974). *Science*, **18**, 529.

May, P.M., Linder, P.W. and Williams, D.R. (1977). *J. Chem Soc Dalton.*, 588.

May, P.M. , Williams, D.R. (1978). in *Metal ions in Biological Systems,* Vol. 12 (H Sigel, ed), Marcel Dekker, New York, 1978, p285.

Rafter, G.W. (1982). *Medical Hypothesis*, **9**, 437.

Reynolds, P.G.M. (1976). *Rheumatoid Arthritis, Medical News*, Postgraduate Series on Rheumatism, Nov., 10.

Sass-Kortsak, A. (1967). *J. Can. Med. Ass.*, **96**, 367.

Sorenson, J.R.J. (1976). *Inflammation*, **1**, 317.

Sorenson, J.R.J. (1976). *Med. Chem.*, **19**, 135.

Sorenson, J.R.J. (1981). 'Trace elements in the pathogenesis and treatment of inflammatory conditions', in *Agents and Actions,* Suppl. 8, K Brune, K., K D Rainsford, K.D. and MW Whitehouse, M.W. (eds.),Birkhäuser, Basel, pp 305ff).

Sorenson, J.R.J. (1979). In 'Copper in the Environment', Part 2 , *Healty Effects*, Nriagu, J.O. (ed.), Wiley-Interscience, New York, pp. 83 ff.

Sorenson, J.R. (1978). *Copper Complexes-A Unique Class of Anti-Athritic Drugs*, Progress in Medicinal Chemistry, **15**, 211, (Ellis G.P. and West G.B. eds.) Elsevier.

Sorenson, J.R.J. (1978). *Inorg. Perspect. Biol. Med.*, **2**, 1.

Sorenson, J.R.J and Hangarter, W. (1979). *Inflammation*, **2**, 217.

Underwood, E.J. (1977). Trace Elements in Human and Animal nutrition, 3rd edition, Academic Press, New York, pp 57 ff.

Vargaftig, B.B., Trainer, Y. and Chignard, M. (1975). *Europ. J. Pharmacol.*, **33**, 19.

Walker, W.R. (1977). *Chem. Aust.*, **44**, 247.

Weber, C.E. (1984). *Medical Hypotheses*, **15**, 333.

Whitehouse, M.W., Field, L., Ryall, R.G. and Denko, C.W. (1975). 'Is penicillamine a precursor drug?' *Scand J. Rheumatol.*, **4**, Suppl. 8 (VII Eur. Rheum. Congr.).

Whitehouse, M.W. (1976). *Agents and Actions* ,**6**, 201.

CHAPTER 2

Ligand design

2.1 Introduction

The investigation of large chemical systems such as the sea, lakes, aquifers and biological fluids is difficult due to their complexity and the extremely low concentrations of the constituents. The analytical techniques currently used perturb the system (May, Linder and Williams,1976) and do not provide information about the distribution of the components amongst the various forms in which it occurs.

Simulation of the system is one of the techniques that has been used to investigate these systems. Early examples of this technique are the studies on seawater by Sillén (Sillén, 1967), and blood plasma by Perrin and co-workers(Perrin, 1965; Hallman, Perrin, and Watt, 1971). While limitations to this approach exist in the form of inadequate description of the system, lack of thermodynamic and kinetic data to describe the reactions taking place and the extent and accuracy of component analysis (Jènne, 1979), it is an effective way to increase the understanding the chemistry of the system and of the factors that may influencing it. The use of high speed computers has enabled workers investigating such systems to use larger and more representative models.

2.2 Speciation modelling

In biological systems there are many aspects that need to be considered. In multicellular organisms the solutions on either side of the cell membrane are usually different. An example of this could be the gastric juices in the stomach, which are at a low pH, while that of the cells lining the stomach are near neutral pH. These differences influence the chemistry and hence the bioavailability of metal ions.

The bioavailability of a species such as a metal ion varies, depending on the type and concentration of ligands in that solution (Sandstead, 1988).

The design of drugs has been dominated by a 'black box' approach, in which numerous compounds were screened in the hope of finding an active substance. As this approach is expensive and time consuming, alternative methods have been employed. These include structure activity relationships, and molecular modelling approaches when the mechanism of action is known. These methods are not particularly successful where labile metal complexes are concerned, as the active substance may not bear any relationship to the administered drug. An alternative approach to this problem, speciation design, has developed out of speciation modelling of biological systems.

The essential feature of speciation models is to define a series of chemical equilibria, which represent as complete a description of the equilibria in the system under investigation as possible. This series of equilibria, together with the concentrations of all components in the system constitute the data base of the model. Computer models exist which can interrogate such databases, and solve for individual species concentrations.

Such models are often criticized because they are generally incomplete due to limitations of our understanding of complex systems, such as blood plasma. However, provided cognisance is taken of the restrictions, useful information can still be extracted from the models.

One limitation of present day speciation modelling is that no account is taken of the kinetics of the system. The system is assumed to be at equilibrium, which is rarely the case in biofluids. In cases where the complexes are kinetically inert, even though it is predicted that at equilibrium the metal ion would be redistributed amongst the available ligands, in reality the complex is excreted before significant redistribution can occur.

Since speciation modelling is a quick and relatively easy way of predicting the *in vivo* distribution of an administered ligand or complex, it is a useful tool in the design of new drugs aimed at influencing the distribution of metal ions. In this process the metal ion coordinating characteristics of a ligand are varied and the effect of these changes on the metal ion speciation are calculated using an appropriate model.

2.3 Blood plasma model

The blood plasma model used in this study was developed by May *et al* (May, Linder and Williams, 1977). This model includes data for 10 metal ions and 43 ligands, giving rise to nearly five thousand equilibria. The model also includes the important ternary complex equilibria. This database is efficiently and conveniently interrogated by the ECCLES computer program.

One limitation of the model, or in fact a deliberate omission of the model, are protein equilibria. Metal-protein equilibria are ill-defined, and cannot be effectively included in simulation models. For this reason the model uses the concept of a plasma mobilising index, P.M.I., to obtain results that are largely independent of the protein equilibria (May and Williams, 1977). In this approach the distribution of the metal ions in the low molecular weight (l.m.w.) fraction is considered. This concept depends on the fact that while the

absolute concentration of the metal ions is dependent on the extent of protein binding, the distribution amongst the l.m.w. ligands is not. Owing to the very low free metal concentration, the amount of complex formed is negligible in comparison to the ligand concentration. Consequently the free ligand concentrations are also not significantly affected, they are 'concentration buffered'. Under these circumstances the concentrations of the complexes are dependent only on the free metal concentration. As this is the case for all mononuclear species, the total concentration of each metal in the l.m.w. fraction is also dependent on the free metal concentration. The percentage of metal appearing in a given species is constant, regardless of the exact free metal concentration, and is therefore independent of the metal-protein equilibria that determines the free metal concentration.

The ability of different administered ligands, drugs in this case, to move a metal ion from the protein bound fraction to the l.m.w. fraction can be expressed as a Plasma Mobilizing Index (P.M.I.), which is defined as:

$$\text{P.M.I.} = \frac{\textbf{Total concentration of l.m.w. metal complex species in the presence of the drug}}{\textbf{Total concentration of l.m.w. metal complex species in normal plasma}}$$

It is the l.m.w. fraction of copper that is postulated to be involved in the transport of the ion across membranes and between active sites, and it is this fraction that can be most effectively manipulated in an attempt to increase the availability of copper to anti-inflammatory processes.

2.4 Ligand design

As outlined in Chapter One, the design of copper based anti-inflammatory drugs is based on the assumption that (a) their therapeutic effect arises from an increase in the total labile l.m.w. concentration of copper in the inflamed tissue and (b) that the labile concentration may be increased by an increase in the tissue permeable neutral fraction of copper in plasma.

In thermodynamic terms what is required is a strong dianionic chelator which is specific for copper, as it must be effective in competition with *in vivo* metal ions and ligands. Ultimately the only way of testing a drugs efficiency is with animal screens, but we can carry out preliminary *in vitro* assessment with computer modelling. It is not sufficient to just compare the equilibrium constants of the different possible drugs, as this does not make allowances for competition from other ligands and metal ions. The danger of ignoring this competition is illustrated by Edta, in Figure 2.1. A concentration of 10^{-8} Edta causes a 10-fold increase

in l.m.w. copper. The introduction of zinc into the model, at its physiological concentration, decreases the mobilizing ability of edta by a factor of 10^5. The effect of Ca^{+2} is even more dramatic. The reason for these effects is that, although the $[Cu(edta)]^{2-}$ complex is more stable than the Zn^{+2} and Ca^{+2} complexes, the *in vivo* concentrations of these two metal ions is much higher than that of Cu^{+2}.

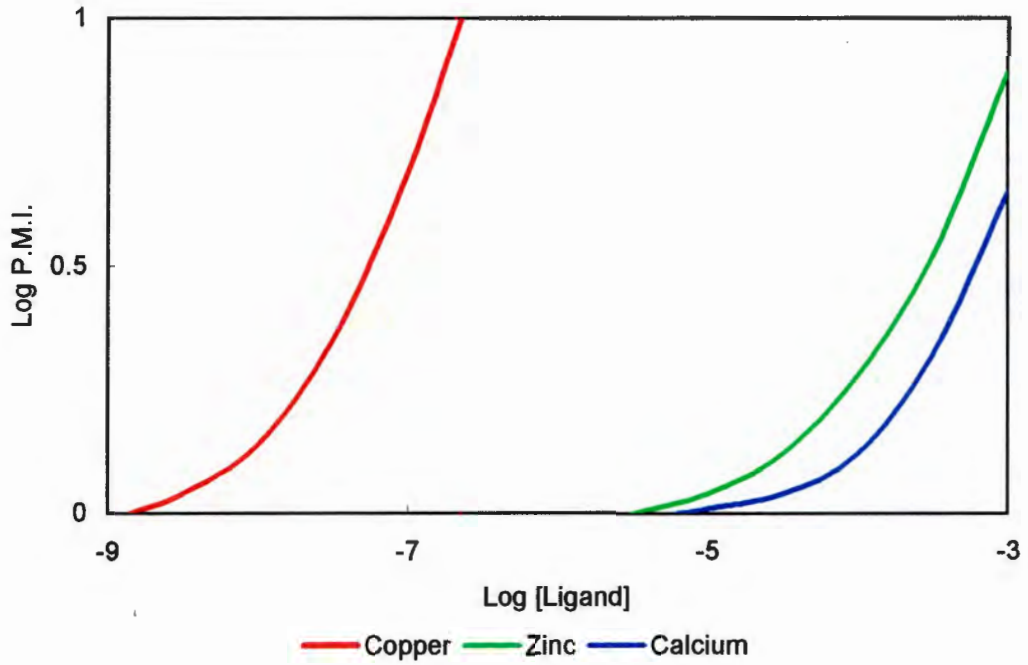

Figure 2.1: The effect of Ca^{+2} and Zn^{+2} upon the Cu^{+2} Plasma Mobilizing Index of edta

Speciation modelling can simulate the effect of structural changes of a ligand on its ability to mobilise copper in plasma. In order to achieve this simulation, the structural features of ligands which would influence the strength or selectivity of complexation with copper were identified, and several ligands selected which contained these features. The stability constants of these ligands were extracted from the literature, or estimated if they were not available, and added to the blood plasma data base. The influence of these features on the l.m.w. concentration of copper was then assessed by calculating the P.M.I. over a range of ligand concentrations.

Donor atom

The first structural feature considered in the design of the ligand is the donor atom. Copper is considered a borderline soft acid according to the HSAB theory (Pearson, 1963). The most

important competitor metal ions in plasma, Zn(II) and Ca(II), are both hard, so a soft donor ligand should favour copper. As the atom changes from O to S to N, the mobilizing efficiency of the ligand increases dramatically- the nitrogen analogue being 10^6 times more efficient than its sulphur counterpart, Figure 2.2. Note that the thiol group, which is known to form very stable copper complexes, was not considered for two reasons. Firstly, the copper undergoes reductive chelation with thiols, and secondly the thiol group is notoriously toxic.

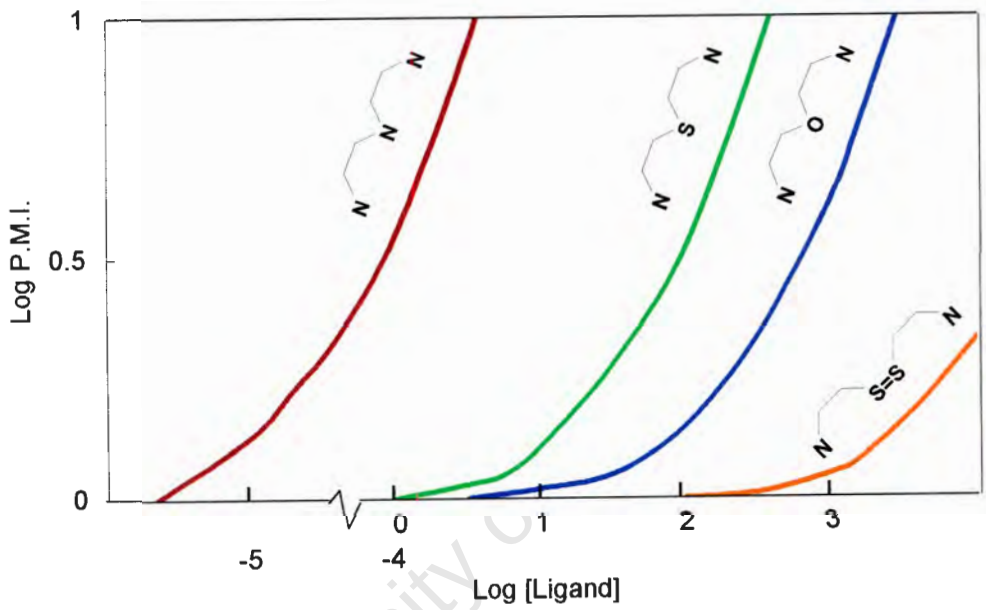

Figure 2.2: The effect of the donor atom upon the Plasma Mobilizing Index of Cu^{+2}

Donor strength

The strength of the ligand is measured by its basicity. Several *N,N'*-disubstituted ethylenediamine compounds were used to examine the effect of the nitrogen ligand used. A comparison of 2-aminobenzyl-, 2-methyleneimidazolyl-, 4-methyleneimidazolyl-, 2-methylenepyridyl- and 2-aminoethyl-substituents (referred to in the Figure as An, 2-imid, 4-imid, py and amine, respectively) is shown in Figure 2.3.

2-aminobenzyl is understandably poor, but in view of the wide biological use of histidine as a chelating agent, it is surprising how poorly 4-methyleneimidazolyl performs. Under physiological conditions, it appears that the straight chain polyamine is the best mobiliser of

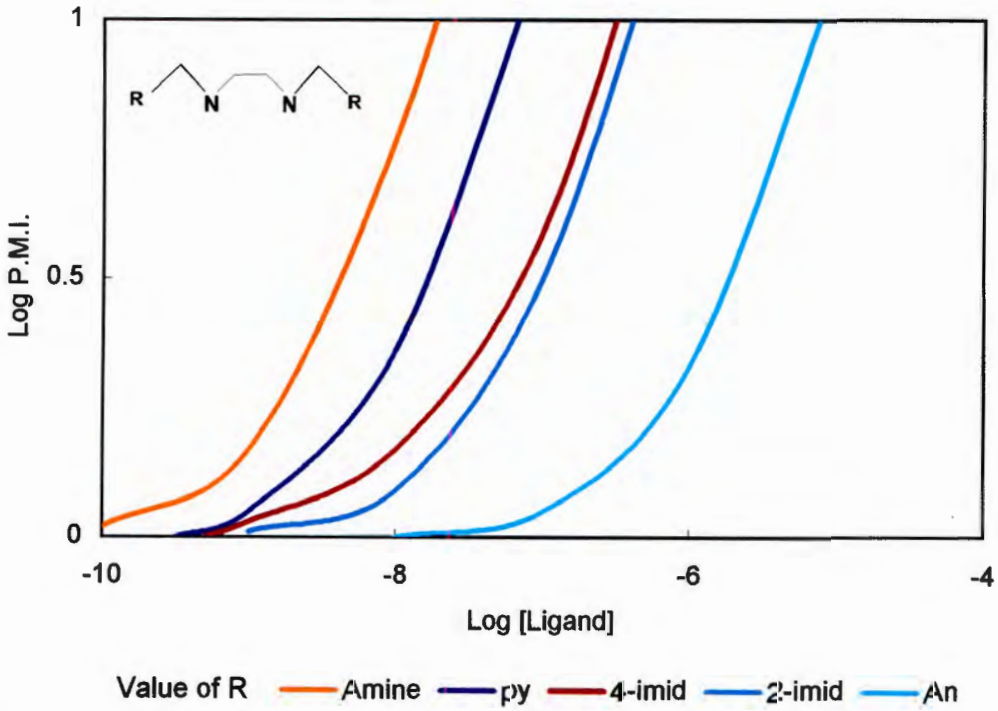

Figure 2.3: The effect of the basicity of the donor atom upon the Plasma Mobilizing Index of Cu^{+2}

copper. Unfortunately, the situation is not as simple as shown because the site of substitution is also important.

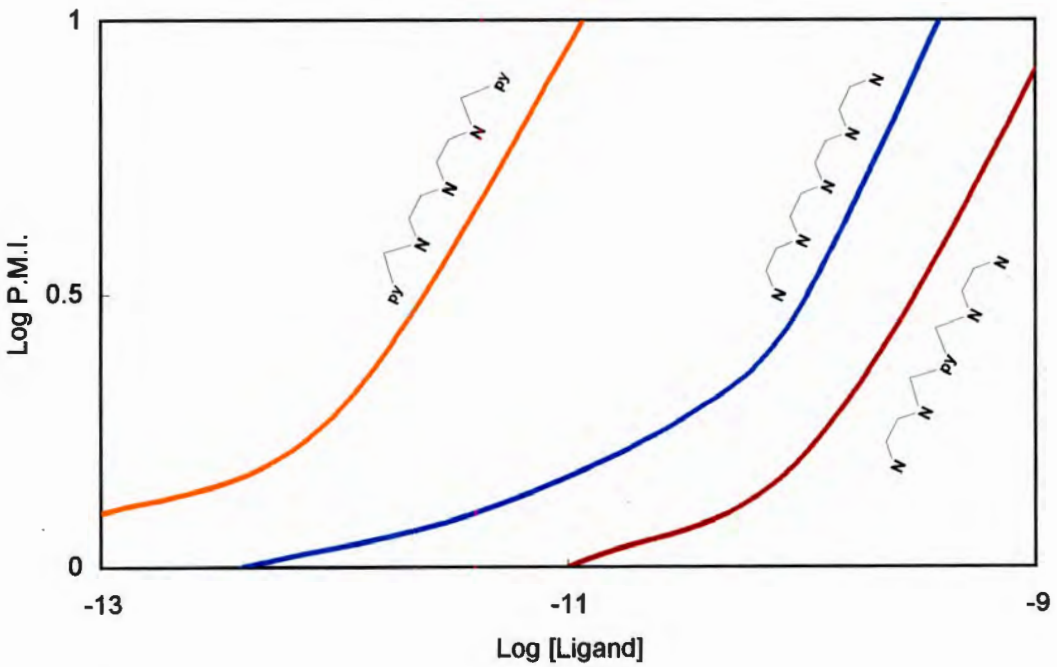

Figure 2.4: The effect of the site of substitution upon the Plasma Mobilizing Index of Cu^{+2}

The effect of the site of substitution is shown in Figure 2.4, using pyridine as the substituent. Substituting the central amino group with pyridine results in a decrease in mobilisation, whereas substitution at the terminal groups increases the mobilization.

Number of donor atoms

Since our ligands are all chelate ligands, the question of denticity arises. Figure 2.5 shows the effect of changing the number of coordinating atoms. The large increase in mobilization in going from mono- to bidentate reflects not only the increased stability of the copper complex, but also the increased difference in stability between the Ca^{2+} and Cu^{2+} complexes. Above a coordination number of 4 there is no significant increase in mobilizing ability. This is because copper complexes are generally Jahn-Teller distorted, so the addition of the fifth donor group to an axial position on the metal is not very favourable.

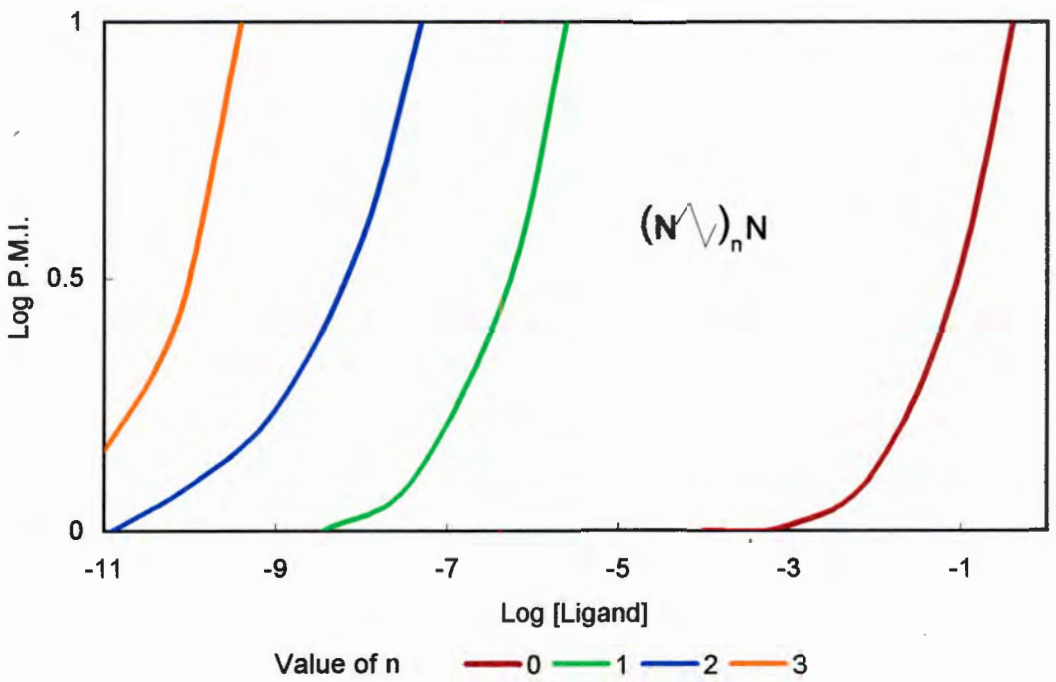

Figure 2.5: The effect of the coordination number upon the Plasma Mobilizing Index of Cu^{+2}

Ring size

The effect of ring size is illustrated in Figure 2.6, using a quadradentate ligand as an example. $H_2N(CH_2)_3NH(CH_2)_3NH(CH_2)_3NH_2$ forms three 6-membered rings upon coordination

and, as expected, is far less effective at mobilizing copper than $H_2N(CH_2)_3NH(CH_2)_2NH(CH_2)_3NH_2$, which gives rise to one 5-membered ring and two 6-membered rings upon coordination. Triethylenetetramine, which forms three 5-membered rings upon coordination is 1000-fold more efficient at mobilizing copper. The introduction of one 6-membered ring in the middle of the ligand results in a substantial increase in the copper mobilizing index, presumably as a result of decreased ring strain within the complex.

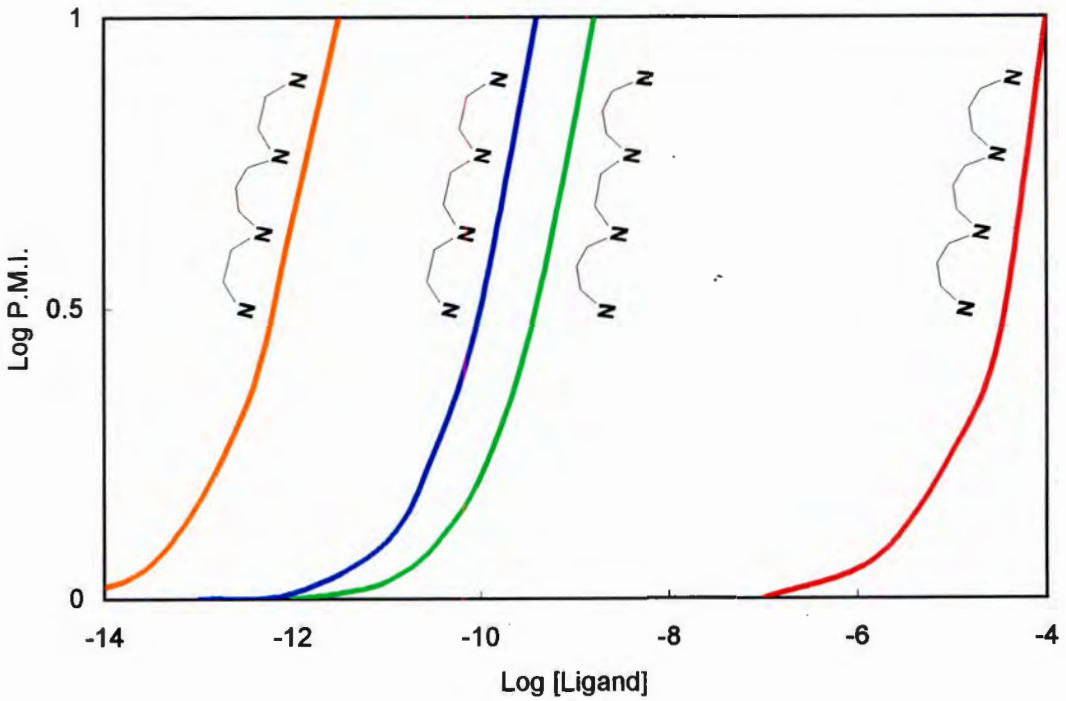

Figure 2.6: The effect of ring size upon the Plasma Mobilizing Index of Cu^{+2}

Anionic groups

Since we wish to form a neutral Cu^{2+} complex, the ligand has to contain two anionic groups. In Figure 2.7 the effect of phosphonate, phosphate, carboxylate and phenolate is compared. There appears to be little to choose between the last three groups, which are all more efficient than phosphonate. Since each phosphate is dianionic, we should really consider the monoester of the phosphate in order to form a neutral complex. Interestingly, methyl substitution increases the efficiency 10-fold. This is probably due to the inductive effect of the methyl group.

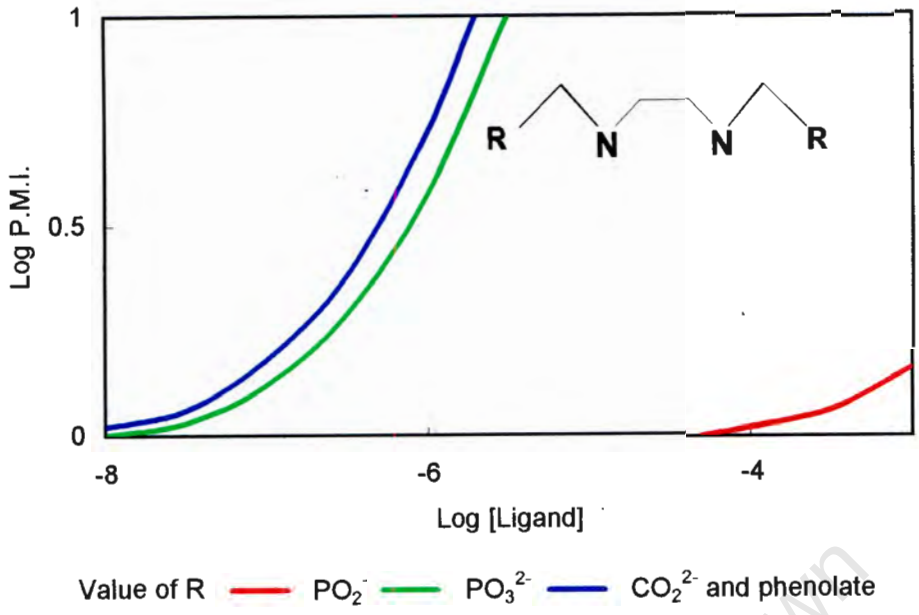

Figure 2.7: The effect of the anionic substituents upon the Plasma Mobilizing Index of Cu^{+2}

Based on the results of the computer simulation studies, the characteristics giving rise to a thermodynamically desirable mobilising agent for copper are a linear, diphenolate, dicarboxylate or dialkyl phosphate substituted polyamine. While a dianionically substituted macrocycle would also have satisfied these thermodynamic conditions, they are unacceptable on kinetic grounds (Jones, 1985).

This last point illustrates one of the limitations of computer modelling. The absence of kinetic data from the model can produce misleading results in situations where kinetics has a large influence on the equilibrium. The interpretation of the results must also include a critical analysis of the effects of other chemical influences.

2.5 Ligand selection

From the characteristics identified above, a number of possible ligands were considered. Two were selected for investigation, these being ttda and dtda. The structural formulae are given below. Neither ligand had been reported in the literature.

ttda

dtda

References

Hallman, P.S., Perrin, D.D., AND Watt, A.E. (1971). *Biochem. J.*, **121**, 549.

Jenne, E.A. (1979) *Chemical Modelling- Goals, Problems, Approaches, and Priorities*, in Chemical Modelling in Aqueous Systems, Jenne, E.A. (ed), American Chemical Society, Washington.

Jones, M.M. (1985). *Inorg. Chim. Acta*, **107**, 235.

May, P.M. and Williams, D.R. (1977). *FEBS Letters*, **78**, 134.

May, P.M., Linder, P.W. and Williams, D.R. (1976). *Experientia*, **32**, 1492.

May, P.M., Linder, P.W., and Williams, D.R. (1977). *J. Chem. Soc., Dalton Trans.*, 588

Pearson, R. (1963). *J. Chem. Educ.*, **45**, 581.

Perrin, D.D. (1965). *Nature*, 206, 170.

Sandstead, H.H. (1988), In *'Metal Speciation; Theory, Analysis and Application'*, Kramer, J.R. and Allen, H.E. (ed), Lewis Publishers, Chelsea, 315.

Sillén, L.G. (1967). *Chemistry in Britain*, 291.

CHAPTER 3

Synthesis

3.1 Introduction

The results of the computer simulation, described in Chapter 2, indicated that an unbranched aliphatic polyamine containing 4 amino groups would be a strong coordinator of Cu(II) under *in vivo* conditions. Further, it was shown that a ligand which formed a 5,6,5 or a 5,5,5 chelate ring system in metal complexation would have considerably enhanced stability. It was also necessary that the ligand would form a neutral complex with divalent metal ions. This requirement dictated that the anionic groups themselves would have to coordinate with the metal at pH 7.4. The computer simulation results did not give a definite indication of superiority between any of the tested anionic groups, so the carboxylate group was chosen, as this group was more accessible synthetically.

As this study was intended to be part of an ongoing project, the synthetic approach selected needed to be versatile. This would allow development of the structure of the target ligand, as the work progressed, without requiring extensive modification of the synthetic route.

Two ligand structures chosen as target molecules were

$HOOCCH_2NH(CH_2)_2NH(CH_2)_2NHCH_2COOH$ (I) (dtda)

and

$HOOCCH_2NH(CH_2)_2NH(CH_2)_2NH(CH_2)_2NHCH_2COOH$ (II) (ttda).

(I) being a dicarboxylate derivative of diethylenetriamine, and (II) a dicarboxylate derivative of triethylenetetramine.

The use of the sulphonate ester as a leaving group in organic synthesis is well known (Morrison and Boyd, 1973) and the *p*-toluene sulphonate group was used extensively in protein synthesis until the appearance of more efficient protecting groups. These two uses of this group have been combined (Richman and Atkins, 1974; Hart, Boeyens, Michael and Hancock, 1983; Koyama and Yoshino 1972) in the synthesis of varying size heterocycles. Generally, bisulphonamide sodium salts were condensed with the required compound containing the sulphonate ester leaving group.

The first attempt to synthesise the target molecules used an adaptation of this general procedure. The appropriate aminoalcohol was converted to the sulphonate ester (tosylate), by reaction with *p*-toluenesulphonyl chloride. At the same time the sulphonamide was formed, thus protecting the amine from further reaction. The tosylate was then reacted with

a 2 molar equivalent of the sodium salt of the sulphonamide derivative of glycine. This was a particularly attractive scheme, as many amino acids are readily available commercially. Unfortunately repeated attempts failed to produce the required product.

The approach was changed, and the sodium salt of the sulphonamide derivative of the required polyamine (trien or dien) was condensed with ethyl bromoacetate. The resulting compounds are thus the sulphonamide derivatives of the ethyl esters of the target molecules. Removal of the sulphonamide protecting group proved elusive. Several methods were tried, sodium in liquid ammonia (Kovacs and Ghatak, 1966), 96% sulphuric acid (Richman and Atkins, 1974), heating under pressure in concentrated HCl (Fabbrizzi, Bencini, and Poggi, 1981) and 47% HBr in glacial acetic acid (Koyama and Yoshino 1972) without any apparent success. A modification of the method used by Hashell and Bowlus (Haskell and Bowlus, 1976), in which the tosyl groups were removed by prolonged heating under reflux with HBr/glacial acetic acid, gave the hydrobromide of the target compounds.

The three step synthetic route is given in Scheme 1 below:

1. $NH_2(CH_2CH_2NH)_xCH_2CH_2NH_2 + TsCl \xrightarrow[\text{ether}]{0\,^\circ C} TsNH(CH_2CH_2NTs)_xCH_2CH_2NHTs$

1. x = 1
2. x = 2

2. **1** or **2** + $2BrCH_2CO_2Et \xrightarrow[THF]{NaH} EtO_2CCH_2NTs(CH_2CH_2NTs)_xCH_2CO_2Et$

3. x = 2
4. x = 3

3. **3** or **4** $\xrightarrow[\Delta]{\text{20\% HBr / glacial acetic}} HO_2CCH_2NH(CH_2CH_2NH)_xCH_2CO_2H$

5. x = 2
6. x = 3

Scheme 1: Synthetic route for ttda and dtda.

3.2 Synthesis

At each stage of the synthesis of the two ligands, ttda and dtda, the products were fully characterised using I.R. and n.m.r. spectrometry. Micro analysis and melting points were also determined and found to be satisfactory.

As the preparation of the two ligands is similar, only the details for ttda will be given. The data for the preparation of dtda are summarised in Table 3.2.

3.2.1 Preparation of Triethylenetetraminetetra-*p*-toluene sulphonamide:

10.25g (0.07mol) of trien was placed in a 1 litre flask. 11.22g (0.28mol) of sodium hydroxide was dissolved in 200ml of distilled water in a beaker. The solution of base was added to the amine, and the reaction vessel placed in an ice water bath. The mixture was stirred vigorously with a mechanical stirrer while 55g (0.288mol, required 53.4g) of *p*-toluenesulphonylchloride in 300ml of ether was added drop wise over approximately 6 hours. Stirring was continued for a further 2 hours after the addition was complete. The mixture was kept at <5° C throughout the reaction. The gummy white precipitate was collected by filtration and washed with ethanol. The product was refluxed with ethanol for one hour, and cooled. The fine white product was collected by filtration, washed with ethanol and air dried. The product was recrystallised from an ethanol/pyridine mixture. This preparation was carried out three times for a combined yield of 67.7g, 42,4% overall. The data are summarised in Table 3.2.

3.2.2 Preparation of the ethyl acetate derivative

Sodium hydride (0.6g, 0.018mol, req 0.55g), was suspended in 200ml of freshly dried THF in a large nitrogen flushed round bottom flask. The sulphonamide (7.0g, 0.0092mol) was added to the suspension and allowed to stir for 2 hours. A pasty solid resulted. Using a calibrated syringe, ethyl bromo acetate (2.1ml, 0.019mol, req .018moles) was added dropwise. The mixture was stirred for an additional 3 hours, giving a pale yellow solution with a fine white suspension (probably NaBr). As the suspension was too fine to filter, the reaction mixture was centrifuged at 2500 rpm for 1 hour, and the supernatant liquid removed. The solid was washed with THF and centrifuged several times. The washings were added to the original supernatant solution. The volume of the reaction mixture was reduced to approximately 50ml, giving a viscous yellow solution. Hot ethanol (120ml) was added, followed by distilled water until the hot solution just turned turbid. The product

precipitated as fine white crystals on cooling. At this stage it was necessary to exercise some care, as the addition of an excess of water gave an oil, and this adversely affected the yield. The precipitate was collected by filtration, and recrystallised from ethanol. The reaction was repeated several times to give a combined yield of 54.1g, 79.0%.

The data are summarised in Table 3.2.

3.2.3 Hydrolysis of the p-toluenesulphonyl protecting group.

An approximately 20% m/m HBr in glacial acetic acid solution was prepared by bubbling HBr gas, produced by reaction of bromine with tetralin (Vogel, 1956, p 182), through glacial acetic acid. The ethyl acetate derivative of the sulphonamide (2.5g) was added to 250ml of the HBr/glacial acetic acid solution. The solid dissolved to give a light yellow solution, which turned red after about one hour. The solution was refluxed for 60 hours, after which the red solution contained a cream-coloured precipitate. The volume was reduced on a rotary evaporator and then poured into 200ml of dry diethyl ether with agitation. The mixture was cooled and the precipitate collected on a fine glass frit. The product was recrystallised several times from 90% ethanol and concentrated hydrochloric acid, yielding a fine white microcrystalline solid. The reaction was performed several times for a combined yield of 12.6g, 64%, of the tetra hydrochloride of ttda. A yield of 12.6g represents an overall yield of 14.7%, based on the total mass of trien used (30.6g).

The data are summarised in Table 3.2.

Table 3.2: Data of the synthesis of ttda and dtda.

Compound formula	Yield (%)	Micro analysis (%)				m.p. (°C)
		C		H	N	
$C_{34}H_{42}N_4S_4O_8$	42.4	calc.:	53.52	5.54	7.34	212-215
		found:	53.5	5.45	7.35	
$C_{42}H_{54}N_4S_4O_{12}$	79.0	calc.:	53.94	5.82	5.99	135-138
		found:	53.85	5.75	5.95	
$C_{10}H_{26}N_4O_4Cl_4$ (ttda.4HCl)	64.0	calc.:	29.42	6.42	13.73	163-177
		found:	29.3	6.4	13.6	(decomposition)
Overall yield	14.7					
$C_{25}H_{31}N_3S_3O_6$	65.5	calc.:	53.07	5.52	7.43	177-178
		found:	53.2	5.7	7.5	(lit 173; Peacock and Dutta, 1934)
$C_{33}H_{43}N_3S_3O_{10}$	74.0	calc.:	53.71	5.87	5.69	98-101
		found:	53.45	5.9	5.7	
$C_8H_{20}N_3O_4Cl_3$ (dtda.3HCl)	59.9	calc.:	29.24	6.14	12.79	137-150
		found:	28.9	6.3	12.6	(decomposition)
Overall yield	29.0					

3.3 Spectral assignment

The spectroscopic data pertaining to the intermediate compounds, as well as for ttda, are summarised in Table 3.3.

In the Ir spectrum of this compound the C=O stretch shifts to 1738 cm^{-1}, which compares well to the C=O stretch at 1740 cm^{-1} for the hydrochloride salts of edda and edta reported by Kawato et al (Kawato, Kanatomi and Murasc, 1973). For a similar molecule, with the acetic acid residues at N^2, N^3, the C=O stretch was reported at 1720 cm^{-1}, supporting the site of substitution of this molecule as N^1, N^4. The N-H stretch arising from a secondary amine salt occurs as a broad peak between 2931 and 2970 cm^{-1}. Several spikes at 2382, 2429, 2458 and 2502 confirm a secondary amine hydrochloride salt (Igi, 1975; *The Aldritch Library of infrared Spectra*, 1981).

Table 3.3: Summary of the spectral data for ttda

Compound	δ (ppm)	multiplicity	integration	assignment
N_4Ts_4	2.22	singlet	9H	$ArCH_3$
(In pyridine-d_5)	3.60	singlet	8H	$R\text{-}CH_2\text{-}R$
	3.37	singlet	4H	$R\text{-}CH_2\text{-}R$ (central)
	5.64	broad singlet	1.3H	N-H (removed by D_2O wash)
	7.73	multiplet	12H	ArH
	Wave no. (cm^{-1})	intensity	bond	assignment
	3275	s	N-H stretch	R-NH
	1600	m	C=C stretch	Ar
	1492	m		
	1360-1250	m	C-H bend	$RR'C\text{-}H_2$
Compound	δ (ppm)	multiplicity	integration	assignment
$N_4Ts_4(EtAc)_2$	1.15	triplet	6H	$EtCH_3$
($CDCl_3$, ref TMS)	2.42	singlet	12H	$ArCH_3$
	3.30	singlet	4H	$RR'CH_2$ (central)
	3.42	singlet	8H	$RR'CH_2$
	4.04	quartet	8H	acetate CH_2
	4.06	singlet		$EtCH_2$
	7.54	multiplet	16H	ArH
	Wave no. (cm^{-1})	intensity	bond	assignment
	1748	s	C=O	RCOOR'
	1213	m	C-O	RCOOR'
	1030	m	C-O	RCOOR'
Compound	δ (ppm)	multiplicity	integration	assignment
ttda (4HCl)	3.60	Singlet	12H	Ethylene CH_2
(D_2O)	4.00	Singlet	4H	Acetate CH_2
	Wave no. (cm^{-1})	intensity	bond	assignment
	3175	w	O-H stretch	RCOO-H
	2970-2931	s	N-H stretch	RN^+H_2
	2502-2382	m		N^+H_2Cl salt
	1738	s	C=Ostretch	RCOO-H
	1226	m	C-O stretch	RCOO-H
	1091	m	C-N stretch	RC-N
	747	m(broad)	N-H wag	$RR'N^+H_2$

The spectroscopic data for dtda is presented in summary in Table 3.4.

Table 3.4: Summary of the spectral data for dtda

Compound	δ (ppm)	multiplicity	integration	assignment
N_3Ts_3	2.26	singlet	9H	$ArCH_3$
(In pyridine-d_5)	3.64	singlet	8H	$R\text{-}CH_2\text{-}R$
	7.69	multiplet	12H	ArH
	Wave no. (cm^{-1})	intensity	bond	assignment
	3288	s	N-H stretch	R-NH
	3060-3040	s	C-H stretch	ArC-H
	3000-2850	s	C-H stretch	$RR'C\text{-}H_2$
	1597	m	C=C stretch	Ar
	1493	m		
	1340-1305	m	C-H	$RR'C\text{-}H_2$
Compound	δ (ppm)	multiplicity	integration	assignment
$N_3Ts_3(EtAc)_2$	1.15	triplet	6H	$EtCH_3$
(In $CDCl_3$ ref TMS)	2.40	singlet	9H	$ArCH_3$
	3.40	singlet	8H	$RR'CH_2$
	4.06	singlet	8H	acetate CH_2
	4.06	quartet		$EtCH_2$
	7.52	multiplet	12H	ArH
	Wave no. (cm^{-1})	intensity	bond	assignment
	1753	s	C=O	RCOOR'
	1211	m	C-O	RCOOR'
	1054	m	C-O	RCOOR'
Compound	δ (ppm)	multiplicity	integration	assignment
dtda (3HCl)	3.60	Singlet	8H	Ethylene CH_2
	4.04	Singlet	4H	Acetate CH_2
	Wave no. (cm^{-1})	intensity	bond	assignment
	3149	w	O-H stretch	RCOO-H
	2978-2931	s	N-H stretch	RN^+H_2
	2779	s	C-H stretch	$RR'CH_2$
	2462-2381	m		N^+H_2Cl salt
	1739	s	C=Ostretch	RCOO-H
	1222	m	C-O stretch	RCOO-H
	1070	m	C-N stretch	RC-N
	745	m(broad)	N-H wag	$RR'N^+H_2$

3.4 Experimental

The chemicals used in the reactions are listed in Table 3.1 below.

Table 3.1: Starting materials for the synthesis of ttda and dtda.

Chemical	Source	Purity	Comments
Trien	Merck	Technical 70%	purified by distillation under vacuum.
Dien	Fluka	Technical 96%	purified by distillation under vacuum.
NaOH	Saarchem	Analar	
p-Toluenesulphonyl chloride	Merck	Technical	Used without further purification
Sodium Hydride	Merck	80%	Suspension in oil
Ethyl Bromo Acetate	-	-	Prepared in these laboratories. (Vogel 1956, p 429)
Tetralin	Saarchem	UniLab 99%	
Bromine	Saarchem	UniLab 99%	

The solvents used for the preparations were of laboratory grade or better, and those used for purification were of analytical grade. T.H.F was dried by reflux over sodium wire under nitrogen and transferred directly into the reaction flask under a stream of nitrogen.

^{1}H and ^{13}C n.m.r. spectra were recorded on a Varian XL200 Fourier Transform instrument. Chemical shifts are given in p.p.m with T.M.S. (δ scale) as internal reference. When some other internal reference was used, the chemical shifts were adjusted to correspond to T.M.S.

Infra red spectra were recorded on a Perkin Elmer 983 instrument as nujol and HCBD mulls between KBr plates. The spectra were recorded between 4000 and 500 cm^{-1}.

Low resolution mass spectra were recorded on a V.G. Micromass 16F spectrometer operating at 70eV with an accelerating voltage of 4kV. The unprocessed mass spectrum was also recorded as a U.V. trace on an EM1 SE6150 UV oscillograph so that metastable peaks could be observed.

Melting points were determined on a Kofler hotstage microscope and are uncorrected.

References

Fabbrizzi, L., Bencini, A. and Poggi, A. (1981). *Inorg. Chem.*, **20**, 2544.

Hart, S.M., Boeyens, J.C.A., Michael, J.P. and Hancock, R.D. (1983). *JCS Dalton*,1601.

Haskell, B.E. and Bowlus, S.B. (1976). *J. Org. Chem.*, **41**, 159.

Igi, K. (1975). *PhD Dissertation.*

Kovacs, J. and Ghatak, U.R. (1966). *J. Org. Chem.*, **31**, 119.

Koyama, H. and Yoshino, T. (1972). *Bull. Chem. Soc. Japan*, **45**, 481.

Morrison, R.T. and Boyd, R.N. (1973). *Organic Chemistry*, 3rd edition, Allyn and Bacon, Boston.

Peacock, D.H. and Dutta, U.C. (1934). *J. Chem. Soc.*,1303.

Richman, J.E. and Atkins, T.J. (1974).*JACS*, **96(7)**, 2268.

Kawato, T. Kanatomi, H. and Murasc, I. (1973). *Bull. Chem. Soc. Japan*, **46**, 1723.

The Aldritch Library of N.m.r. Spectra, (1983). Edition II, Pouchert, CJ (ed), Vol II.

The Aldritch Library of infrared Spectra, (1981). Edition III, Pouchert, CJ (ed), Vol II.

Vogel, A.I., (1956). *A textbook of practical Organic Chemistry*, 3rd edition, p 429, Longman, London.

Vogel, A.I., (1956). *A textbook of practical Organic Chemistry*, 3rd edition, p 182, Longman, London.

CHAPTER 4

Potentiometry

4.1 Introduction

In the study of metal ion equilibria in biological systems, the use of stability constants provides a ready means of estimating the speciation of the metal ion of interest within the system.

If some care is taken, comparison of the values of the constants for the equilibria of interest with those of similar compounds can provide information concerning the binding and structure of the complexes formed.

In this study there were two purposes in measuring the stability constants for the ligands synthesised .

Firstly the measured constants would be used as input to the blood plasma model, and the P.M.I. calculated for the ligands.

Secondly some knowledge of the complex chemistry of these ligands would be gained.

4.2 Theory

The general theory of formation constants and the techniques used to determine them is covered extensively in the literature (Rossotti and Rossotti,1961; Beck, 1970; Martell and Motekaitis,1988). A brief description will be given here to define the terms and to outline the procedures used.

For the typical reaction below, the equilibrium constant is defined as the ratio of activities of the products and reactants of a reaction at equilibrium (eqn 4.1)

$$aA + bB \rightleftharpoons cC + dD \qquad K_{eq} = \frac{a_C^c \cdot a_D^d}{a_A^a \cdot a_B^b} \tag{4.1}$$

The difficulties associated with the determination of activities has lead to the wide spread use of concentration, or conditional, constants, where the equilibrium is studied in a large excess of a non-reacting background electrolyte. The above equation then becomes

$$aA + bB \rightleftharpoons cC + dD \qquad K_{eq} = \frac{[C]^c \cdot [D]^d}{[A]^a \cdot [B]^b} \tag{4.2}$$

In terms of metal-ligand equilibria, the complexation can be described by the following set of reactions

$$M + L \rightleftharpoons ML \qquad K_1 = \frac{[ML]}{[M][L]} \tag{4.3}$$

$$ML + L \rightleftharpoons ML_2 \qquad K_2 = \frac{[ML_2]}{[ML][L]} \tag{4.4}$$

Comparison of these stoichiometric constants, when measured under the same conditions then becomes meaningful.

The equilibria represented by equations 4.3 and 4.4 can also be expressed as overall formation constants, denoted by β, and these are given below. The charges of the species have been omitted.

$$ML + L \rightleftharpoons ML \qquad \beta_1 = K_1 = \frac{[ML]}{[M][L]} \tag{4.5}$$

$$ML + 2L \rightleftharpoons ML_2 \qquad \beta_2 = K_1 \cdot K_2 = \frac{[ML_2]}{[ML][L]^2} \tag{4.6}$$

In general this can be written as

$$\beta_n = \prod_{i=1}^{n} K_i \tag{4.7}$$

The possibility of formation of protonated, hydroxo or oligonuclear complexes can be depicted by the subscripts of β. In this work, the subscripts follow the order of metal, ligand, proton. So for the complex $M_pL_qH_r$ the formation constant will be given by

$$\beta_{pqr} = \frac{[M_pL_qH_r]}{[M]^p[L]^q[H]^r} \tag{4.8}$$

When r = -1 this refers to a proton removed to a water molecule or to a hydroxide ligand added.

Any method which can determine the concentration of at least one of the species in the equilibrium with reasonable accuracy can be used to obtain the equilibrium constant (Martell, and Motekaitis, 1988). Potentiometry is one of the most convenient and widely used of the techniques. The glass electrode, which measures hydrogen ion concentration (activity), is widely used, although metal ion selective electrodes are also used.

At any point in a titration the total concentration of a component is given by the sum of the concentrations of all species containing that component, including the free concentration. For example the total ligand concentration , T_L will be given by:

$$T_L = [L] + [ML] + 2[ML_2] + ... \tag{4.9}$$

And in general by:

$$T_L = [L] + \sum_{p=1}^{P}\sum_{q=1}^{Q}\sum_{r=0}^{R} \beta_{pqr}[M]^p q[L]^q[H]^r \tag{4.10}$$

There are three mass constraints in terms of total ligand, total metal and total hydrogen ion concentrations. The total ligand, total metal and total hydrogen ion concentrations are known, the free hydrogen ion concentration is measured at each point in the titration, and the βs, free metal and ligand concentrations are the unknowns which must be calculated from the mass balance equations. If there are n_p titration points and $n_{M.B.E.}$ mass balance equations at each point, there will be a total of $n_p \times n_{M.B.E.}$ free concentrations. As the free hydrogen ion concentration is known at each point, there will be $n_c = n_p(n_{M.B.E.} - 1)$ unknown free concentrations. If there are m unknown βs, there will be a total of n_c + m parameters to be determined.

The hydrogen ion concentration is obtained from the emf readings delivered by the glass electrode according to the following equation:

$$E_{cell} = E_r + E_l + E_g^o + \frac{RT}{F}\ln\{H^+\} \qquad (4.11)$$

Where:

E_{cell} = the measured emf of the cell
E_r = contribution arising from the reference electrode
E_l = contribution arising from the liquid junction
E_g^o = Standard glass-electrode potential at unit activity
R = universal gas constant
T = absolute temperature
F = Faraday constant
$\{H^+\}$ = Hydrogen ion activity

If the ionic strength of the test solution is kept constant, the hydrogen ion activity can be expressed as a concentration, equation 4.12 can be obtained by putting $s = 2.303RT/F$ and collecting together all the constants as E_{const}:

$$E_{cell} = E_{const} + s \log[H^+] \qquad (4.12)$$

4.3 Data analysis

Computer analysis of equilibrium data has replaced the graphical methods used earlier, and many programs exist to analyse potentiometric data (Martell and Motekaitis, 1988). In this study, the program MAGEC (Williams, May, Linder and Torrington, 1982) was used to calibrate the electrode and to determine the value of pK_w. Extensive use of features within the ESTA (Murray and May, 1984) suite of programs was made to model the equilibria in the test solutions and to compute the βs.

In the optimisation section a Gauss-Newton least squares method is used to minimise the objective function, U, given by

$$U = (N - n_p)^{-1} \sum_{n=1}^{N} n_e^{-1} \sum_{i=1}^{n_e} w_{ni} (y_{ni}^o - y_{ni}^c)^2 \qquad (4.13)$$

where

N = total number of experimental titration points

n_e = total number of electrodes (one in this study)

w_{ni} =weight of i^{th} residual at n^{th} point

y_{ni} = either T_{ni} = total concentration of electrode ion i at the n^{th} titration point

or E_{ni} = emf of electrode i at the n^{th} titration point

(o = obs., c = calc.)

Use was made of the $\bar{Z}$ function, the average number of ligands attached to the metal, which is given below.

$$\bar{Z} = \frac{T_L - [L]}{T_M} = \frac{\sum i\, \beta_i\, [L]^i}{1 + \sum \beta_i\, [L]^i} \qquad (4.14)$$

This definition of the function applies only to mononuclear binary complexes. A plot of $\bar{Z}$ against -log [L], pL, gives a pictorial representation of the equilibria. If only mononuclear binary species are formed in solution, the titrations performed under different conditions of concentration and concentration ratios of the metal and ligand should give overlapping curves. Any deviation from this is an indication that there are species other than mononuclear binary complexes present. This can assist with the selection of models for the refinement process.

As the curve is characteristic of the equilibria existing in the solution, a test of the validity of the refined model is to generate a set of titration data using the determined formation constants and experimental titration conditions and to construct a $\bar{Z}$ plot using this data. The degree of agreement between the experimental plot and the simulated plot is an indication of the validity of the proposed chemical model. This process is termed pseudoplotting (Vacca, Sabatini and Gristina, 1972).

The deprotonation function, $\bar{Q}$, is the average number of protons released per metal ion, as a result of complexation and is defined according to equation 4.15, where T_H and T_{M^*} are the total proton and metal concentrations respectively;

$$\bar{Q} = (T_{H^*} - T_H)/T_M, \qquad (4.15)$$

T_{H^*}, given by equation 4.16,

$$T_{H^*} = [H] - [OH] + S_r B_{0qr}[L]^q[H]^r, \quad (4.16)$$

is the calculated total concentration of protons that would be necessary to give rise to the observed pH if no complexation took place. The summation is over all protonated species. In order to evaluate T_{H^*} it is necessary to solve for the free ligand concentration using equation 4.17. If we define a formation function for the ligand subsystem according to equation 4.18, then F, the average number of dissociable protons in a complex (assuming that it is the predominant complex), is given by equation 4.19.

$$T_L = [L] + S_q B_{0qr}[L]^q[H]^r \quad (4.17)$$

$$\bar{n} = (T_{H^*} - [H] + [OH])/T_L \quad (4.18)$$

$$F = q \times \bar{n} - \bar{Q} \times p \quad (4.19)$$

Here $\bar{Q}$ represents the average number of protons released from the ligand as a result of complexation, while $\bar{n}$ is the average number of protons which would be bound to the ligand in the absence of metal complexation. The difference between the two therefore gives the average number of dissociable protons remaining on the ligand after complexation. Clearly, cognizance of metal-ligand stoichiometries has to be taken.

4.4 Results and interpretation

The protonation and formation constants determined for the systems studied are given in Table 4.1.

Table 4.1 Log β for the species $M_pL_qH_r$ at 25°C and I=0,15 M NaCl .
M = Metal $^{2+}$ ion, L = Ligand, H = H^+, σ = standard deviation in log constant, n = number of titration readings for each system, R is the crystallographic R-factor.

L	M	p q r	log β	σ	n	R
ttda	H^+	0 1 1	9.766	0.002	800	0.003
		0 1 2	18.603	0.004		
		0 1 3	24.947	0.007		
		0 1 4	28.09	0.01		
		0 1 5	29.53	0.04		

L	M	p q r	log β	σ	n	R
	Mg^{2+}	1 1 0	2.34	0.003	779	0.004
		1 1-1	-8.54	0.04		
	Ca^{2+}	1 1 0	3.17	0.007	216	0.008
		1 1-1	-8.19	0.04		
	Mn^{2+}	1 1 0	9.47	0.006	214	0.01
		1 1-1	0.048	0.054		
	Co^{2+}	1 1 0	15.977	0.0064	243	0.005
		1 1 1	19.72	0.01		
	Ni^{2+}	1 1 0	19.59	0.007	184	0.004
		1 1 1	22.35	0.01		
	Cu^{2+}	1 1 0	21.34	0.02	140	0.0024
		1 1 1	24.92	0.01		
		1 1 2	26.67	0.04		
	Zn^{2+}	1 1 0	15.65	0.004	112	0.004
		1 1 1	19.14	0.02		
dtda		0 1 1	9.662	0.002	672	0.0028
		0 1 2	18.097	0.005		
		0 1 3	22.349	0.008		
		0 1 4	24.47	0.02		
	Mg^{2+}	1 1 0	2.62	0.003	694	0.004
	Ca^{2+}	1 1 0	2.64	0.02	240	0.005
		1 1-1	-8.53	0.04		
	Mn^{2+}	1 1 0	7.633	0.005	96	0.03
	Co^{2+}	1 1 0	13.097	0.009	181	0.005
		1 1 1	17.27	0.01		
	Ni^{2+}	1 1 0	16.508	0.0034	279	0.002
		1 1 1	18.48	0.02		
	Cu^{2+}	1 1 0	19.16	0.01	400	0.0059
		1 1 1	21.35	0.02		
		1 1-1	8.24	0.02		
	Zn^{2+}	1 1 0	13.19	0.004	324	0.003
		1 1 1	16.720	0.02		
trien		0 1 1	9.880	0.0016	425	0.0017
		0 1 2	19.065	0.0018		
		0 1 3	25.763	0.0025		
		0 1 4	29.207	0.0035		

L	M	p q r	log β	σ	n	R
	Cu^{2+}	1 1 0	20.323	0.0091	406	0.0022
		1 1 1	23.437	0.008		
		1 1-1	8.61	0.03		
ttda/trien	Cu^{2+}	1 1 0	21.15	0.03	437	0.0038
		1 1 1	24.75	0.02		
		1 1 2	26.81	0.04		
dtda/trien	Cu^{2+}	1 1 0	18.96	0.01	483	0.0026
		1 1 1	21.07	0.02		

4.4.1 Protonation

The stepwise protonation constants for ttda and dtda, with the exception of the last protonation step which occurs beyond the reliable range of the glass electrode, show a low standard deviation. The low R factor indicates the correctness of the protonation model. The experimental protonation curves are given in Figure 4.1 for ttda and in Figure 4.2 for dtda. The theoretical curves calculated using the constants given in the table are given on the clear sheet for comparison . The order of protonation was studied by n.m.r. under conditions of varying pH, and is discussed in Section 5.4. As triethylenetetramine (trien) was to be used as a competing ligand, its protonation constants for were also determined, and are given in Table 4.1. With the exception of the minor 11-1 species, the agreement of the constants determined in this study with those in the literature is good. Literature values are given in Table 4.2 for comparison.

Table 4.2 Formation constants for trien, at 25°C and ionic strength of 0.1 mol dm^{-3}. (Martell and Smith, 1989).

L	M	p q r	log β
trien	H^+	0 1 1	9.74
		0 1 2	18.81
		0 1 3	25.40
		0 1 4	28.67
	Cu^{2+}	1 1 0	20.05
		1 1 1	23.75
		11-1	10.7

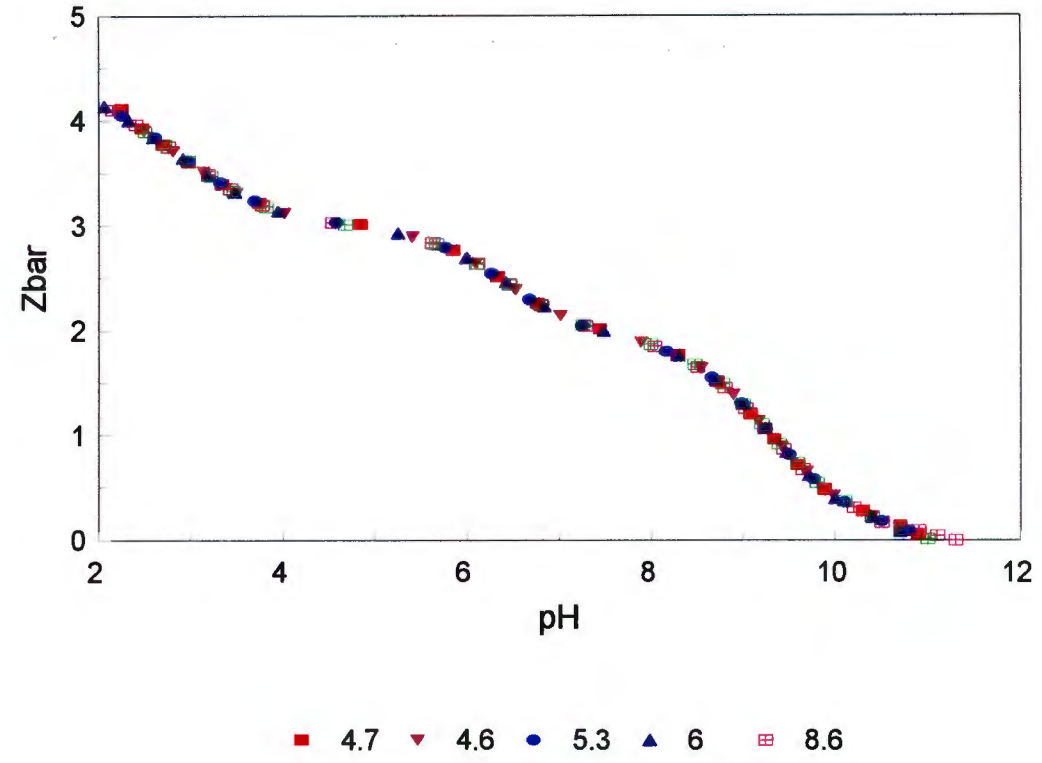

Figure 4.1: Experimental and calculated protonation curves for ttda. The different symbols represent titrations performed with different ligand concentrations (mM).

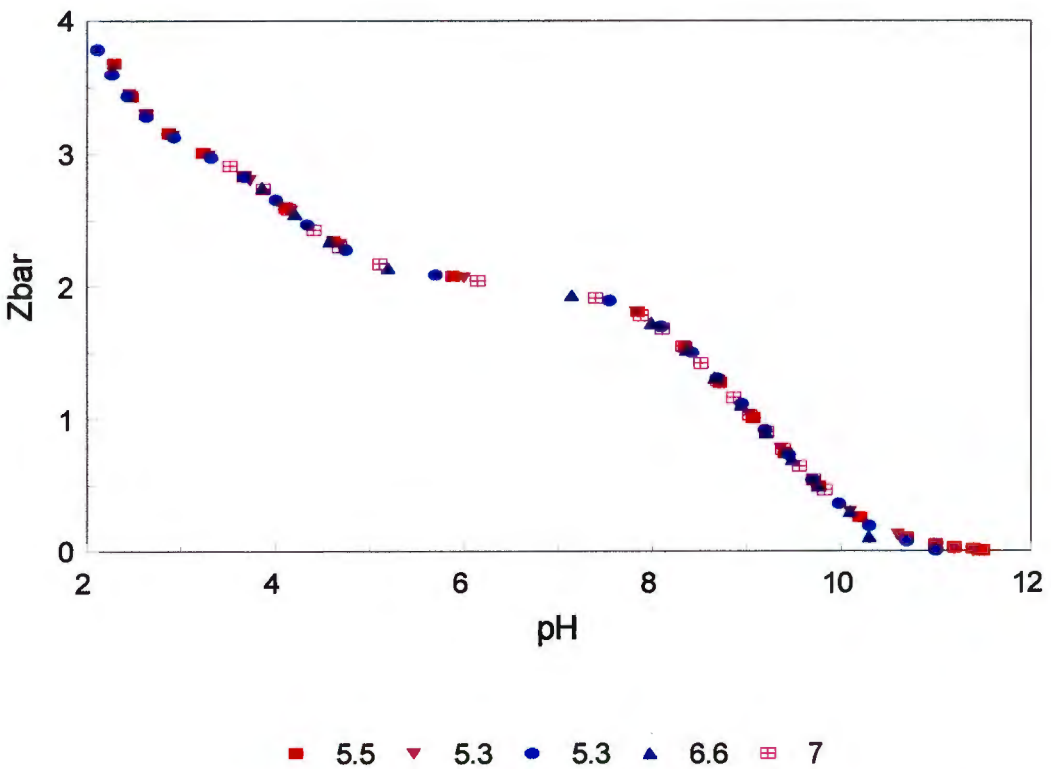

Figure 4.2: Experimental and calculated protonation curves for dtda. The different symbols represent titrations performed with different ligand concentrations (mM).

For the three ligands β_{011} is similar, but decreases from trien to dtda. It is possible to rationalise these results in terms of protonation occurring at a central amine. The decrease in β_{011} can then be attributed to the inductive effect of the acetate groups, which is greatest for dtda where the acetate groups are in closer proximity to the central amine. The second protonation step of ttda and dtda is significantly weaker than trien, which is consistent with protonation at a terminal amine. In the case of the third protonation step β_{013} for ttda is somewhat lower than that for trien, but that for dtda is more than two log units lower as the last remaining nitrogen in the dtda chain is protonated.

4.4.2 Copper

ttda

The formation and deprotonation curves of the Cu(II)ttda system are shown in Figures 4.3 and 4.4. The pH range over which the data could be analysed is very narrow, and this is not an ideal situation as far as the computer analysis is concerned.

As the complex was fully formed above pH 4, inclusion of data in this region in the modelling analysis did not result in a more acceptable model, and merely increased the error statistics. For this reason only the pH region 2-4 could be used to refine the betas. The formation curves are not superimposable, indicating that species other than simple mononuclear binary species are present. The curves rise towards a limiting value of 0.75, independent of component ratios and concentration, suggesting a complex stoichiometry of 1:1 and a high proportion of protonated species. At the start of the titration (pH of approximately 2), $\bar{Q}$ is approximately 2 indicating that complexation has already commenced. Within the data range analysed, $\bar{Q}$ did not rise above 3, and never reached the $\bar{n}$ curve implying that the MLH species was still present at this point in the titration. The data collected over the full pH range of the titration, that is from 2 to 11, was analysed, but the models chosen gave no significant improvement in the optimisation statistics and the high pH data was discarded.

The very narrow effective titration range is a result of the high stability of the copper complexes relative to the pK_a's of the ligands. Because of this narrow pH range computer analysis of these data is not ideal. The study was, therefore, repeated using trien as a competing ligand. This enabled the titrations to be carried out over a much wider pH range. The results of these experiments are discussed later. The species distribution calculated using the constants determined in this study is given in Figure 4.5.

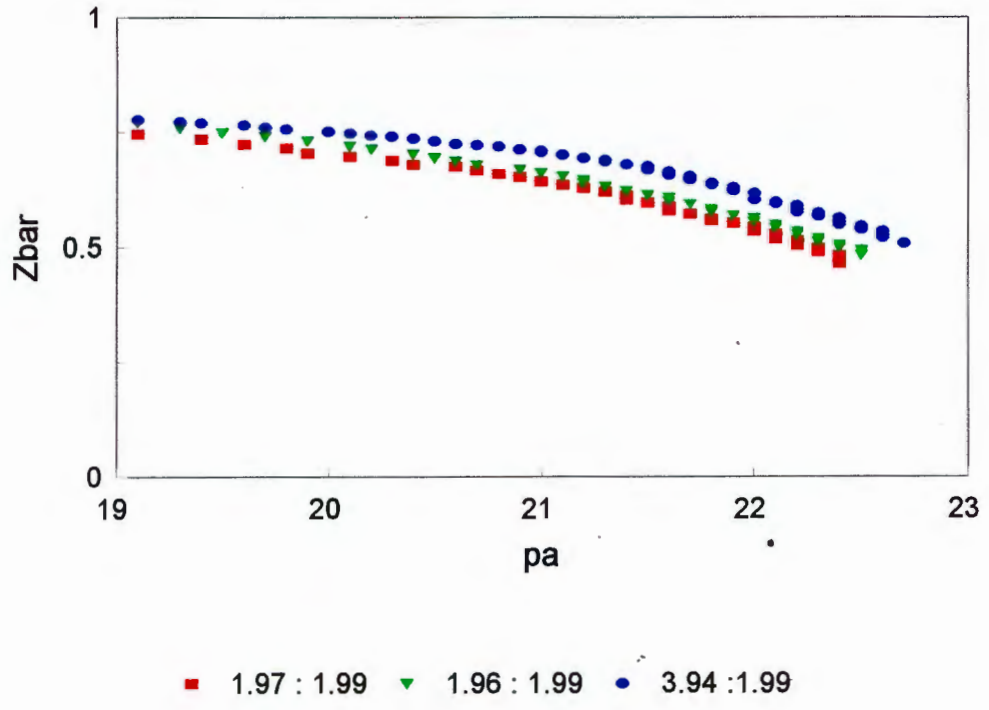

Figure 4.3: Experimental and calculated formation curves for the Cu(II)ttda system. The symbols represent titrations with different concentrations (mM) and [ttda]:[Cu] ratios.

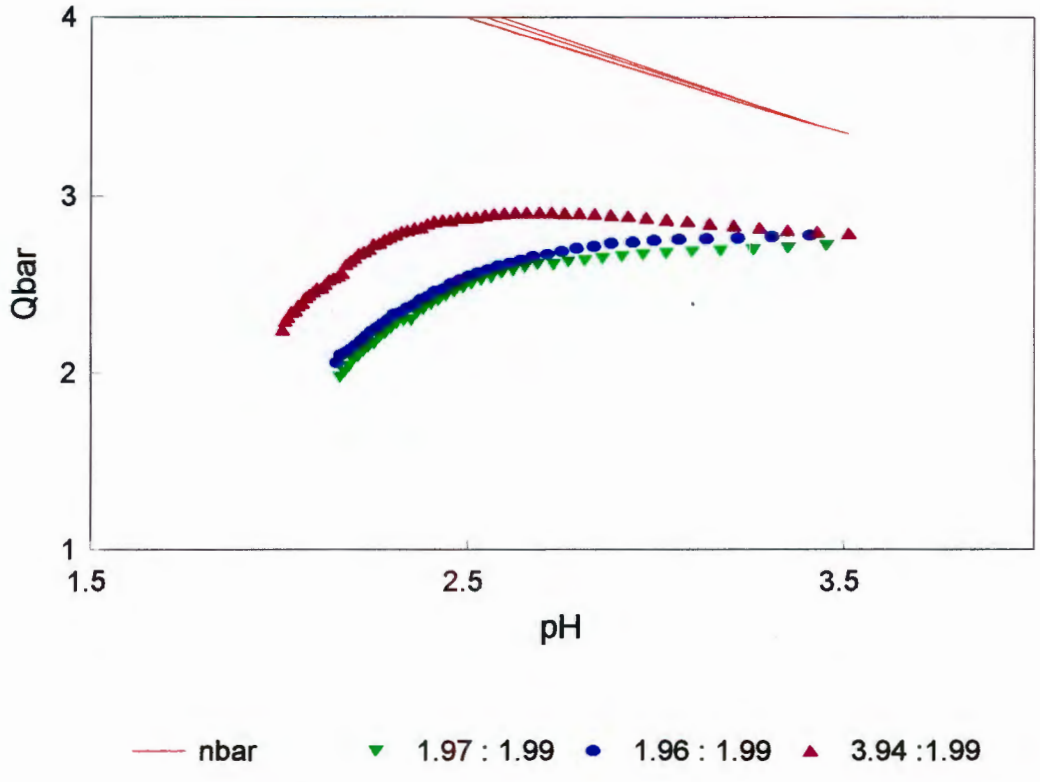

Figure 4.4: Experimental and calculated deprotonation curves for the Cu(II)ttda system. The symbols represent titrations with different concentrations (mM) and [ttda]:[Cu] ratios.

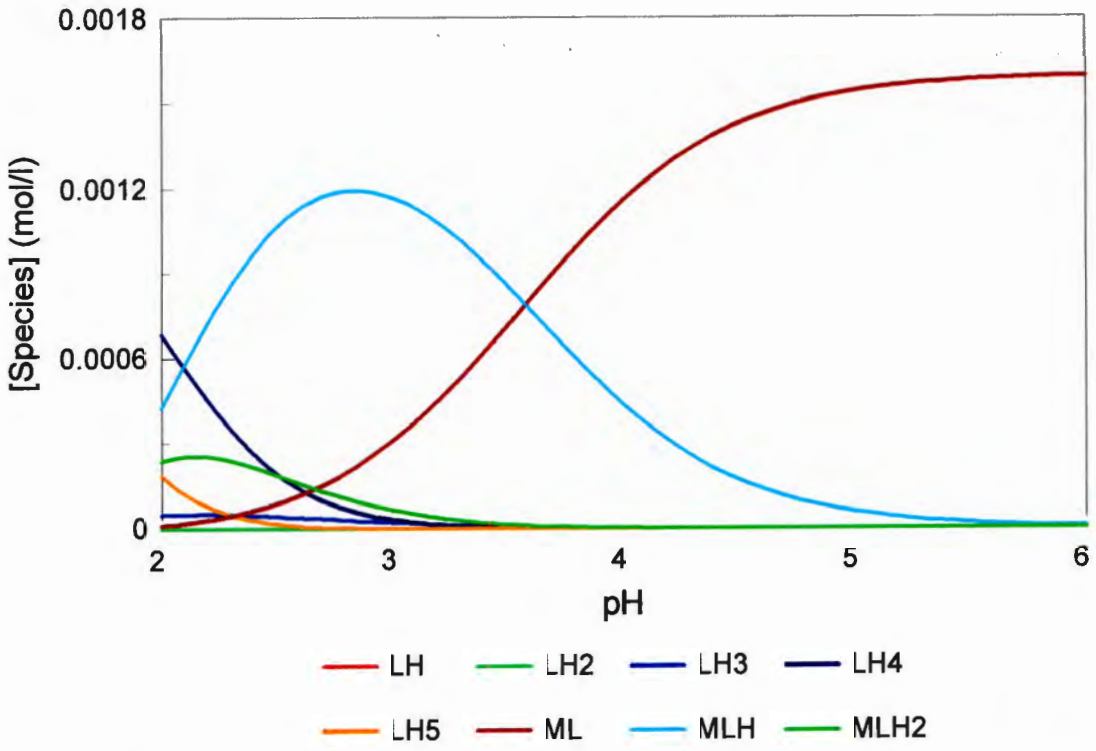

Figure 4.5: Species distribution curves for [Cu(ttda)]; Total [Cu(II)] = 1.6 mM = Total [ttda]

dtda

The formation and deprotonation curves are shown in Figures 4.6 and 4.7 for the dtda system.

The formation curves are largely superimposable, indicating that only mononuclear binary species are present. The curves rise towards a limiting value of 1, independent of component ratios and concentration, suggesting a complex stoichiometry of 1:1. At the start of the titration, at a pH of approximately 2, $\bar{Q}$ is > 1 indicating that complexation has already commenced. The ñ curve shows that at pH 3,6 there are essentially three protons to be displaced from the ligand while $\bar{Q}$ indicates that at this pH these protons have already been displaced by the metal ion. At higher pH values the ñ and $\bar{Q}$ curves are coincident indicating that no further complexation takes place.

At pH > 10 the $\bar{Q}$ curve rises above the ñ curve, which could indicate hydrolysis of the metal ion. A hydroxy species was refined in the computer optimisation, and this is also reflected in the fanning back of the Zbar curves.

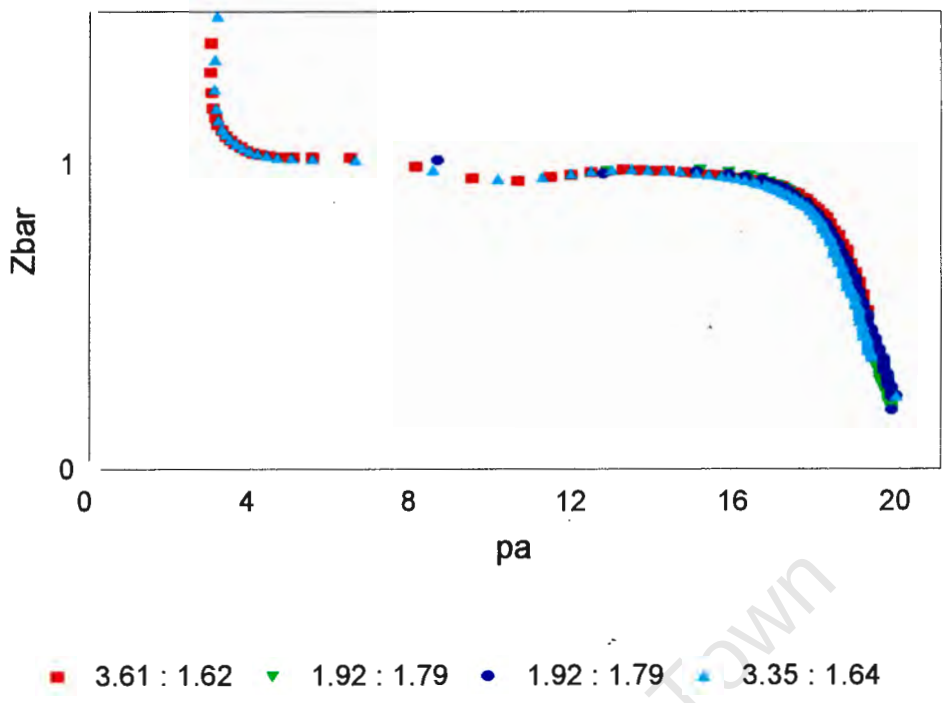

Figure 4.6: Experimental and calculated formation curves for the Cu(II)dtda system. The symbols represent titrations with different concentrations (mM) and [dtda]:[Cu] ratios.

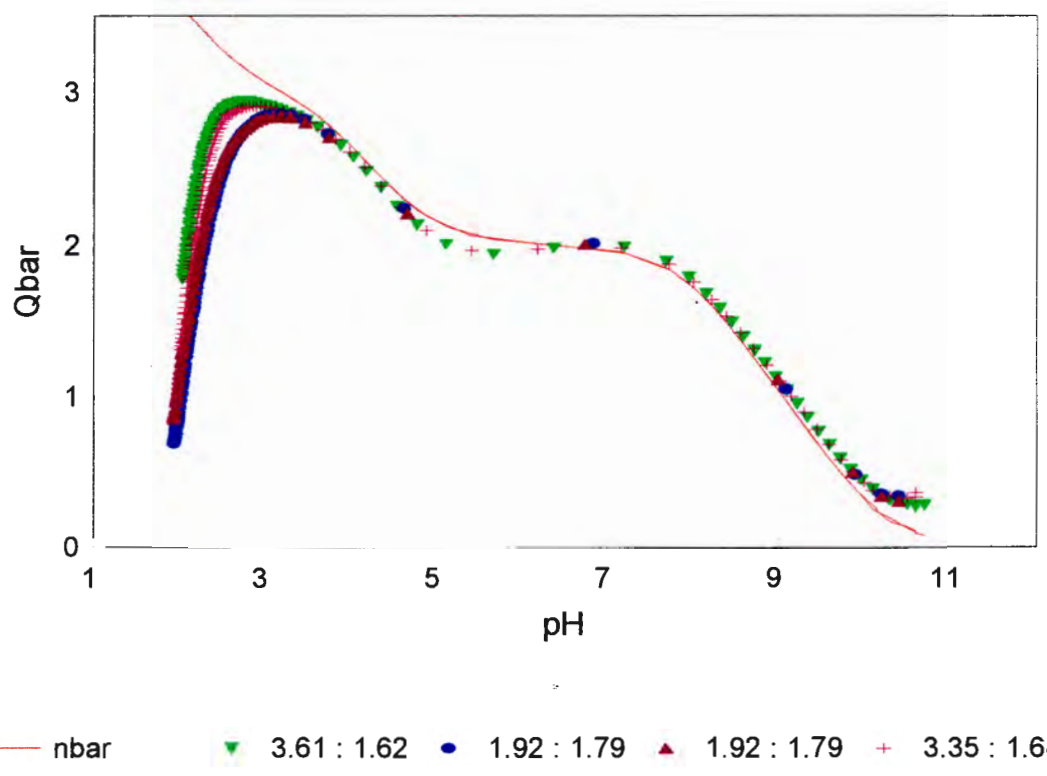

Figure 4.7: Experimental and calculated deprotonation curves for the Cu(II)dtda system. The symbols represent titrations with different concentrations (mM) and [ttda]:[Cu] ratios.

The species distribution calculated using the constants determined in this study is given in Figure 4.8.

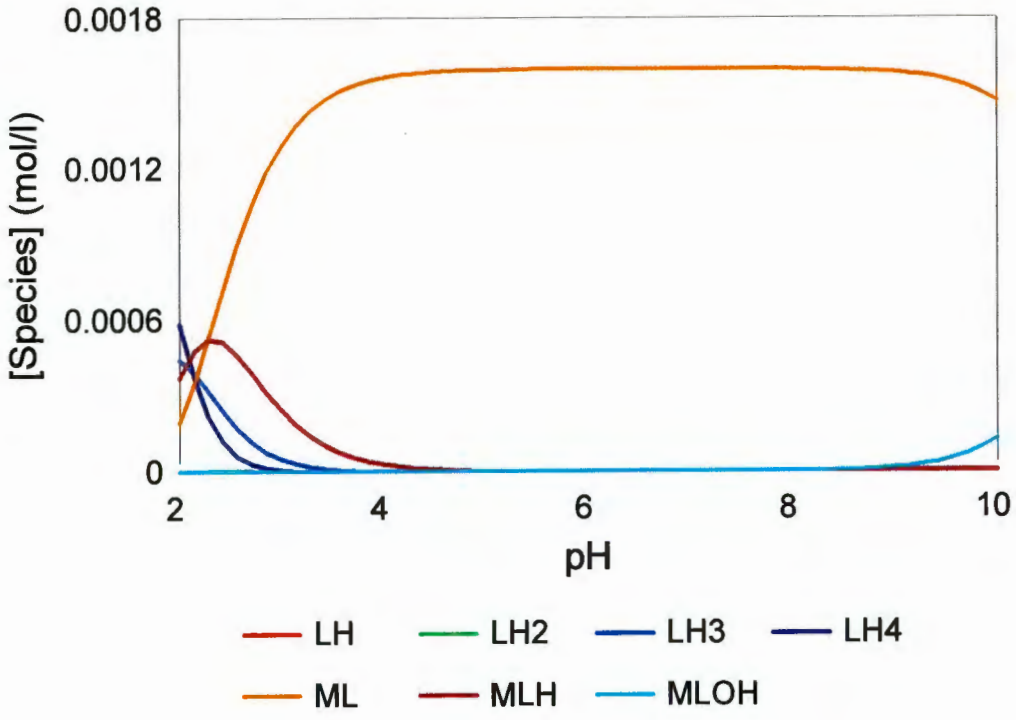

Figure 4.8: Species distribution curves for [Cu(dtda)]; Total [Cu(II)] = 1.6 mM = Total [dtda]

trien-ttda-dtda

The formation curves at the different concentration ratios are moderately non-superimposable, indicating that although mononuclear binary species predominate, other species are present. The curves rise towards a limiting value of 1, independent of component ratios and concentration, suggesting a complex stoichiometry of 1:1. A β_{110} and β_{111} model was refined for this system, and this agrees well with literature results, both in terms of the model and formation constant values. Some literature values are given in Table 4.2.

The results of the ternary system Cu-dtda-trien are essentially in agreement with those obtained in the binary Cu-dtda system, and show improved statistics. Similar results were obtained for the Cu-ttda-trien system, although in this case the results for the binary system were somewhat better than the ternary system.

Comparison of the results for the most predominant ML (metal-ligand) species of trien, ttda and dtda shows that the [Cu(ttda)] complex is the most stable, which is expected. The

increase in stability of the copper complex of ttda over that of trien must be due to the increased denticity of ttda. Comparison with trienda, Table 4.3, shows that the [Cu(trienda)] complex is only marginally more stable than the [Cu(ttda)] complex even though the basicity of trienda is significantly higher than ttda. Within the complex, ring strain about the tertiary amines may account for this difference. It has been shown that in $[Ni(edta)]^{2-}$ (edta = ethylenediaminetetra-acetate) the ligand is quindentate, the sixth co-ordination site being occupied by a water molecule (Smith and Hoard, 1959).

Table 4.3 Formation constants for [Cu(trienda)] (Chang and Douglas, 1981).

L	M	p q r	log β
Trienda	H^+	0 1 1	10.54
		0 1 2	20.40
		0 1 3	27.10
		0 1 4	30.88
	Cu^{2+}	1 1 0	21.78
		1 1 1	26.57

The potentiometric results show that a significant amount of the protonated M(HL) species is formed at a low pH. For this species there is a relatively large difference in stability between trien and ttda [log K = 12.5 and 15.1 respectively for the equilibrium M + HL ⇌ MHL], and a much smaller difference between ttda and trienda (log K = 16.03). These results could be accounted for by protonation occurring at a carboxylate site in the case of ttda and trienda. It would also support the hypothesis of ring strain about the tertiary amine of trienda being responsible for the decreased stability of the [Cu(trienda)] complex, as protonation would relieve this strain, making the $[Cu(trienda)H]^+$ complex more stable than the $[Cu(ttda)H]^+$ complex. The postulate that protonation of a carboxylate group occurs is also supported by the electronic spectra of the ttda complexes, and this is discussed in Section 5.2.

4.4.3. Zinc

ttda

The formation and deprotonation curves are shown in Figures 4.9 and 4.10.

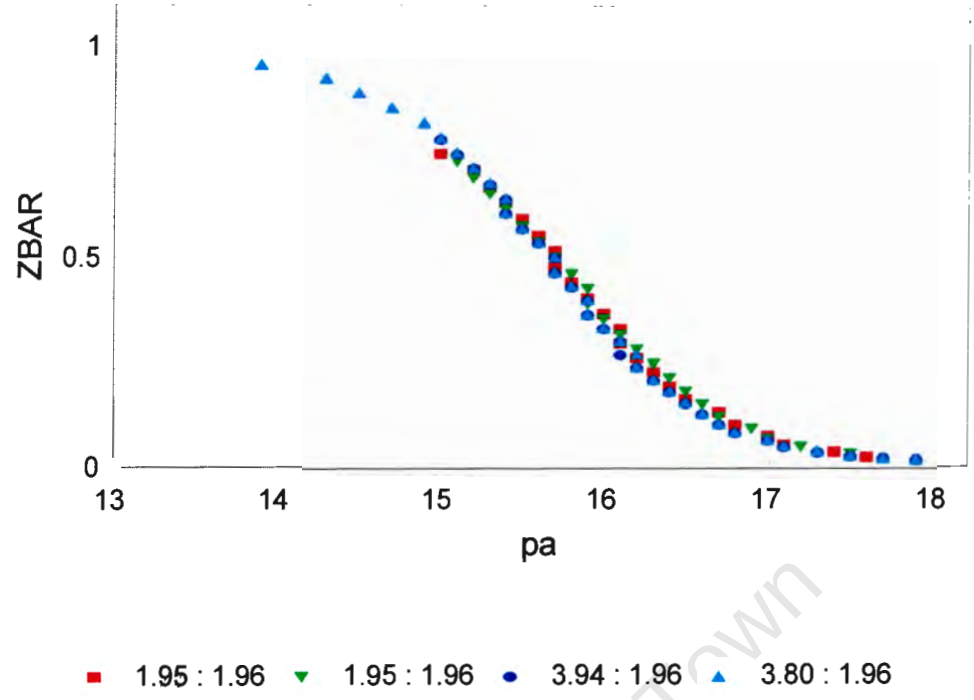

Figure 4.9: Experimental and calculated formation curves for the Zn(II) ttda system. The different symbols represent titrations with different concentrations (mM) and [ttda]:[Zn] ratios.

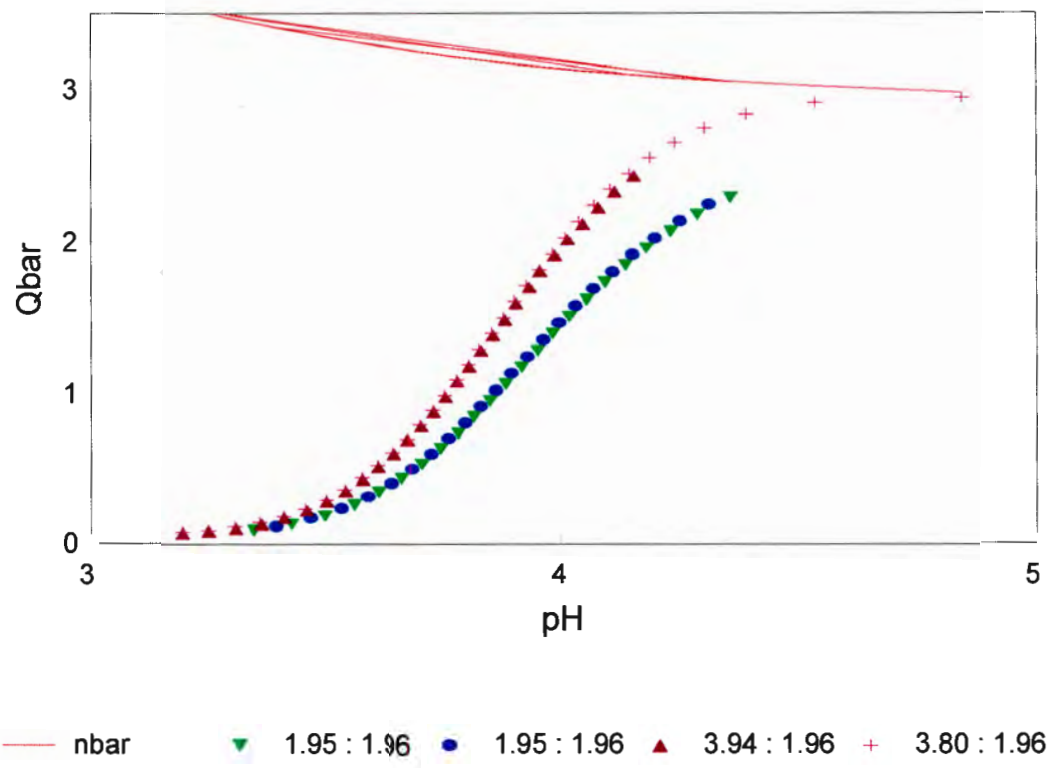

Figure 4.10: Experimental and calculated deprotonation curves for the Zn(II) ttda system. The different symbols represent titrations with different concentrations (mM) and [ttda]:[Zn] ratios.

The formation curves are superimposable, indicating simple, stepwise, mononuclear complexation. The curves rise towards a limiting value of 1, independent of component ratios and concentration, suggesting a complex stoichiometry of 1:1. The $\bar{Q}$ function is not as simple, indicating the presence of protonated species. This illustrates the complementary nature of the these two functions. The formation function is sensitive to the number of co-coordinate metal ions, while the deprotonation function is sensitive to the number of protons (or hydroxyl ions) in the complex. Within the data range analysed, $\bar{Q}$ did not rise above 3, and reached the $\bar{n}$ curve at a pH of 5. This implies that the MLH species was still present at this point in the titration.

The species distribution calculated using the constants determined in this study is given in Figure 4.11.

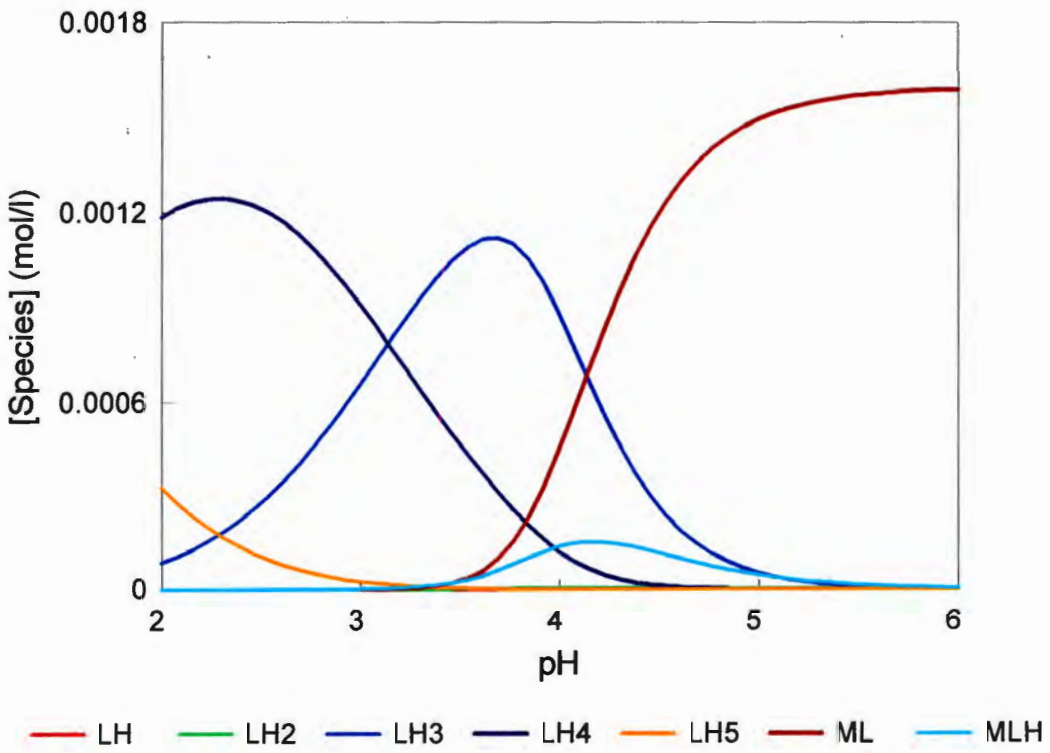

Figure 4.11: Species distribution curves for [Zn(ttda)];Total [Zn(II)] = 1.6 mM = Total [ttda]

The constants reported for the [Zn(trienda)] complex are given in Table 4.4, and are substantially different from those determined in this study for the analogous ligands ttda and dtda.

Table 4.4 Formation constants for [Zn(trienda)] (Chang and Douglas, 1981).

L	M	p q r	log β
trienda	Zn^{2+}	1 1 0	19.13
		1 1 1	24.66
		1 1 2	28.01

It is difficult to rationalise these discrepancies in terms of the structural differences between the ligands, especially as the protonation and copper(II) complex formation constants of ttda and trienda are in much closer agreement.

Inspection of the thermodynamic data (Martell and Smith, 1974-1989) for zinc(II) complexes of related ligands shows that the enthalpy factors make the biggest contribution towards the stability of the amino complexes. The neutralisation of the charge, and hence decrease in hydration is most likely responsible for the importance of entropy in determining the stability of acetate ligand complexes. The presence of two acetate groups on ethylenediammine (en) lowers $\Delta H°$ for zinc(II) complexation by about 4 kJ mol^{-1} [$\Delta H°$(en) = -29.3, $\Delta H°$(ethylenediammine-*N*,*N*'-diacetate) = -25.5 kJ mol^{-1}], hence it is estimated that $\Delta H°$ for zinc complexation of ttda to be of the order of -33.2 kJ mol^{-1} [$\Delta H°$(triethylenetetrammine) = -37.2 kJ mol^{-1}]. Similarly $\Delta H°$ for zinc complexation of dtda is estimated to be -23.2 kJ mol^{-1} [$\Delta H°$(diethylenetriamine) = -27.2 kJ mol^{-1}]. At the same time the data show that $\Delta S°$ increases by about 30 J K^{-1} mol^{-1} per acetate group. Hence $\Delta S°$ is estimated to be about 165 J K^{-1} mol^{-1} for zinc(II) complexes of ttda and dtda. This leads to values for $\Delta G°$ of -82.4 and -72.4 kJ mol^{-1} and equilibrium constants of $10^{14.4}$ and $10^{12.7}$ at 25°C for the formation of [Zn(ttda)] and [Zn(dtda)] respectively. This is in reasonable agreement with the values of 15.65 and 13.19 obtained for β_{110} in this work.

dtda

The formation and deprotonation curves are shown in Figures 4.12 and 4.13 for the zinc(II)dtda system.

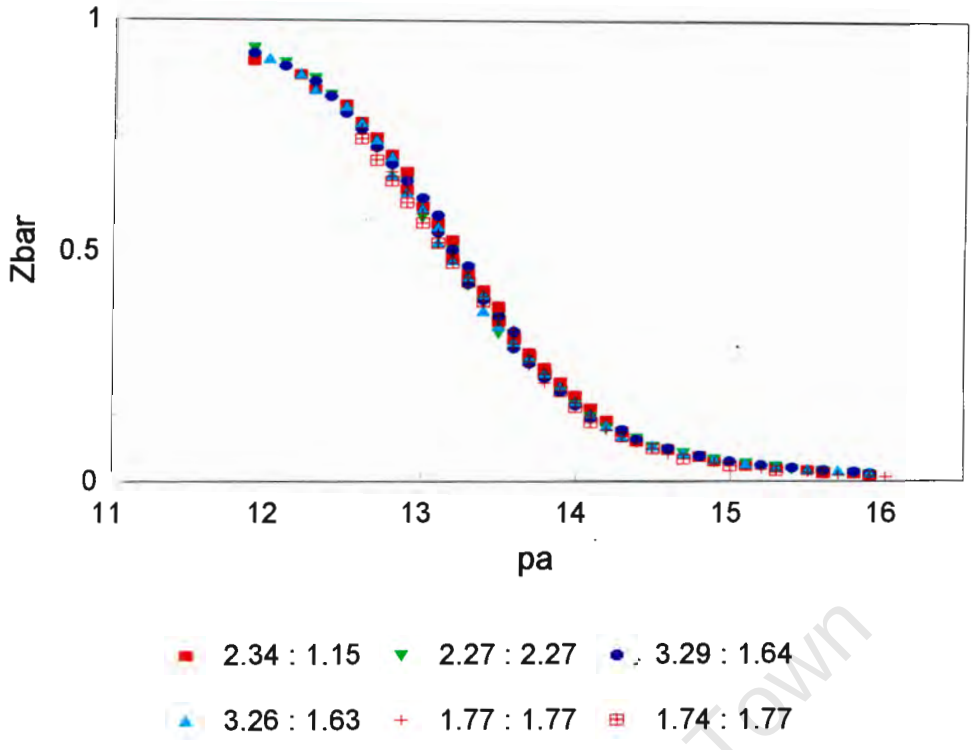

Figure 4.12: Experimental and calculated formation curves for the Zn(II)dtda system. The symbols represent titrations with different concentrations (mM) and [dtda]:[Zn] ratios.

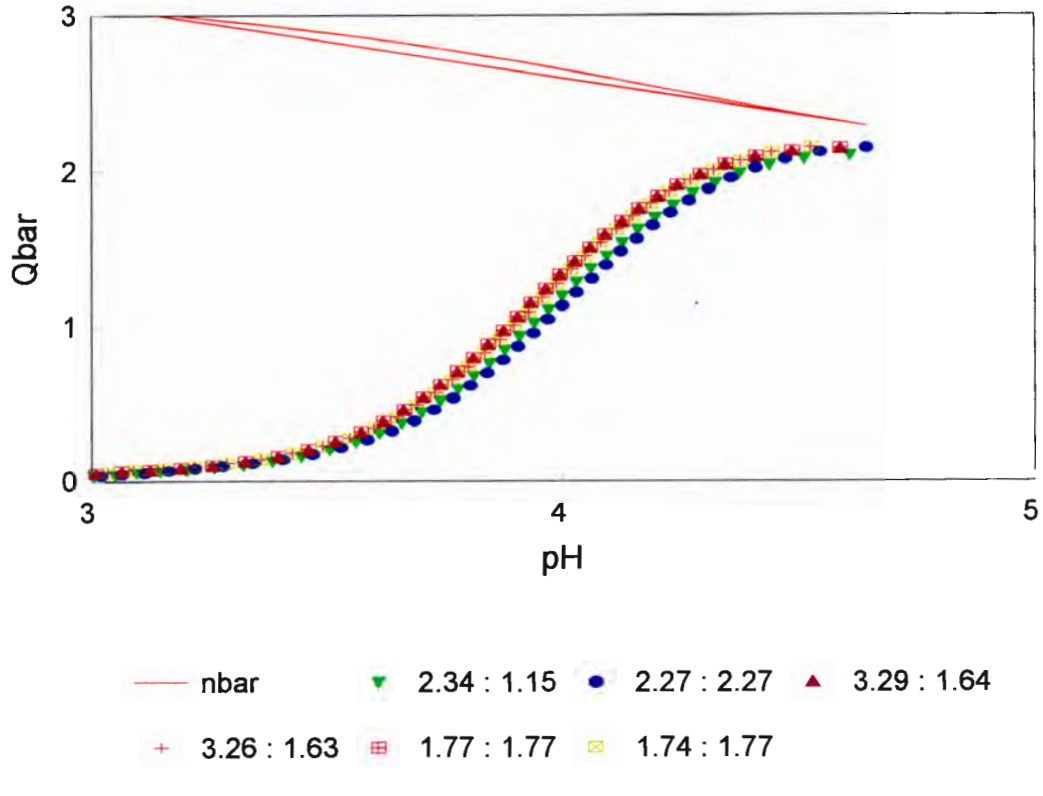

Figure 4.13: Experimental and calculated deprotonation curves for the Zn(II) dtda system. The symbols represent titrations with different concentrations (mM) and [dtda]:[Zn] ratios.

The formation curves are largely superimposable, indicating that only mononuclear binary species are present. The curves rise towards a limiting value of 1, independent of component ratios and concentration, suggesting a complex stoichiometry of 1:1. At the start of the titration, at a pH of approximately 3, $\bar{Q}$ is zero indicating that as with nickel, zinc complexation commenced after the start of the titration. The $\bar{n}$ curve shows that at pH 3,6 there are essentially three protons to be displaced from the ligand while $\bar{Q}$ indicates that at this pH the displacement of these protons by the metal ion is beginning. As the titration continues the curves arising from different initial titration concentrations diverge, as the ratio of metal to displaceable proton varies. At higher pH values the $\bar{n}$ and $\bar{Q}$ curves are coincident indicating that no further complexation takes place.

The species distribution calculated using the constants determined in this study is given in Figure 4.14.

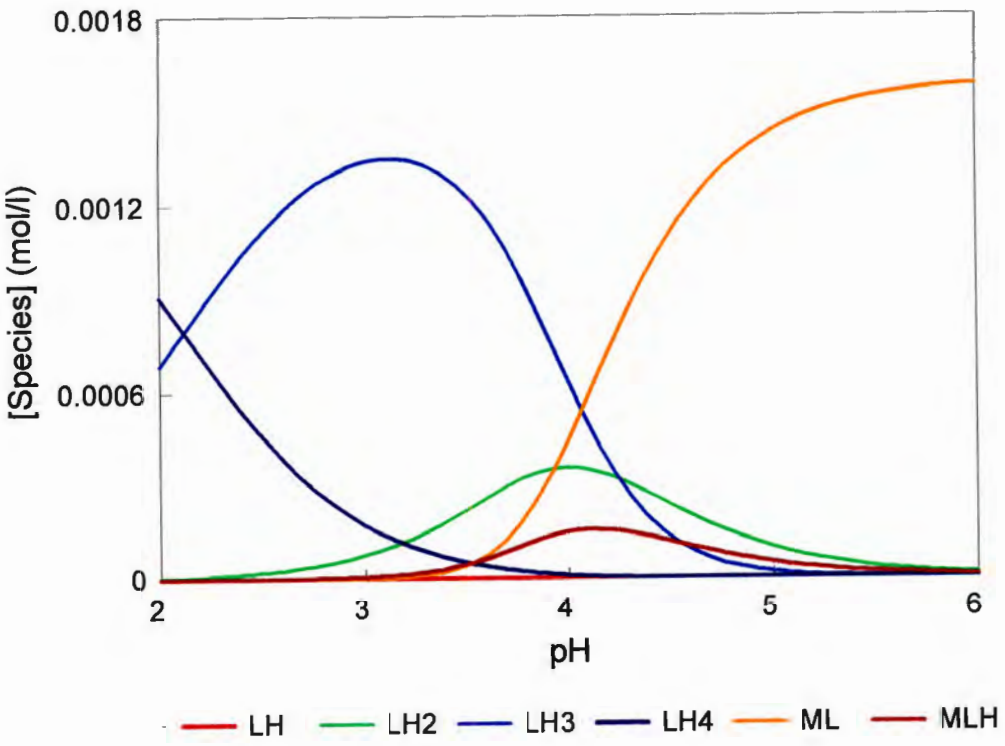

Figure 4.14: Species distribution curves for [Zn(dtda)]; Total [Zn(II)] = 1.6 mM = Total [dtda]

4.4.4 Nickel and Manganese

ttda and dtda

Inspection of the results of the potentiometric study of these system showed that there were many similarities in their behaviour under these conditions. The analysis of the results for these systems are therefore described together.

The formation and deprotonation curves are shown in Figures 4.15 to 4.22 below. The speciation curves are given in Figures 4.23 to 4.26 (see appendix II)

The formation curves are not entirely superimposable. This could indicate that species other than mononuclear complexes were present. The curves rise towards a limiting value of 1, at higher ligand to metal ratios and ligand concentration, but the 1:1 ratio titrations begin to plateau at smaller values of $\bar{Z}$, suggesting a complex stoichiometry other than 1:1, but refinement of models including stoichiometries other than 1:1 did not improve the optimisation statistics. It must be concluded that the data contains some error. The $\bar{Q}$ function indicates the presence of protonated species in most of the systems. In the Mn(II)dtda system the 'best' fit was obtained with a model comprising only the ML species.

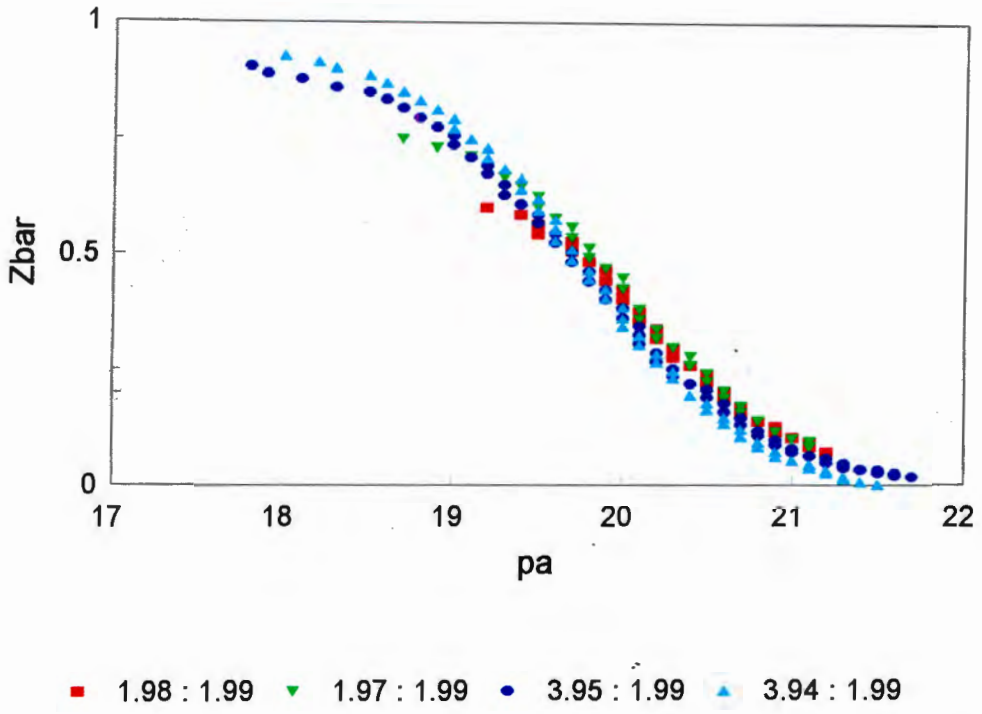

Figure 4.15: Experimental and calculated formation curves for the Ni(II)ttda system. The symbols represent titrations with different concentrations (mM) and [ttda]:[Ni] ratios.

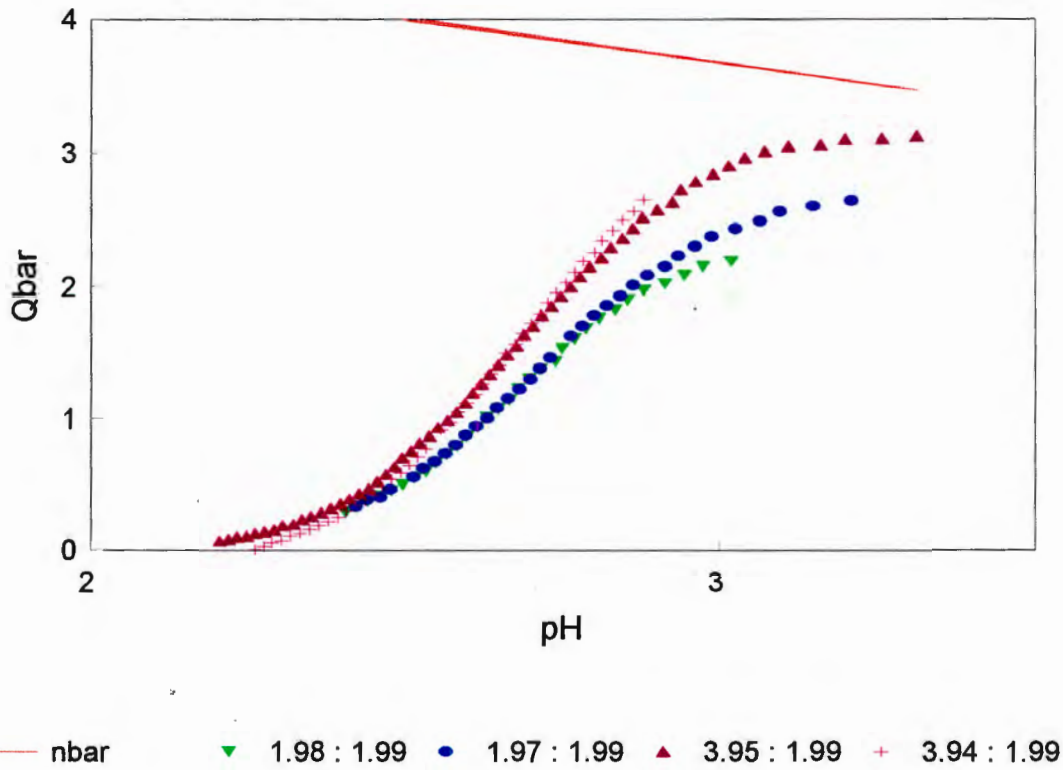

Figure 4.16: Experimental and calculated deprotonation curves for the Ni(II)ttda system. The symbols represent titrations with different concentrations (mM) and [ttda]:[Ni] ratios.

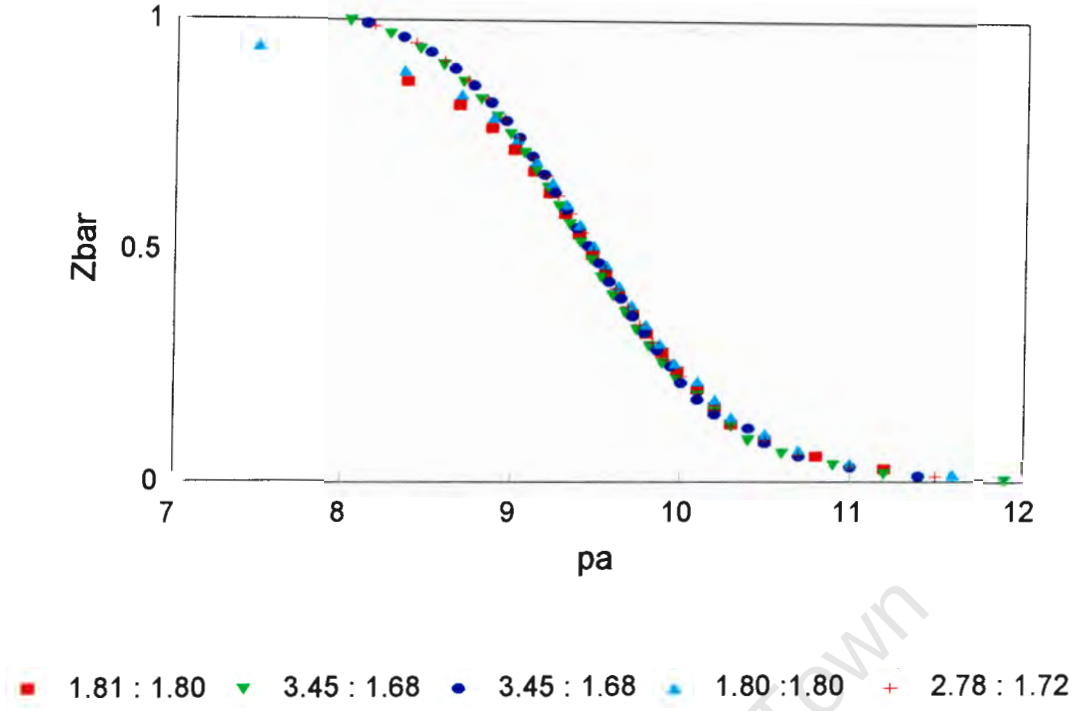

Figure 4.17: Experimental and calculated formation curves for the Mn(II)ttda system. The symbols represent titrations with different concentrations (mM) and [ttda]:[Mn] ratios.

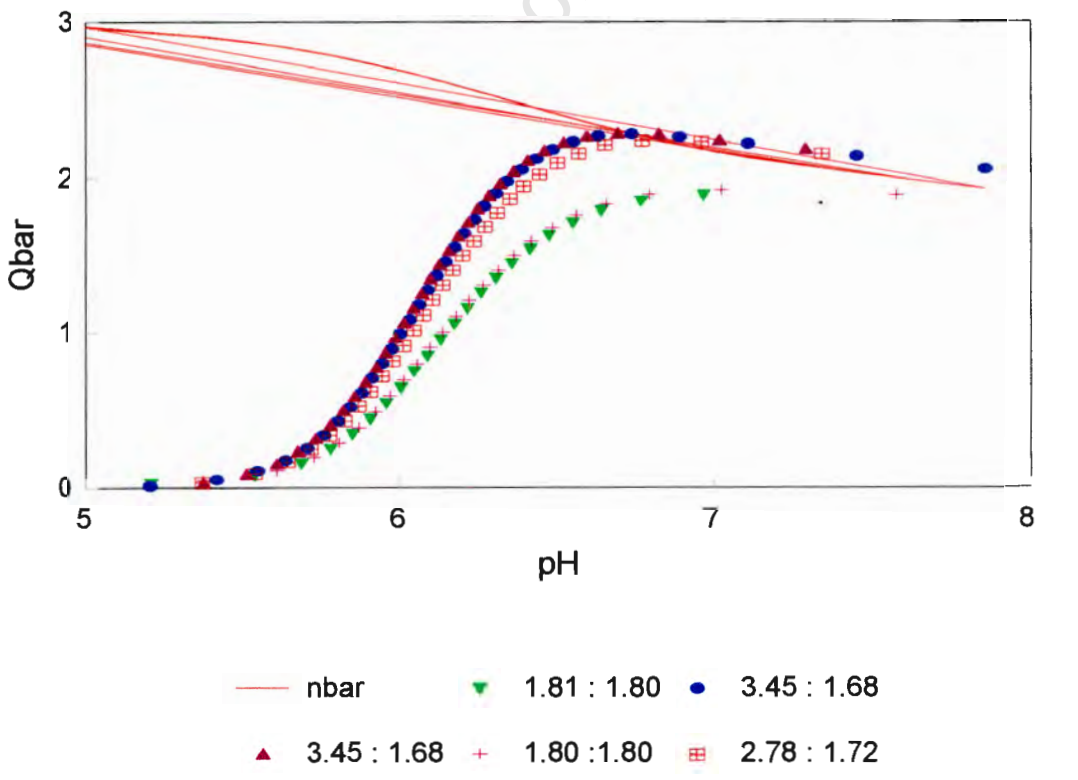

Figure 4.18: Experimental and calculated deprotonation curves for the Mn(II)ttda system. The symbols represent titrations with different concentrations (mM) and [ttda]:[Mn] ratios.

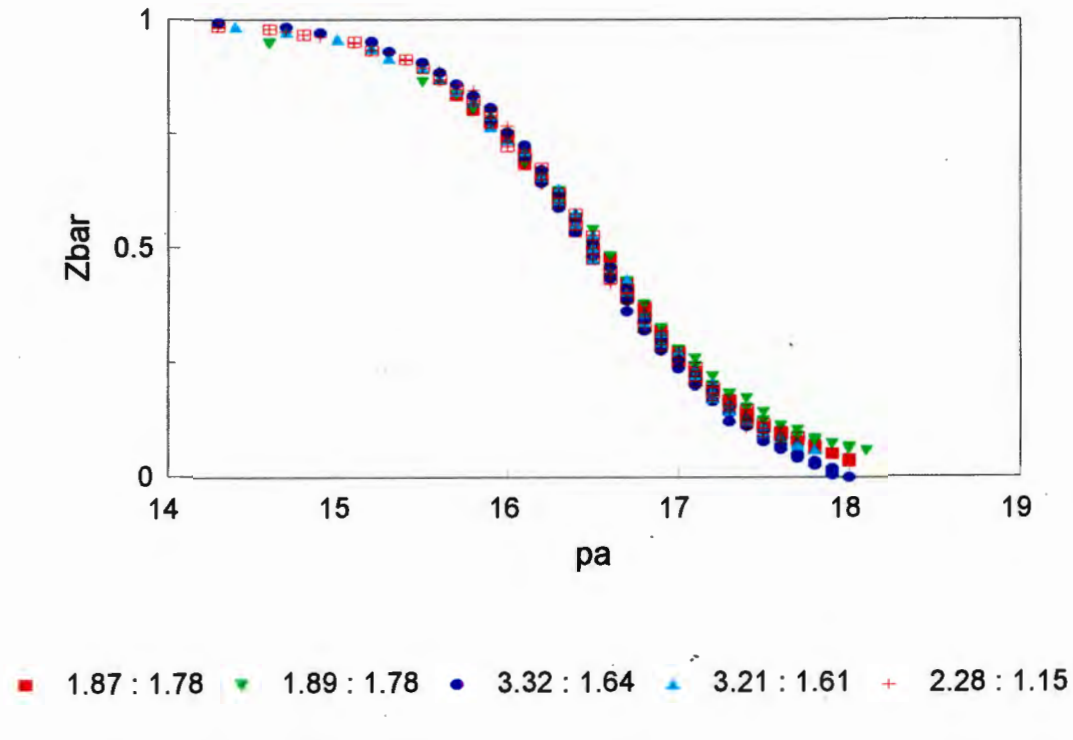

Figure 4.19: Experimental and calculated formation curves for the Ni(II)dtda system. The symbols represent titrations with different concentrations (mM) and [dtda]:[Ni] ratios.

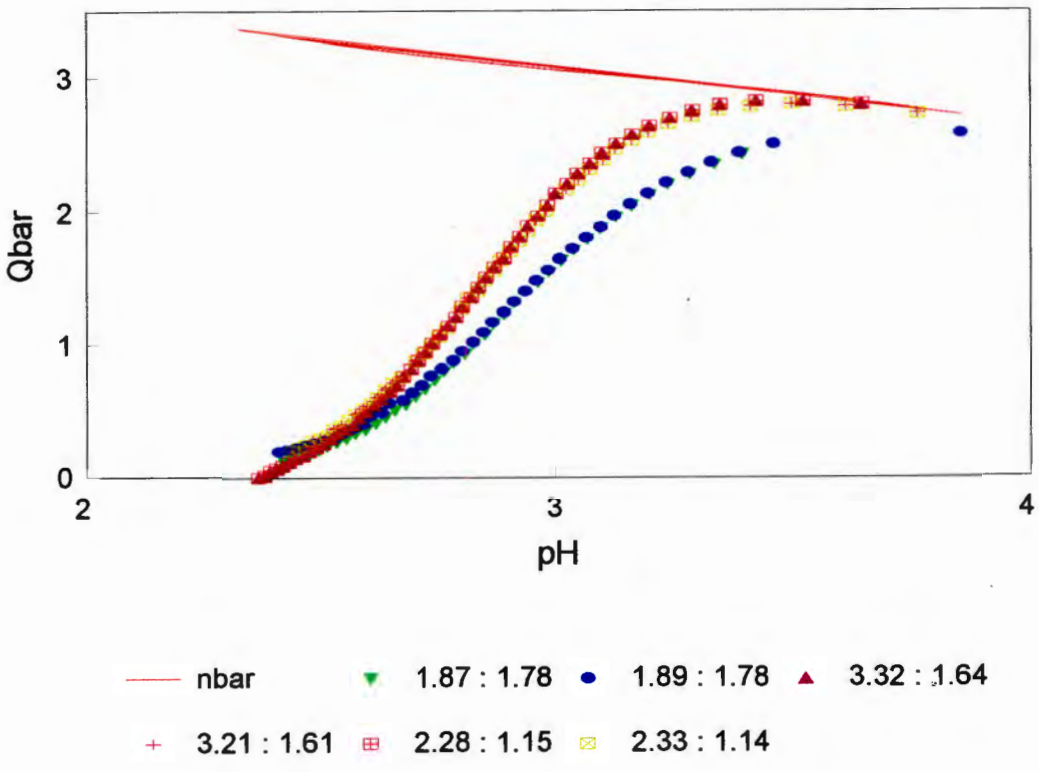

Figure 4.20: Experimental and calculated deprotonation curves for the Ni(II)dtda system. The symbols represent titrations with different concentrations (mM) and [dtda]:[Ni] ratios.

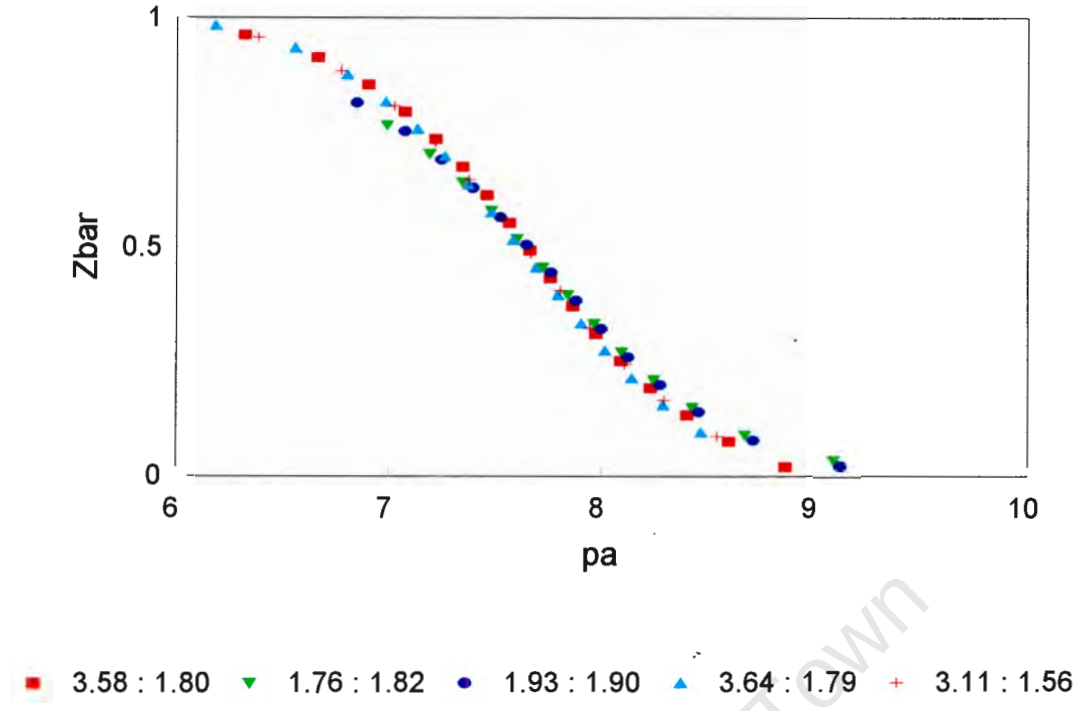

Figure 4.21: Experimental and calculated formation curves for the Mn(II)dtda system. The symbols represent titrations with different concentrations (mM) and [dtda]:[Mn] ratios.

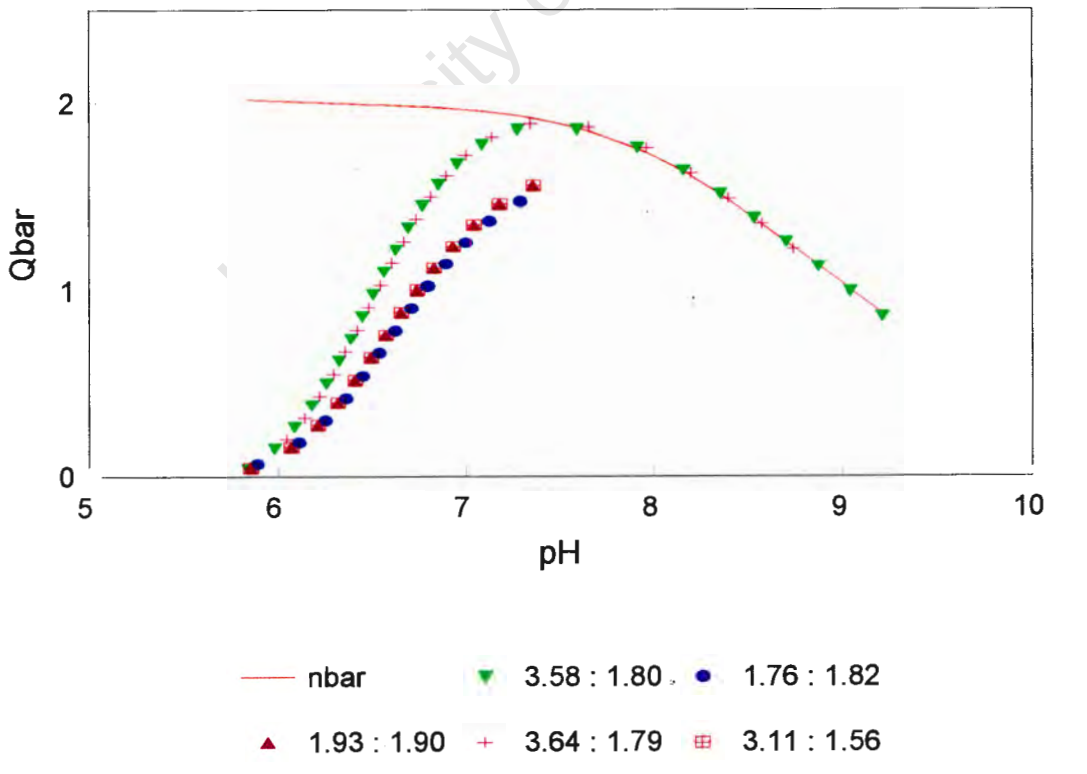

Figure 4.22: Experimental and calculated deprotonation curves for the Mn(II) dtda system. The symbols represent titrations with different concentrations (mM) and [dtda]:[Mn] ratios.

4.4.5. Cobalt

ttda

The formation and deprotonation curves are shown in Figures 4.27 and 4.28 for this system. The formation curves are largely superimposable, indicating that only mononuclear binary species are present. The curves rise towards a limiting value of approximately 0.9, and curves representing different component ratios and concentration begin to diverge at approximately $\bar{Z}$ = 0.6, suggesting a complex stoichiometry other than 1:1. The levelling off of the formation curve at a value less than 1 could also indicate the presence of precipitate (Smith, Motekaitis, and Martell,1985). During the titration of these solutions no precipitate was observed, but the solution changed colour. As oxidation to Co(III) was considered to be a possibility, the reaction mixture was back titrated to check that the system was reversible. The colour change was not reversible, and the data was not superimposable with the forward titration. The conclusion drawn was that at higher pH the deviation from the expected curve was due either to the formation of a very fine precipitate, or to oxidation of the cobalt (II) to cobalt(III). Data from the non superimposable region was not included in the data analysis. There is good agreement between the experimental $\bar{Z}$ plot and the theoretical pseudoplot, indicating that the model and betas are essentially correct. At the start of the titration, at a pH of approximately 2, $\bar{Z}$ is zero, and begins to increase at a pH of approximately 3,3, indicating the commencement of complexation. The $\bar{n}$ curve shows that at pH 4 there are essentially three protons to be displaced from the ligand while indicates that at this pH just over two of these protons have been displaced by the metal ion. The agreement between the experimental and theoretical plots is good.

The speciation curves, Figure 4.29, show that the formation of the ML complex begins at pH 3, and by pH 5 it is the only complex of significance in the solution. The degree of formation of the MLH complex is low, explaining the relatively high standard deviation of the β calculated for this complex. Due to the low percentage formation, the question must be asked as to whether this is not a 'computer' complex, arising from error within the data.

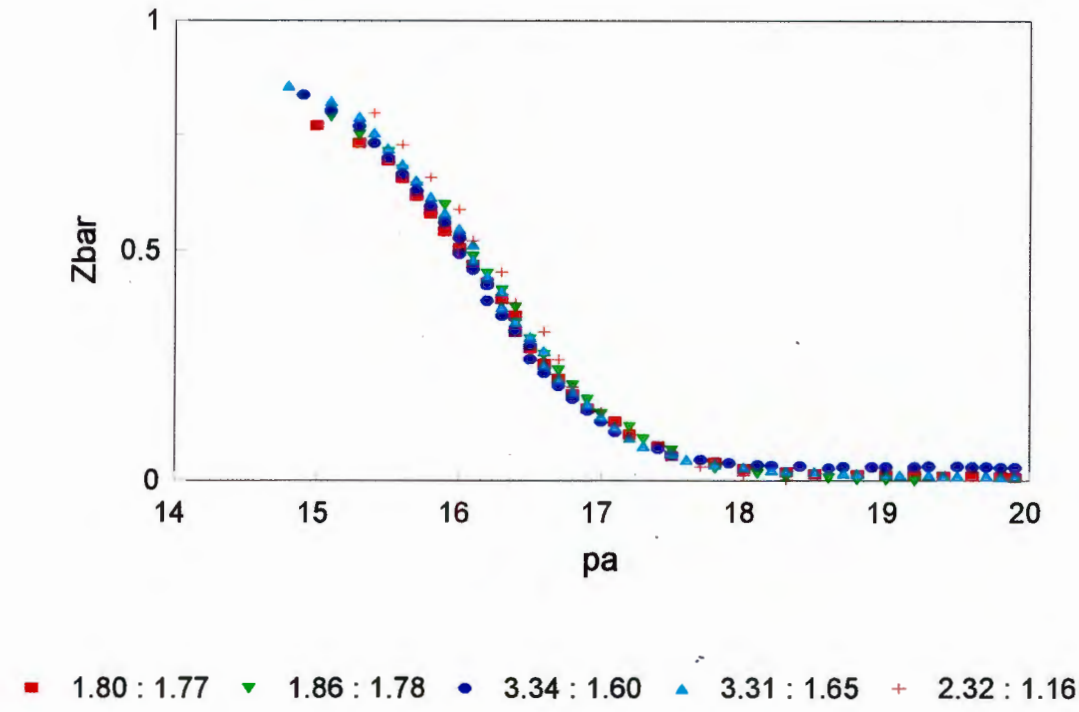

Figure 4.27: Experimental and calculated formation curves for the Co(II)ttda system. The symbols represent titrations with different concentrations (mM) and [ttda]:[Co] ratios.

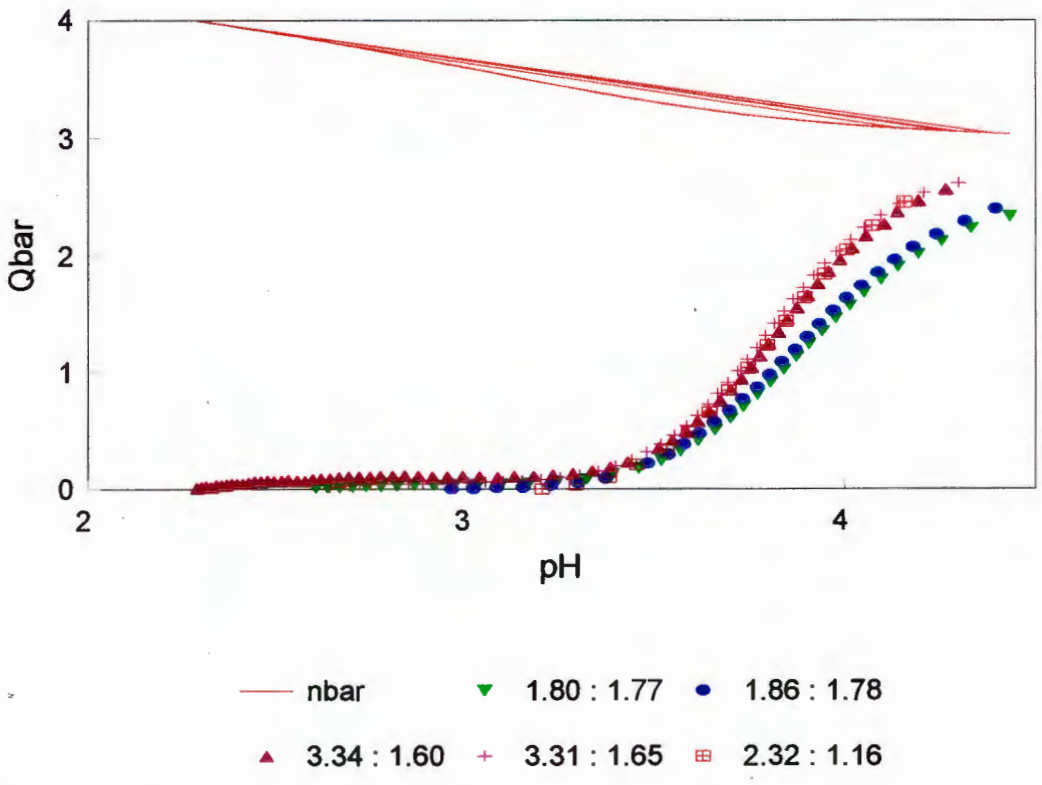

Figure 4.28: Experimental and calculated deprotonation curves for the Co(II) ttda system. The symbols represent titrations with different concentrations (mM) and [ttda]:[Co] ratios.

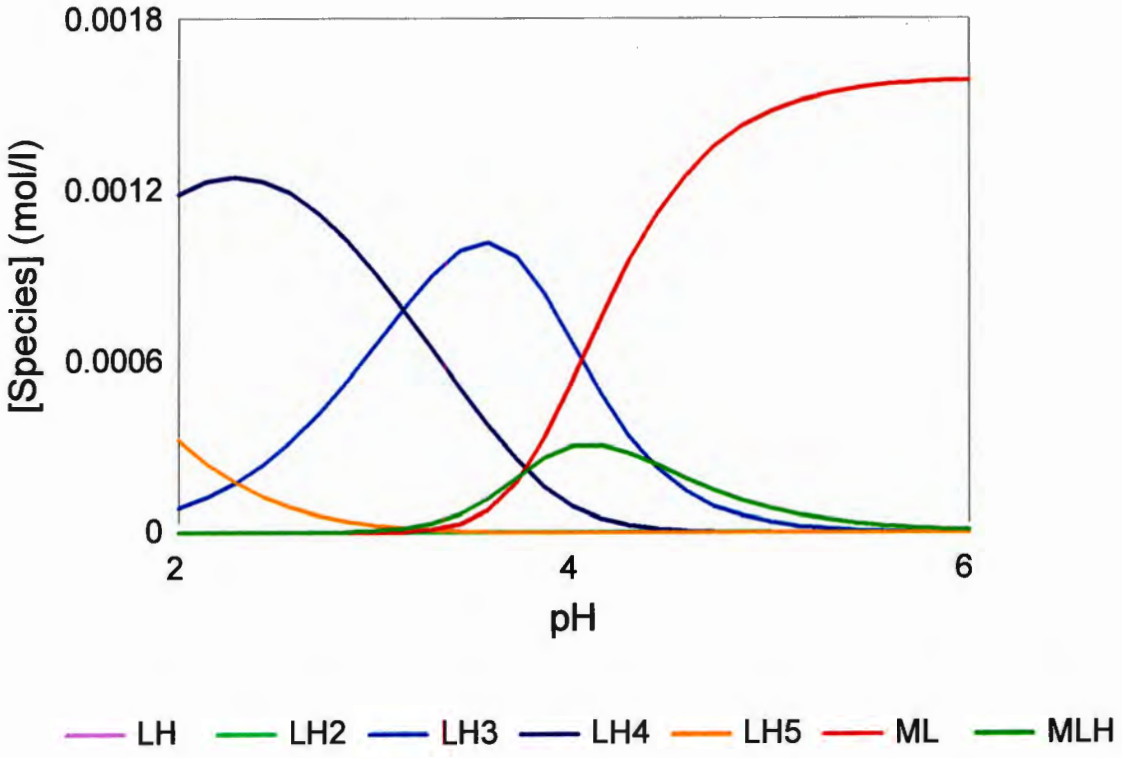

Figure 4.29: Speciation curves for the system [Co(ttda)]; Total [Co(II)] = 1.6 mM = Total [ttda]

dtda

The formation and deprotonation curves are shown in Figures 4.30 and 4.31 for this system. The formation curves are largely superimposable, indicating that mainly mononuclear binary species are present. The curves rise towards a limiting value of approximately 0.8, as is the case with the Co-ttda system, suggesting the possibility of precipitation or oxidation in the vessel. At the start of the titration, at a pH of approximately 2.3, $\bar{Z}$ is zero indicating that complexation commenced after the start of the titration. Complexation begins at a pH of approximately 3.4, at which point the $\bar{n}$ curve shows that there are essentially three protons to be displaced from the ligand. As the pH increases during the titration the $\bar{n}$ and $\bar{Q}$ curves approach each other, but never become coincident, indicating that under the conditions of these titrations complexation is never complete.

The species distribution calculated using the constants determined in this study is given in Figure 4.32 (see Appendix II).

The values for the formation constants obtained for these ligands were compared with literature values (Martell and Smith, 1974-1989) for similar compounds. These values are given in Table 4.5 below.

Table 4.5: Formation constants for compounds similar to dtda

4 co-ordinate	β	5 co-ordinate	β
4 N (trien)	10,9	5 N (tetren)	13,3
2 N 2 O (edda)	11,2	3 N 2 O (dtda)	13,1

The values obtained for the ligands containing only nitrogen donor ligands are similar to those obtained for the mixed donor ligand. It appears from these results that for the cobalt-nitrogen or cobalt-oxygen systems the donor atom has little influence on the stability of the complex.

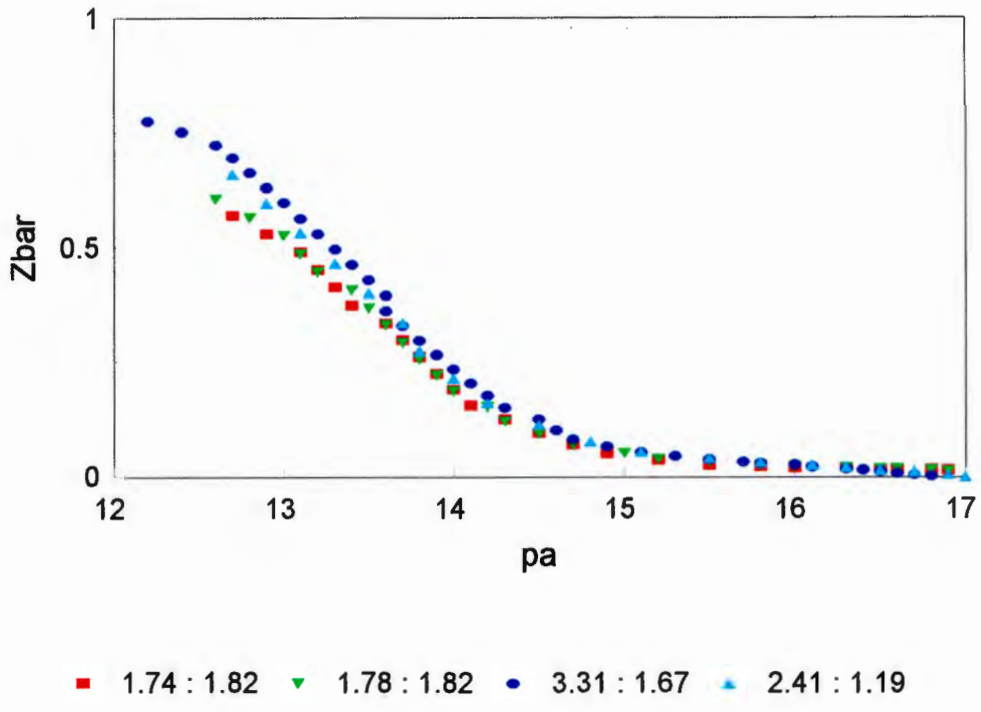

Figure 4.30: Experimental and calculated formation curves for the Co(II)dtda system. The symbols represent titrations with different concentrations (mM) and [dtda]:[Co] ratios.

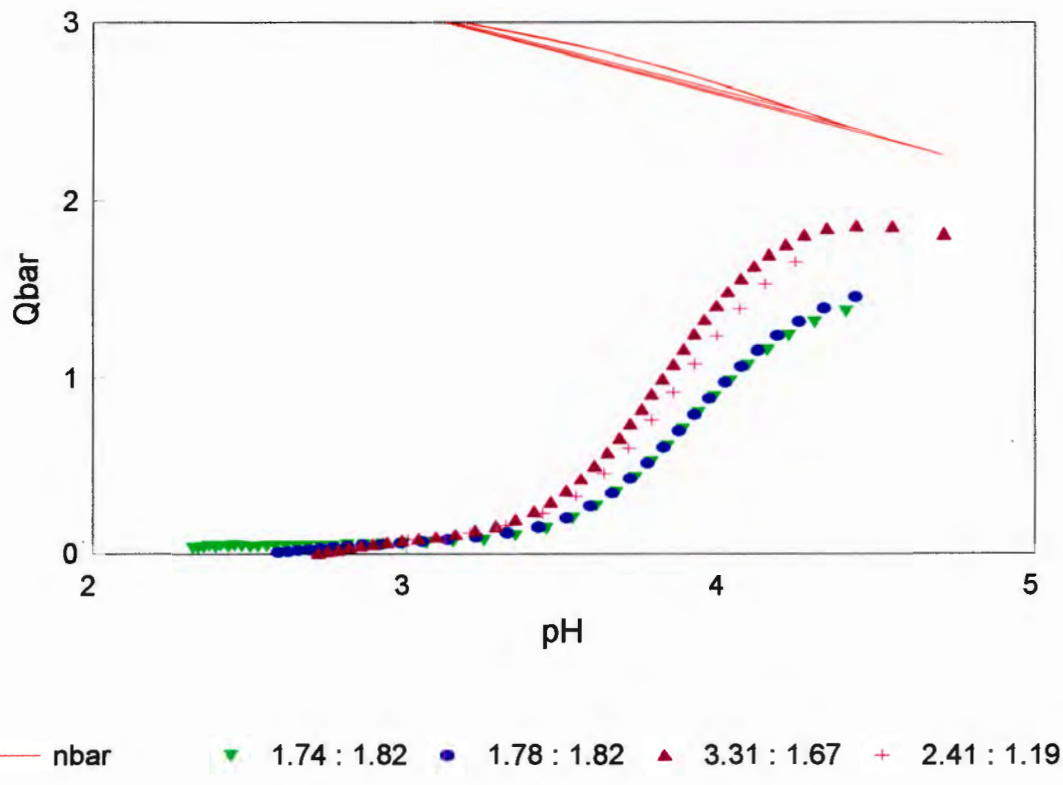

Figure 4.31: Experimental and calculated deprotonation curves for the Co(II)dtda system. The symbols represent titrations with different concentrations (mM) and [dtda]:[Co] ratios.

4.4.6. Calcium and Magnesium

ttda

The formation curves are given in Figure 4.33 and the deprotonation curves in Figure 4.34 for calcium, and in Figures 4.35 and 4.36 for magnesium.

The formation curves for the Ca-ttda system are superimposable, indicating that the major species formed are simple mononuclear complexes. At high pH the formation curves fan back, which is characteristic of hydroxy species formation. This is shown more clearly by the deprotonation function. Computer analysis of the data confirms the presence of only two species, ML and MLH_{-1}. The 'goodness of fit' between the experimental data and the proposed model is indicated by the superimposability of the curves in the Figures on the clear page.

dtda

The formation curves are given in Figure 4.37 and the deprotonation curves in Figure 4.38 for calcium, and in Figures 4.39 and 4.40 for magnesium.

The results obtained are similar to those for the Ca-ttda system. The ML complex is the major complex formed under these conditions, with the calculated formation constant marginally lower than that obtained for the Ca-ttda. This must be due to the higher denticity of the tetramine ligand.

A comparison of the results obtained for the calcium(II) and magnesium(II) systems is interesting. The [Mg(dtda)] complex is more stable than the [Mg(ttda)] complex. Presumably this is due to the small size of the magnesium(II) ion. For the larger calcium(II) ion the expected order of complex stability [Ca(ttda)] > [Ca(dtda)] is seen.

Ionic radius is a common theme running through the co-ordination chemistry of calcium(II) and magnesium(II) (Burgess, 1974). The higher charge density of the magnesium(II) ion tends to make complexes of this metal ion more stable than the corresponding calcium(II) complexes. On the other hand, the small size of the magnesium ion makes multidentate co-ordination difficult. The results of this study are consistent with these observations. The [Ca(dtda)] complex has the same stability as the [Mg(dtda)], while the [Ca(ttda)] complex is more stable than the [Mg(ttda)].

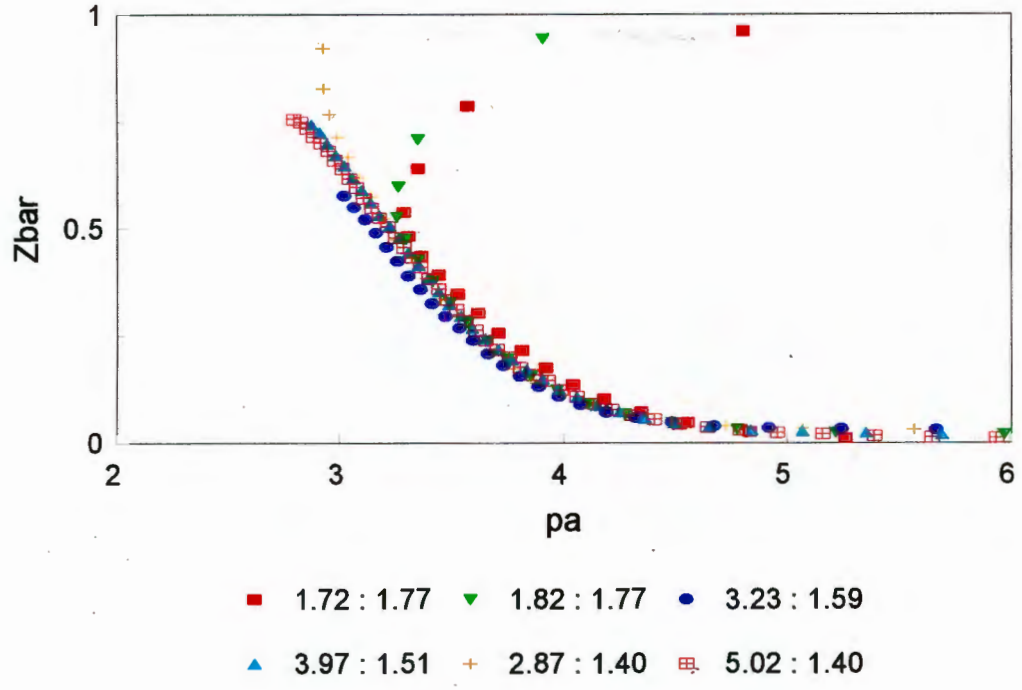

Figure 4.33: Experimental and calculated formation curves for the Ca(II)ttda system. The symbols represent titrations with different concentrations (mM) and [ttda]:[Ca] ratios.

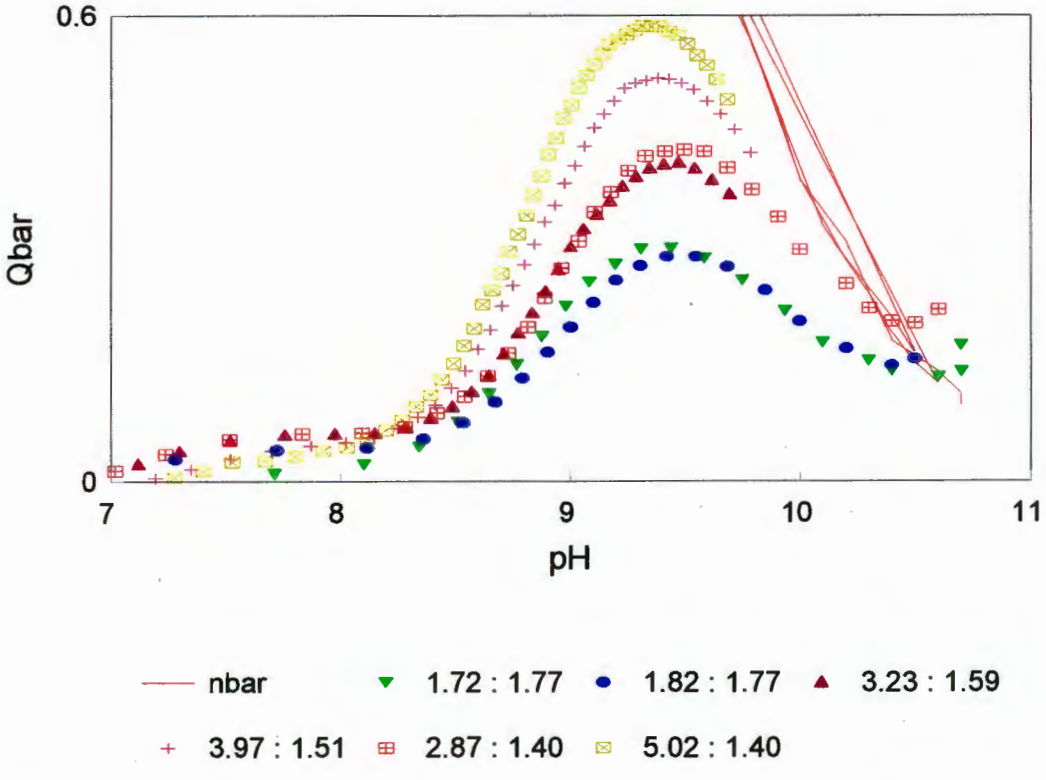

Figure 4.34: Experimental and calculated deprotonation curves for the Ca(II)ttda system. The symbols represent titrations with different concentrations (mM) and [ttda]:[Ca] ratios.

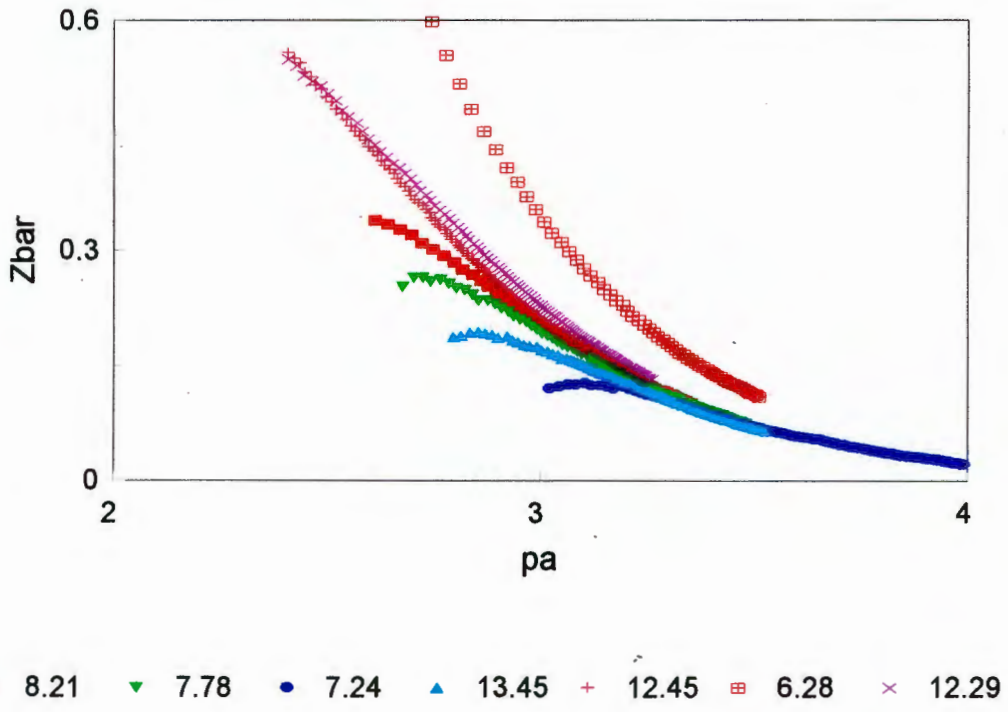

Figure 4.35: Experimental and calculated formation curves for the Mg(II)ttda system. The symbols represent titrations with different concentrations (mM) and [ttda]:[Mg] ratios.

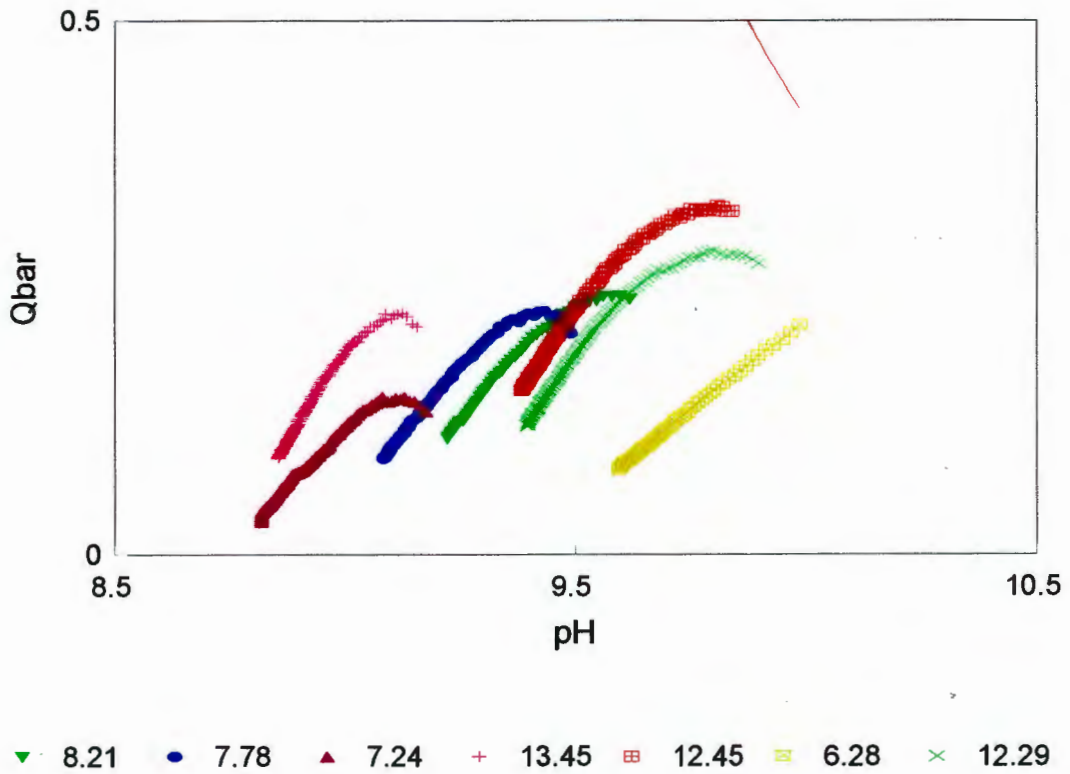

Figure 4.36: Experimental and calculated deprotonation curves for the Mg(II)ttda system. The symbols represent titrations with different concentrations (mM) and [ttda]:[Mg] ratios.

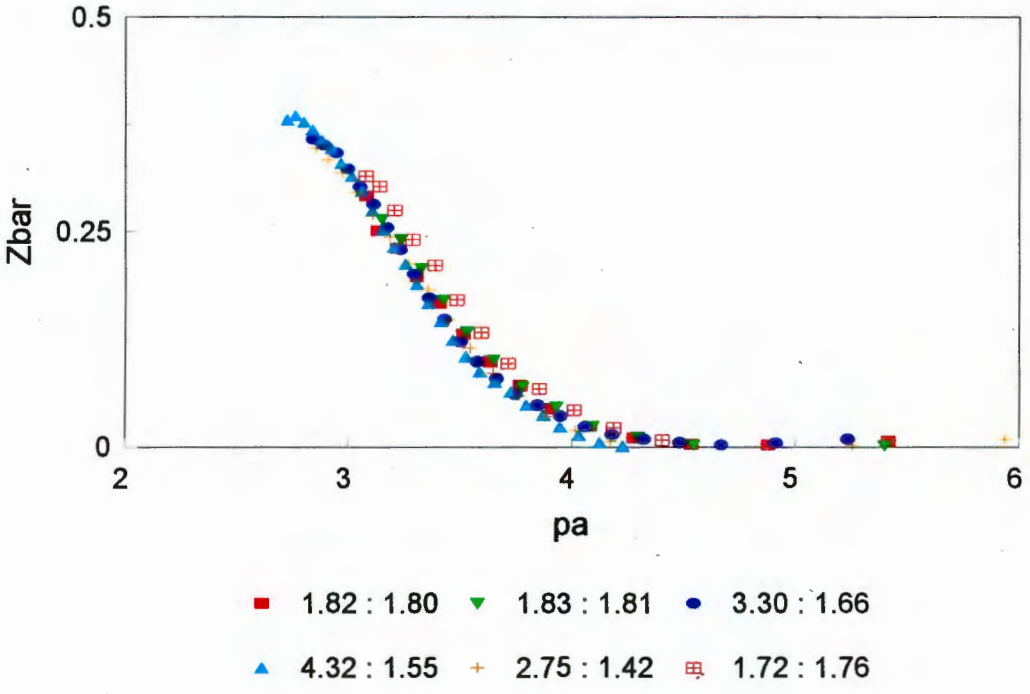

Figure 4.37: Experimental and calculated formation curves for the Ca(II)dtda system. The symbols represent titrations with different concentrations (mM) and [ttda]:[Ca] ratios.

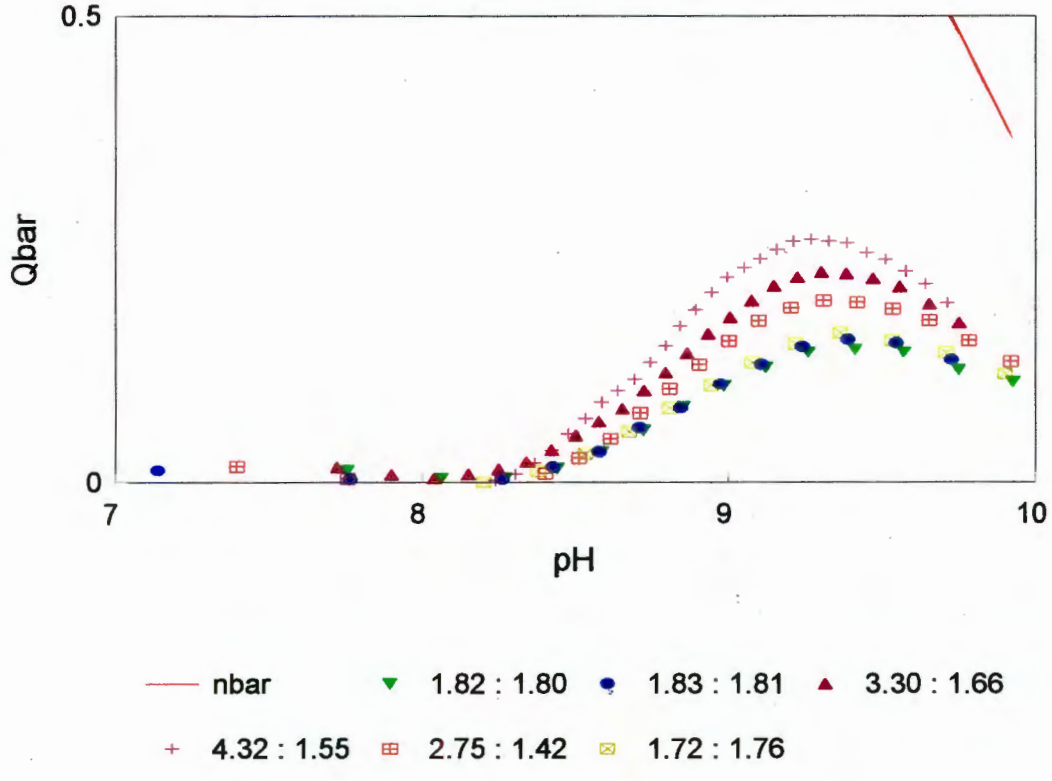

Figure 4.38: Experimental and calculated deprotonation curves for the Ca(II)dtda system. The symbols represent titrations with different concentrations (mM) and [ttda]:[Ca] ratios.

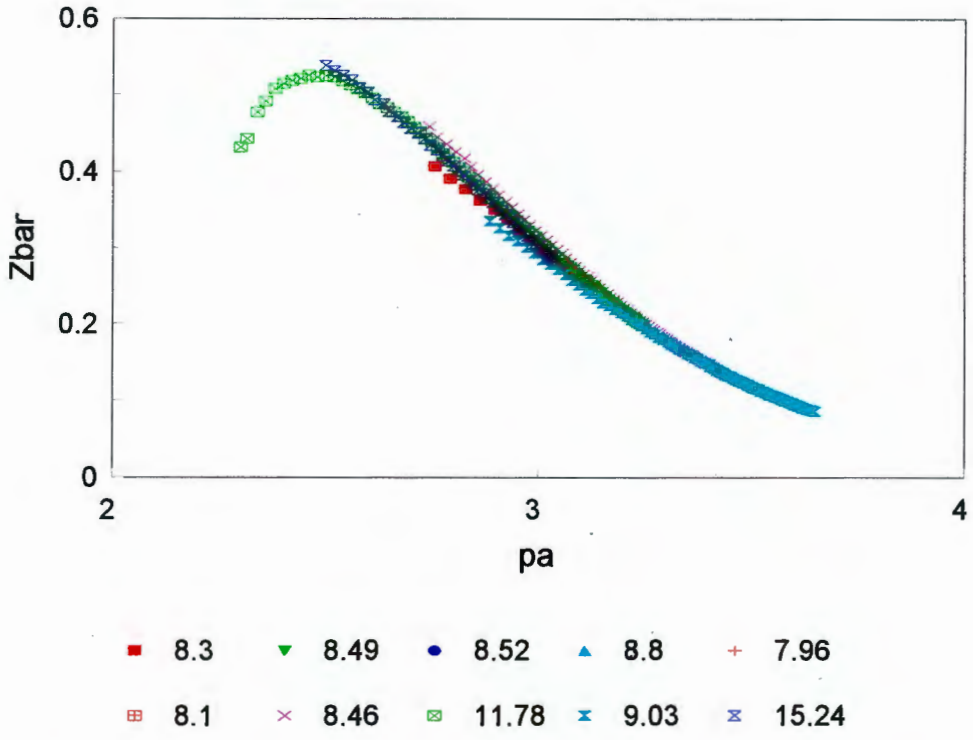

Figure 4.39: Experimental and calculated formation curves for the Mg(II)dtda system. The symbols represent titrations with different dtda concentrations. [Mg] = 0 - 32 (mM).

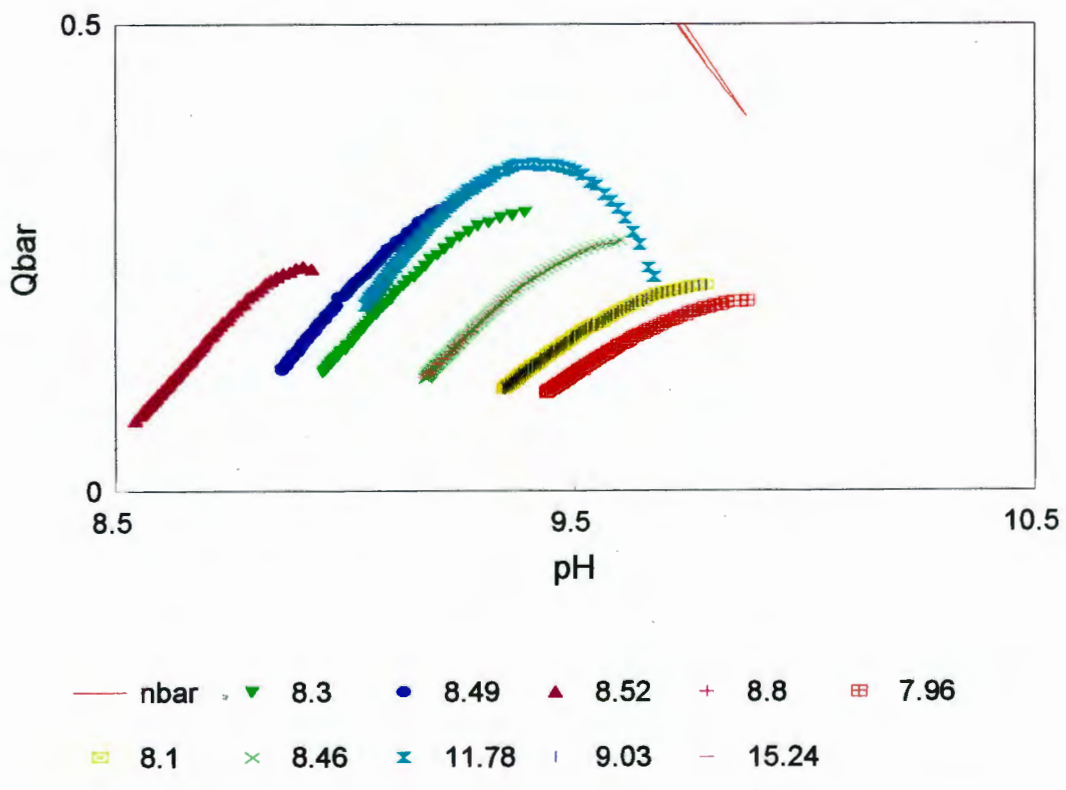

Figure 4.40: Experimental and calculated deprotonation curves for the Mg(II)dtda system. The symbols represent titrations with different dtda concentrations. [Mg] = 0 - 32 (mM).

The species distribution curves for these systems are given in Figures 4.41 and 4.42 for calcium and in Figures 4.43 and 4.44 for magnesium (see appendix II).

4.5 Discussion

The order of stability of the first row transition metal complexes of both ttda and dtda follows the Irving-Williams series (Irving and Williams, 1948;1953). This order is demonstrated graphically in Figure 4.45, where β_{110} is plotted against the metal.

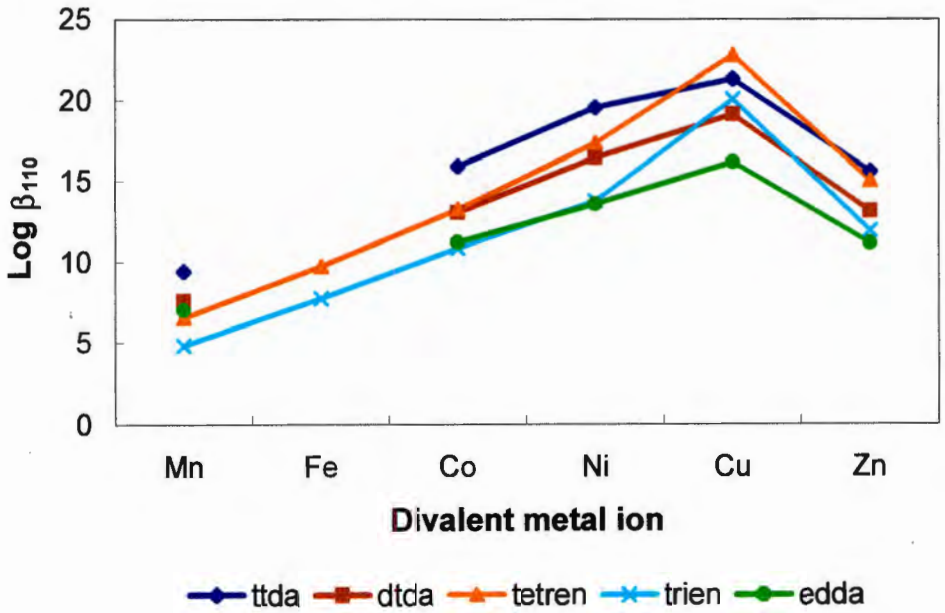

Figure 4.45: Increase in β_{110} for complexes of ttda, dtda, edda, trien and tetren with atomic number of divalent first row transition metal ions.

In all cases, the β_{110} stability constants measured for the ttda complexes are larger than those determined for dtda. This is due to the increased stability afforded by the formation of 5 chelate rings for ttda in comparison to the 4 formed by dtda and can be explained due to an increase in entropy.

The direct comparison of tetren, a five donor site ligand with only nitrogen donor atoms, with dtda, which also has five donor atoms, three nitrogen and 2 oxygen, shows a high relative stability for dtda for the Mn^{+2} complex, while from Co^{+2} onwards the tetren complexes are increasingly more stable. This can be accounted for in terms of the hard and soft acid and bases concept, as the divalent metal ions become increasingly 'soft' from manganese to copper. The same trend is seen of the four donor analogues, trien and edda.

The final point of note is that for trien and tetren there is a large relative increase in the stabilities of the copper complexes compared to those of the complexes with the other metals. This increase is not seen with either ttda or dtda. This is probably due to the coordination of the carboxylate arms, which would reduce the effect of Jahn-Teller stabilisation.

4.6 Experimental

The experimental procedures used are similar to those used by other workers in this field. In essence, solutions containing differing metal and ligand concentrations and ratios were titrated potentiometrically with strong acid or base. The ionic strength of the solutions was kept as constant as possible by the addition of an inert background electrolyte (0.15M NaCl). The resulting data, (ml, mV), was then analysed using the ESTA suite of programmes (Murray and May, 1984) to obtain the "best " set of stability constants. The resulting model, or models , were used to generate theoretical formation curves which could be compared with the experimental curves. The extent of the agreement between the experimental and theoretical curves, together with the optimisation statistics were used to assess the validity of the proposed model. Protonation constants were obtained by excluding the metal ions from the titrand solution.

The chemicals used are given in Table 4.6. These were used without further purification, except where indicated.

Table 4.6: Chemicals used in the potentiometric work

Chemical	Source	Purity	Purification Method
Zinc metal	Merck	G.R.	
edta	NT Lab Supplies	AR	
Potassium hydrogen phthalate	Merck	GR	Recrystallised
NaCl	Saarchem Ltd	AR	
HCl	Merck	Titrisol ampule	
$MgCl_2.6H_2O$	Merck	GR	
$CaCl_2.4H_2O$	Merck	GR	
$MnCl_2.4H_2O$	Merck	GR	
$CoCl_2.6H_2O$	Merck	GR	
$NiCl_2.6H_2O$	Merck	GR	
$CuCl_2.2H_2O$	Merck	GR	
$ZnCl_2$	Merck	GR	
NaOH	Merck	Titrisol ampule	

Chemical	Source	Purity	Purification Method
trien	Merck	Technical, 70%	Distillation under vacuum, followed by fractional crystallisation of the hydrochloride. Recrystallised from dilute ethanol (Sacconi, Paolletti, and Ciampolini, 1961)

Standard zinc solutions were prepared in a calibrated volumetric flask by dissolving zinc metal in concentrated hydrochloric acid and diluting the solution to volume. Temperature corrections were made when calculating the resulting concentration(CRC Handbook of Chemistry and Physics, 1983).

Edta solutions of the required concentrations were prepared and standardised against the appropriate zinc standard solution (Vogel, page 317.).

Metal chloride solutions were prepared as required. Sufficient sodium chloride was added to give a final ionic strength of 0.15M. The solutions were standardised against edta (Vogel, 324-325).

Sodium hydroxide solutions (0.1M) were prepared under a nitrogen atmosphere from Merck titrisol standard ampules. Sodium chloride was added to give a final ionic strength of 0.15M. The solutions were standardised against Potassium hydrogen phthalate using the method of Gran (Gran, 1952).

Hydrochloric acid solutions (0.1M and 0.01M) for titration and electrode calibration were prepared from titrisol ampules and dilution of the bulk solution, respectively. Both solutions were adjusted for ionic strength with sodium chloride and were standardised against sodium hydroxide and borax (Vogel, 320).

With the exception of the 0.01M HCl solution, which was used only for electrode storage and calibration, all solutions were maintained under an atmosphere of purified nitrogen. All the solutions were prepared using double glass distilled deionised water which had been freshly boiled out to remove carbon dioxide and cooled in a container protected by a "Carbosorb" (BDH) filter.

The Titrations were carried out in a double walled titration vessel (Metrohm, cat. No. 6.1405.0001) thermostated at 25.0 ±0.1°C, under an inert atmosphere of nitrogen. The high purity nitrogen was first passed through 4 thermostated wash bottles containing 50% KOH solution, 15 g pyrogallol in 100 ml 30% KOH solution, distilled water and 0.15M sodium chloride, respectively. A gas bubbler was attached to the gas outlet from the titration vessel to prevent back diffusion.

The reaction between each of the ligands and the divalent metal ions of calcium, cobalt, nickel copper and zinc was studied using the following experimental procedure. Sufficient ligand to give an initial concentration between 1.5 and 3.4 mM was weighed out into the titration vessel. An appropriate mass of sodium chloride was added to give an initial ionic strength of 0.15M in 20 ml. The vessel was then attached to the titration apparatus and flushed well with nitrogen. The ligand and salt were then dissolved in 20 ml degassed, distilled water. Concentrations are expressed using the molar scale, ignoring molar partial volumes which are negligible. The pH of the solutions was immediately adjusted to approximately 11 by the addition of sodium hydroxide. The need for this precaution is explained in section 3.2. If metal ions were to be included in the titration, 20 ml of the metal solution was added as well. The solution temperature was stabilised at 25 °C, and then titrated with 0.1M hydrochloric acid. All solutions were introduced via piston burettes (Metrohm, cat no. 6.1521.220), read to a precision of 0.01 ml. All titrations were performed in duplicate. The solution was stirred magnetically.

Analysis of the data obtained with the above method showed that the copper interaction with the ligands was very powerful, with, in the case of ttda, the complex being 50% formed even at pH 2. For this reason the reaction was also studied using a competitive ligand, after the method of Martell et al (Harris and Martell, 1976). Trien was chosen as the competing ligand as its complexation equilibria with copper are well documented in the literature, and it is unlikely to form ternary complexes with ttda or dtda.

The above procedure was followed, with solid trien HCl being weighed into the titration vessel. Sodium chloride was again added to achieve an ionic strength of 0.15M in 20 ml of solution. The protonation and copper formation constants were determined in separate experiments using the same procedure.

When the divalent manganese solution was added to the alkaline ligand solution a brown precipitate, presumably manganese hydroxide, formed, and the titration procedure was modified to avoid this. The pH of the solution was raised to approximately 4, instead of 11, and then titrated with base until a precipitate was observed.

As the binding between the ligands and magnesium was very weak, it was not possible to obtain usable data for these systems, even using high concentrations of the ligand and metal. An upper limit for the possible reactant concentration is imposed by the requirement for constant ionic strength. If the reactant concentrations are too high, their contribution to the total ionic strength of the solution cannot be considered as negligible. In order to overcome this, the reaction solution was adjusted to a pH of approximately 4, and titrated with base to a preselected pH, somewhere between 8.5 and 10.5. The solution was then titrated with a 0.5M solution of Magnesium chloride. Using a large number of titrations it was possible to cover a sufficiently large pH range, and obtain high ligand to metal concentration ratios (Linder, Torrington, and Seeman, 1983).

In all experiments the reaction was followed using a glass electrode sensitive to hydrogen ion (Metrohm, cat.no. 6.0102.000) coupled to a calomel reference electrode (Metrohm, cat.no. 6.0702.000) with a renewable liquid junction. The emf readings were taken on a Radiometer PHM 84 digital pH meter, which was read to a precision of 0.1mV. The titrations were microprocessor controlled using software developed in these laboratories.

The ionisation constant for water, pK_w, was determined from strong acid-strong base titrations, using the computer programme MAGEC (Williams, May, Linder and Torrington, 1982). A value of -13.76 was obtained and used throughout. Table 4.7 gives literature values determined under similar conditions.

Table 4.7: Literature pK_w values, determined at 25.0°C

pK_w	Ionic strength	Electrolyte	Reference
13.74	0.4	NaCl	Dynssen and Hansoon, 1972
13.75	0.14	KNO_3	Jameson and Wilson, 1972
13.72	0.1	NaCl	Teder, 1972
13.67	0.1	NaCl	Whitfield, 1972

The electrode was calibrated using the protonation data after the method of Williams *et al* (Williams, May, Linder and Torrington, 1982). A strong acid reading in 0.01M HCl was correlated to the E° value obtained. A strong acid reading was taken before and after each titration and the mean of these readings used to calibrate the electrode for the metal titrations.

The data were analysed on a Sperry 1100 computer.

References

Beck, M.T. (1970). *Chemistry of Complex Equilibria*, Van Nostrand Reinhold Co., London.

Burgess, J. (1974). *Metal Ions in Solution*, Ellis Horwood, New York.

Chang, C.A. and Douglas, B.E., (1981). *J. Coord.. Chem.*, **11**, 91.

CRC Handbook of Chemistry and Physics, (1983) Weast,R.G. ed. 63rd edition, CRC press, Florida.

Dynssen, D. and Hansoon, I. (1972). *Marine Chem.*, **1**, 137.

Fazakerley, G.V., Jackson, G.E. and Linder, P.W. (1976). *J. Inorg. Nucl. Chem.*, **38**, 1397.

Gran, G. (1952). *Analyst*, **77** 661.

Harris, W.R. and Martell, A.E. (1976). *Inorg. Chem.*, **15(3)**, 713.

Irvine, H. and Williams, J.P.R. (1948). *Nature*, **162**, 746.

Irvine, H. and Williams, J.P.R. (1953) *J. Chem. Soc.*, 3192.

Jameson, R.F. and Wilson, M.R. (1972). *JCS Dalton*, 2607.

Linder, P.W. Torrington, R.G. and Seeman, U.A. (1983). *Talanta*, **30(4)**, 295.

Martell, A.E., and Motekaitis, R.J. (1988). *The Determination and use of Stability Constants*, VCH Publishers Inc., New York.

Martell, A.E. and Smith, R.E. (1976). *'Critical Stability Constants'*, Vol. 4, Plenum, New York.

Murray, K. and May, P.M. (1984). Univ. Of Wales Institute of Science and Technology, .

Rossotti, F., and Rossotti, H. (1961). *The Determination of Stability Constants*, McGraw-Hill, London.

Sacconi, L., Paolletti, P. and Ciampolini, M. (1961). *J. Chem. Soc*, 5115.

Smith, G.S. and Hoard, J.L. (1959).*J. Am. Chem. Soc.*, **81**, 556.

Smith, R.M., Motekaitis, R.J. and Martell, A.E. (1985). *Inorg. Chem.*, **24**, 1132.

Teder, A. (1972). *Svensk Papperstidning*, **75**, 704.

Vacca, A. Sabatini, A. and Gristina, M. (1972). *Coord. Chem. Rev.*, **8**, 45.

Vogel's Textbook of Quantitative Inorganic Analysis, 4th edition, Longman, page 324-325.

Vogel's Textbook of Quantitative Inorganic Analysis, 4th edition, Longman, page 320.

Vogel's Textbook of Quantitative Inorganic Analysis, 4th edition, Longman, page 317.

Whitfield, M. (1972). *J. Chem. and Eng. Data*, **17**, 124.

Williams D.R. (1973). *J.C.S. Dalton*, 1064.

Williams, D.R., May, P.M., Linder, P.W. and Torrington, R.G. (1982). *Talanta*, **29**, 249.

CHAPTER 5

Ancillary Studies

5.1 Introduction

The use of ECCLES, the computer blood model, to design ligands which would selectively mobilise copper in plasma, and the determination of the formation constants of the target ligands with some of the important metal ions present in blood, suggested that the two ligands, ttda and dtda, had the potential to be effective anti-inflammatory agents when combined with copper. The simulation results indicated that the complexes survived the coordinating medium of plasma. This, we believe, is a necessary condition for activity, but is not a sufficient condition. There are other properties of the complexes which are also important for biological activity. These properties include the lipophilicity, biodistribution, pharmokinetics, and superoxide dismutase activity. The ultimate test, however, is animal screens of anti-inflammatory activity

The solution structure of the complexes will have an effect on their behaviour in biofluids. The rapid transport of the complex through cell membranes will be determined by its lipophilicity. The ligands considered were all di-anionic, to neutralise the charge on the divalent copper ion. The degree of bonding of the carboxylic residues is therefore of interest. A situation where the carboxylates are loosely associated will give rise to a larger hydration sphere, and this will reduce the lipophilic nature of the complex.

Several theories exist as to the mode of action of the copper in reducing the inflammation associated with rheumatoid arthritis. Some investigation into the performance of the copper complex in models used to assess the biological potential of the anti-inflammatory agents was of interest in this work. These investigations included an assay of superoxide dismutase (SOD) like activity and animals screens using the adjuvant arthritis model in rats.

5.2 UV/VISIBLE Spectroscopy

5.2.1 Introduction

Studies of the electronic spectra of complexes often allow structural aspects of the complexes to be determined (Nicholls, 1974). Of particular interest in this study are the ligand field spectra, which arise from transitions between non-degenerate metal d-orbitals caused by the low symmetry of the complexes. The octahedral complexes formed by copper (II) ions are generally tetragonally distorted. The degree of distortion is determined by the strength of the bonding and the structure of the complex. In a multi component system, by changing the conditions of the solution, it is possible to change the equilibrium concentration of the individual species. This provides a tool to examine changes in the structure of the predominant complex, as the UV spectrum will change as the relative concentrations of the species present change.

5.2.2 Theory

In complexes of first row transition metal ions the degeneracy of the metal d orbitals is lost as a result of the presence of the ligands. The influence of the ligands on the metal orbitals varies due to the symmetry of the complex, and separates the d orbitals into a set of two e_g orbitals and a set of three t_{2g} orbitals. As the t_{2g} orbitals have their lobes pointing between the axes, and the e_g orbitals point along the axes, in octahedral complexes the e_g orbitals are at higher energy than the t_{2g} orbitals.

When more than one valence electron is present, coupling occurs between the quantum numbers for the individual electrons. For elements up to an atomic number of 30 the Russell-Saunders coupling scheme applies, and in this scheme it is assumed that spin-spin coupling > orbit-orbit coupling > spin-orbit coupling. In spin-orbit coupling the spin and orbital angular momenta on the same electron are concerned.

The information concerning the resultant energy levels is conveyed by means of the Term Symbol

$$\text{Term symbol} = {}^{(2S+1)}L_J$$

S is the spin-spin coupling quantum number
L is the orbit-orbit coupling quantum number
J is the spin-orbit coupling quantum number
$(2S + 1)$ is the multiplicity of the system

For each of the d^1 to d^9 ions the allowed terms can be derived. In the case of the copper (II) ion, there is only a ^2D term.

Under the quantum-mechanical selection rules for light absorption, given below, d-d transitions are forbidden.

1 Spin forbidden: transitions in which there is a change in the number of unpaired electrons are forbidden.

2 Orbitally forbidden (Laporte rule): Transitions involving the redistribution of electrons in a single quantum shell are forbidden. Transitions of the type g→g and u→u are partially forbidden.

The spin forbidden rule is relaxed by spin-orbit coupling, but the absorptions are weak.

If complexes have a centre of symmetry, the Laporte rule can be relaxed by a vibronic mechanism. For complexes that already lack a centre of symmetry, mixing of p and d orbitals allows transitions between orbitals of varying amounts of p character.

In complexes the free ion terms give rise to crystal-field terms. For the d^9 ions these terms are E_g and T_{2g} terms, with the E_g term being the ground state. Thus for octahedral copper (II) complexes a single $^2E_g \rightarrow {}^2T_{2g}$ transition is expected. Jahn-Teller distortion generally leads to broadening of the spectra.

For electronic absorption spectra of solutions containing more than one absorbing species the Beer-Lambert law can be expanded to give a linear combination of terms for each individual species, Equation 5.2.1

$$A^{\lambda} = l(\epsilon_1{}^{\lambda} c_1 + \epsilon_2{}^{\lambda} c_2 + ... + \epsilon_i{}^{\lambda} c_i) = l \sum \epsilon_i{}^{\lambda} c_i \qquad (5.2.1)$$

where

A^{λ} = Absorption at wavelength λ

ϵ_i = molar adsorption coefficient at wavelength λ of the *i* th species ($dm^3mol^{-1}cm^{-1}$)

c_i = concentration at wavelength λ of the *i* th species ($mol\ dm^{-3}$)

l = path length (cm)

5.2.3 Results and discussion

To examine the solution structure of the copper-ttda complex, the UV/visible spectrum of the complex was recorded as a function of pH. The variation in $\varepsilon_{max.}$ with pH is given in Figure 5.2.1. Over the entire pH range there is no change in λ_{max} (624 nm).

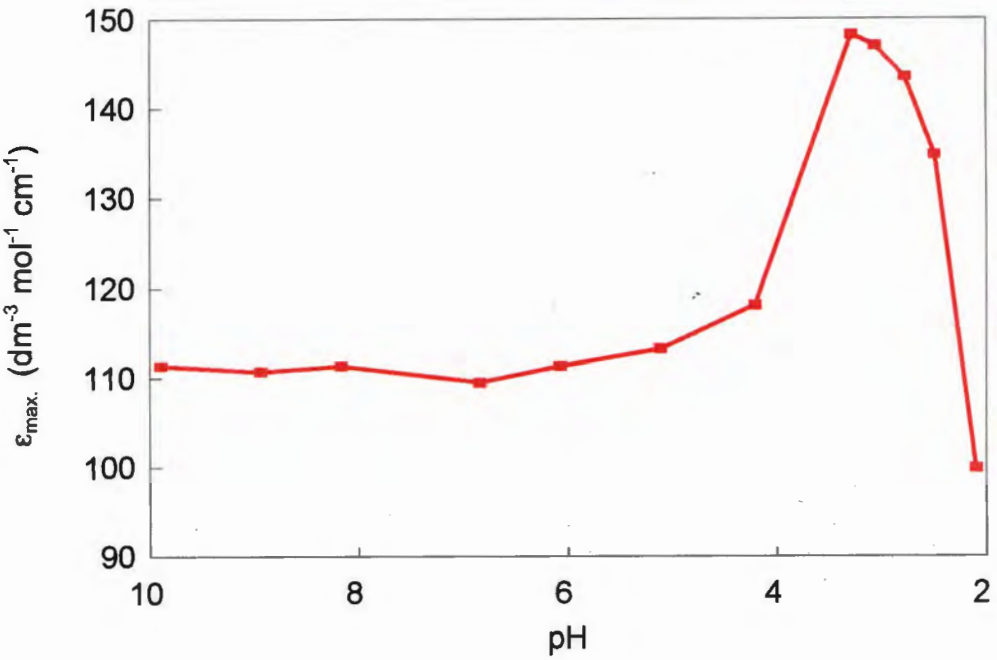

Figure 5.2.1: Variation in $\varepsilon_{max.}$ with pH for the Cu-ttda system. [Cu] = [ttda] = 1.6 mmol dm^{-3}

For regular octahedral copper(II) complexes the separation of the T_{2g}-E_g orbitals is about 770 nm for CuO_6 and about 550 nm for CuN_6 (Lever, 1985). With tetragonal distortion , as the axial bond lengthens the in-plane ligands move in and the absorption band shifts to shorter wavelength, for example for $[Cu(trien)(H_2O)_2]^{2+}$, $\lambda_{max.}$ = 575 nm (Hedwig, Love and Powell, 1970). Constraint of the axial bond by being part of a chelate ligand results in a shift to longer wavelength. In the case of [Cu(ttda)], a $\lambda_{max.}$ of 624 nm is consistent with equatorial co-ordination of the four amine groups and axial co-ordination of the two carboxylate groups.

Above pH 4, where according to the potentiometric results only the ML species is present, see Figure 4.5, there is no change in the electronic spectrum as the pH increases. Below

pH 4, however, $\varepsilon_{max.}$ increases and then decreases as the entire complex dissociates. The increase in $\varepsilon_{max.}$ corresponds to the formation of the M(HL) species, which distorts the structure from regular octahedral and the selection rules are relaxed. This same variation in ε_{max} is shown by $[Cu(NH_3)_n(H_2O)_{6-n}]^{2+}$ as n is varied. There is no change in $\lambda_{max.}$. For $[Cu(trien)]^{2+}$ $\lambda_{max.}$ shifts from 575 to 610 nm upon protonation of a co-ordinated amino group (Sacconi, Paoletti, and Ciampolini, 1961). The change in $\varepsilon_{max.}$ and the lack of change in $\lambda_{max.}$ can be explained by protonation occurring at one of the carboxylate sites. Release of one axially coordinated carboxylate groups from the metal ion increases the tetragonal distortion of the complex resulting in an increase in the absorption coefficient. For the ML species ε_{max} = 110 while for the M(HL) complex ε_{max} = 176 $cm^3mol^{-1}cm^{-1}$.

5.2.4 Experimental

The solutions used in this section were similar to those used in the potentiometric determinations of the formation constants.

The test solution was prepared by dissolving 0.0635 grams of ttda and 0.3822 grams of NaCl in a 50 ml volumetric flask. To this was added 5 ml of a 0.01588 M copper chloride solution. Sufficient NaOH was added to the solution to give a pH of approximately 10 once the solution had been made up to the mark. These quantities gave final concentrations of 0.001588 M with respect to copper, 0.0032 M with respect to ttda. The ionic strength was 0.15 M with respect to NaCl.

The spectra were recorded on a Philips PU 8700 spectrophotometer. A 0.001588 M copper chloride solution made up in 0.15 M NaCl was used as the blank.

5.3 Super Oxide Dismutase (SOD) like activity

5.3.1 Introduction

As outlined in Chapter 1, there is evidence which suggests that superoxide and other free radicles released into the synovial cavity are linked to the inflammatory process and tissue degradation. Suppression of radical production and/or rapid destruction of free radicals is therefore important in tissue protection. Superoxide dismutases, which are metalloproteins containing copper-zinc, manganese or iron, occur naturally in synovial fluid. These proteins are responsible for the destruction of superoxide *in vivo*. It has been suggested that the anti-inflammatory activity of copper complexes is related to their ability to destroy superoxide. For this reason the superoxide dismutase activity of the copper complex of ttda was tested using the method of Roberts and Robertson (Roberts and Robinson, 1985).

5.3.2 Theory

In the Roberts and Robinson procedure, superoxide radicals are produced by the reaction of hypoxanthine with xanthine oxidase, and detected by the reduction of nitrobluetetrazolium (NBT) to a blue formazan. Superoxide like activity is detected by the inhibition of the NBT reduction. Edta, is used as a competing ligand, to approximate the presence of albumen in blood. It's copper complex has no SOD-like activity (Lengfelder and Weser, 1981). The SOD activity of a complex is quoted as the concentration or the complex, with respect to copper, which will inhibit NBT reduction by 50% (I_{50}).

The activity of the complexes determined in this test falls into one of three categories. Those complexes with SOD like activity which are stable in the presence of edta, those which are active but are less stable than the edta complex, and those which do not inhibit NBT reduction.

Inhibition of NBT reduction is calculated from the optical densities at 550 nm as follows.

$$Inhibition = 1 - \frac{test - testblank}{100\%control - controlblank}$$

Where

Test = The assay with the test ligand

Test blank = Assay with the test ligand but without xanthine oxidase

100% control = Assay excluding both copper and test ligand in the presence of xanthine oxidase.

Control blank: = Assay excluding both copper and test ligand in the absence of xanthine oxidase

5.3.3 Results

Several assays were carried out in parallel. $Cu(gly)_2$ was used to check the weak chelator response; the control and blank assays; and the test ligand.

The results of the assay for the ttda copper complex are displayed graphically in Figure 5.3.1. The results indicate that there is no significant catalyses of the dismutation of the superoxide radical by this complex. A single point assay was repeated for the copper complexes of dtda and ttda and these are also given in Figure 5.3.1. In both cases the per cent inhibition was only 4%.

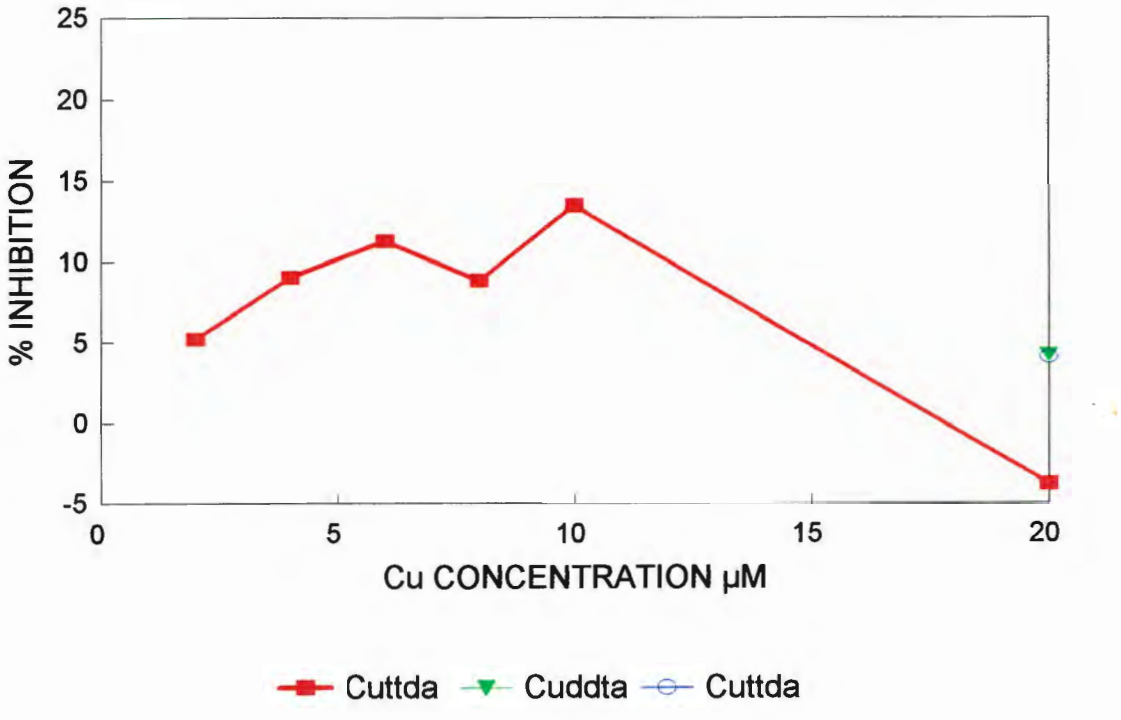

Figure 5.3.1: SOD activity of Cu(ttda), as a function of copper concentration, and a single point assay for the Cu(dtda) complex.

From these results it is apparent that these complexes do not catalyse the dismutation of the superoxide radical.

An assay run with glycine gave an I_{50} of approximately 20μM, which is similar to the results reported by Roberts *et al* (Roberts and Robinson, 1985).

5.3.4 Experimental

Bulk solutions of copper glycinate (9,74 x 10^{-3}M Cu^{+2}, 2,09 x 10^{-2} M glycine), ttda (5,1 x 10^{-3}M) and edta (1,2 x 10^{-3}M) were made up in 100mM Hepes buffer. Bulk solutions of hypoxanthin and NBT were made up. Copper/glycine/ttda bulk test solutions were made up by combining 0,25 ml of the bulk copper/glycine solution and 1 ml of the bulk ttda solution and diluting to 25 ml with Hepes buffer (9.7 x 10^{-5} M Cu^{+2}). Aliquots of this solution were diluted with Hepes buffer to give the required copper-ttda complex concentration. To these solutions, the required amounts of hypoxanthine and NBT were added to provide a final concentration of 20μM hypoxanthine and 500μM NBT in 4 ml of assay solution. The test solutions were incubated at 20°C in the dark, and the reduced NBT was measured at 550 nm using a UV spectrophotometer.

5.4 N.M.R..

5.4.1 Introduction

N.m.r. is an important tool in the investigation of chemical structures and reaction mechanisms and has been extended to whole body imaging in medical diagnosis. The use of this technique in chemistry was initially restricted to study of the proton, but developments in instrumentation and procedures have resulted in the routine study of nuclei with spin other than ½ and with low abundance.

In this work we have used n.m.r. to determine the sequence of protonation of ttda and dtda (Letkeman, 1979), and to investigate the solution structures of the calcium and zinc complexes (Hague and Moreton, 1987). In both protonation and complexation reactions the presence of the proton or metal shifts the n.m.r. signal arising from the protons attached to the neighbouring carbons. The nature of the bonding and the degree of complexation both influence the resulting signal. The chemical shifts of the ^{1}H and ^{13}C spectra were analysed by plotting the shift against the pD (or Ca concentration). Rapid changes in the chemical shift indicate complexation at the nitrogen closest to the proton concerned. From the data the value of the equilibrium constant can also be calculated.

5.4.1 Theory

The general theory of n.m.r. is well known and is dealt with in many standard texts (for example Akitt, 1983). As the main use of n.m.r. in this work was to study the change in chemical shift on complexation of the ligand with either protons or metal ions, the basic theory was applied. However, it is also possible to determine formation constants from n.m.r. data, and the theory for this is given below (Hague, and Moreton, 1987).

Assuming rapid exchange between the various species present in solution, the observed chemical shift for a particular atom is the average of the chemical shifts of that atom in the various species (δ_i), weighted according to their fractional populations (p_i):

$$\delta = \Sigma p_i \delta_i$$

Thus for ttda, which can exist in un-protonated up to hexa-protonated forms (L, HL, up to H_6L), the chemical shift is given by

$$\delta = p_L \delta_L + p_{HL} \delta_{HL} + p_{H2L} \delta_{H2L} + p_{H3L} \delta_{H3L} + p_{H4L} \delta_{H4L} + p_{H5L} \delta_{H5L} + p_{H6} \delta_{H6L}$$

The fractional populations are also related through the acid dissociation constants.

Addition of an appropriate concentration of a metal ion to the solution will result in a change in the chemical shift if complexation takes place. The chemical shift at a particular pH is given by

$$\delta' = \Sigma p_u \delta_u + \Sigma p_c \delta_c$$

where the first term on the right is a composite one containing all the contributions from the uncomplexed ligand and the second represents the contributions from the various complexes.

5.4.2 Results and discussion

5.4.2.1Protonation

The structures for ttda and dtda are given in Figure 5.4.1, to indicate the labelling of the proton and carbon sites used in the discussion below.

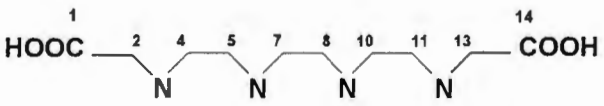

ttda

dtda

Figure 5.4.1: Structures of ttda and dtda giving the numbering of the carbon atoms.

The order of protonation of ttda and dtda were determined by measuring the ^{1}H and ^{13}C n.m.r. as a function of pD.

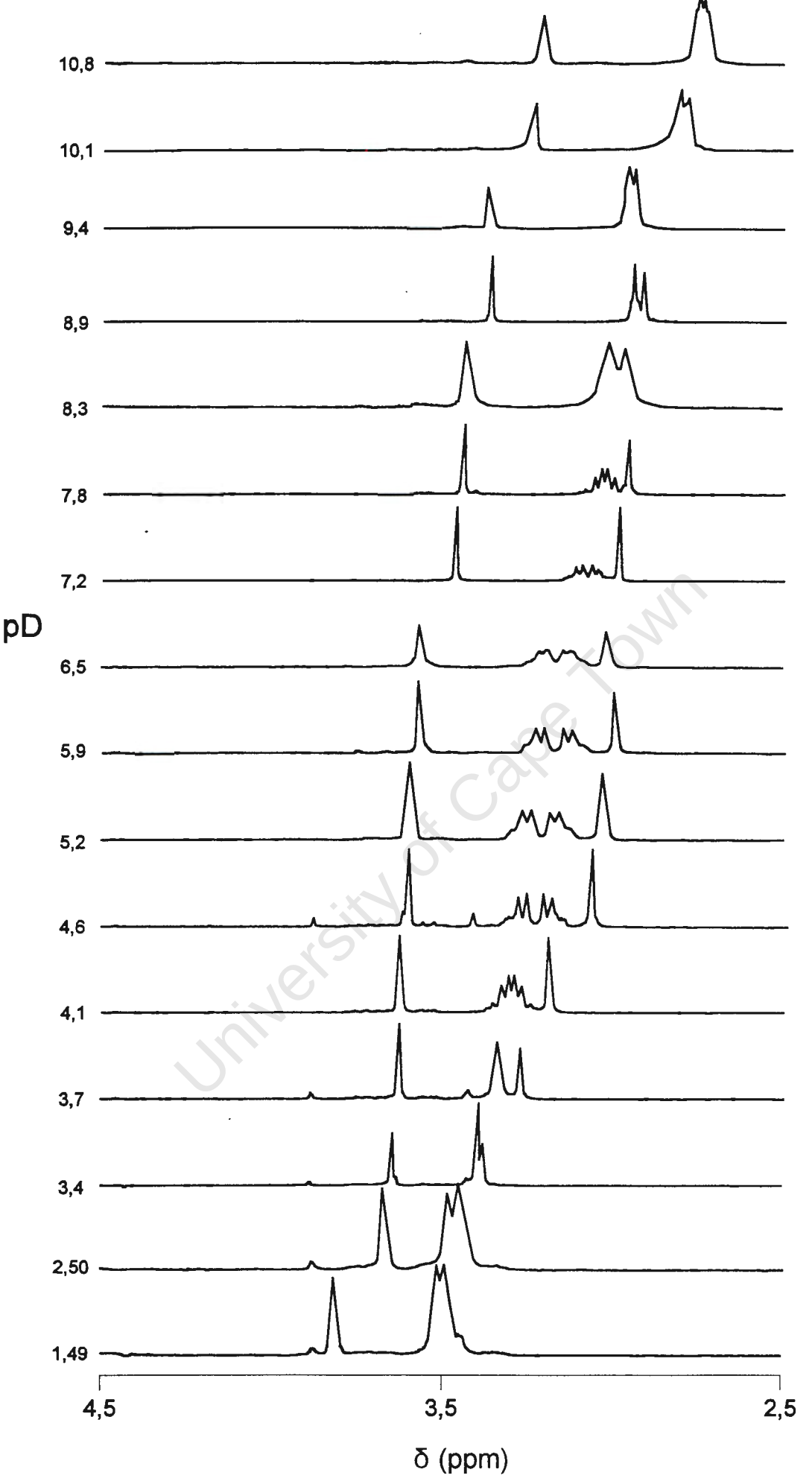

Figure 5.4.2: Proton n.m.r. spectra of ttda as a function of pD

The variation of the chemical shift of ttda with changing pD for ^1H is given in Figure 5.4.3, and for dtda in Figure 5.4.4.

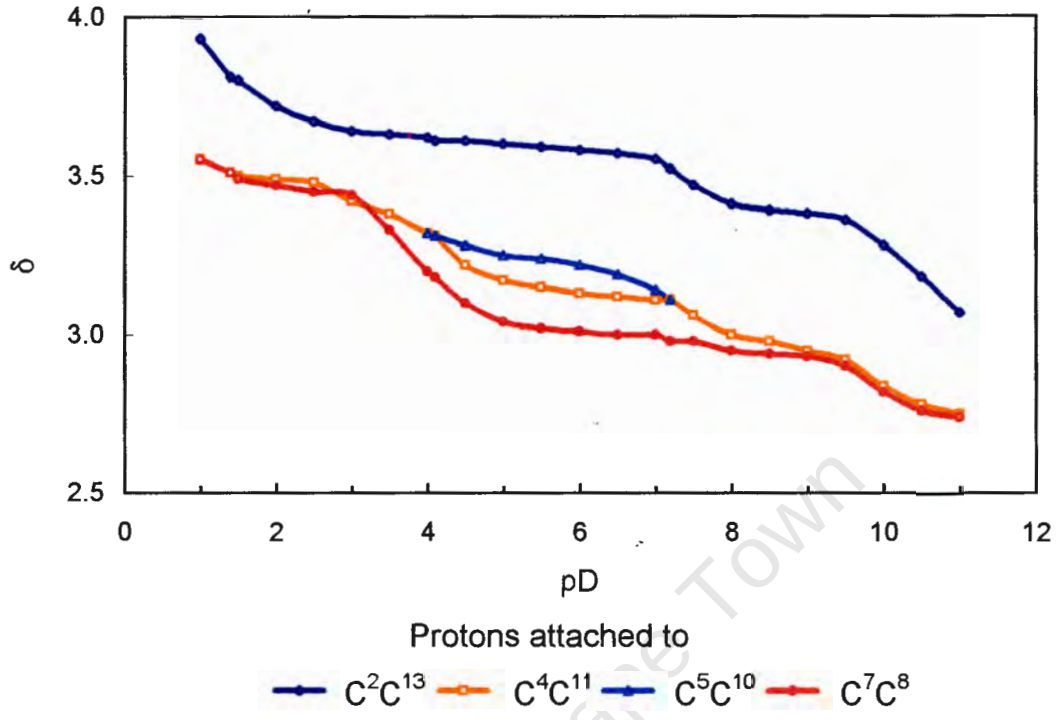

Figure 5.4.3: pD Dependence of the ^1H n.m.r. chemical shifts for ttda

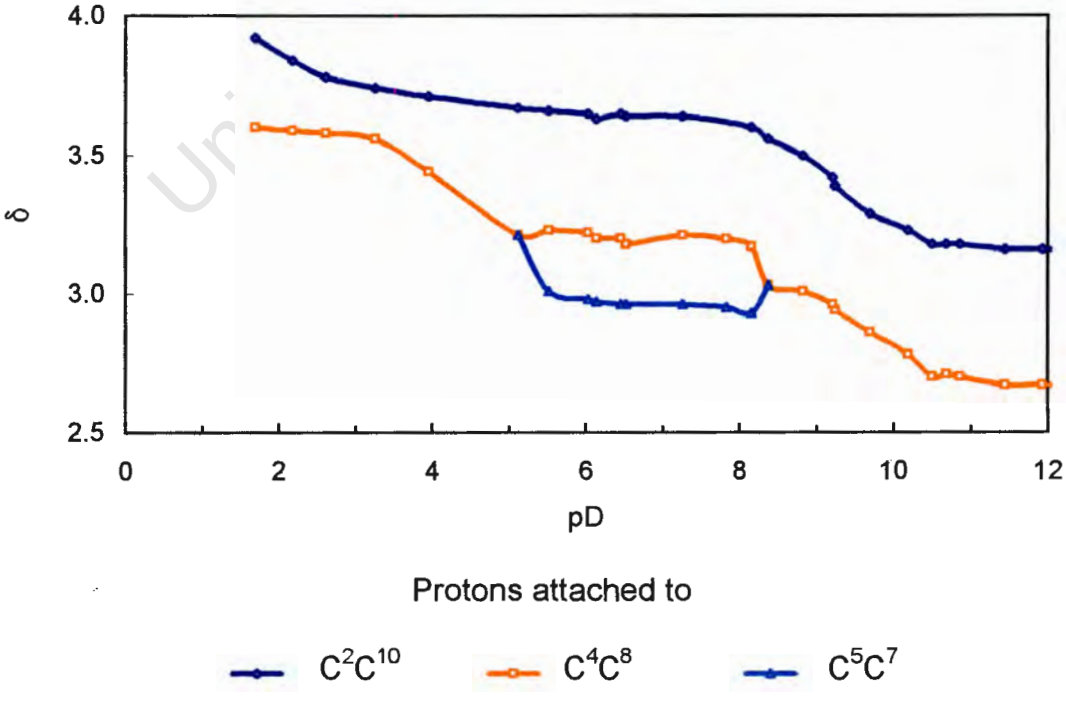

Figure 5.4.4: pD Dependence of the ^1H n.m.r. chemical shifts for dtda

With the addition of the first proton to ttda, all ^1H resonances are shifted to higher δ, that is they are all shielded, and hence protonation must be occurring to the same degree at all four nitrogen sites. The second step is clearly at $N^1(N^4)$ with the third proton $N^4(N^1)$. The signals for the protons attached to C^4,C^{11} and C^5, C^{10} exhibit a complex fine structure that is consistent with an A_2B_2 system, and the signal arising from the protons attached to carbon atoms C^2,C^{13} moves upfield to approximately the same extent. The signal arising from the protons attached to carbon atoms C^7,C^8 show no fine structure throughout the change in pD, and relative to the other protons, a small change in chemical shift. The addition of the fourth proton at pD 4 has the greatest influence on the C^7,C^8 protons, indicating the protonation is at the central nitrogens. The relatively rapid shift in the resonance of the C^2,C^{13} protons below pD 3 is consistent with addition at the acetate sites. This protonation scheme is given in Figure 5.4.5.

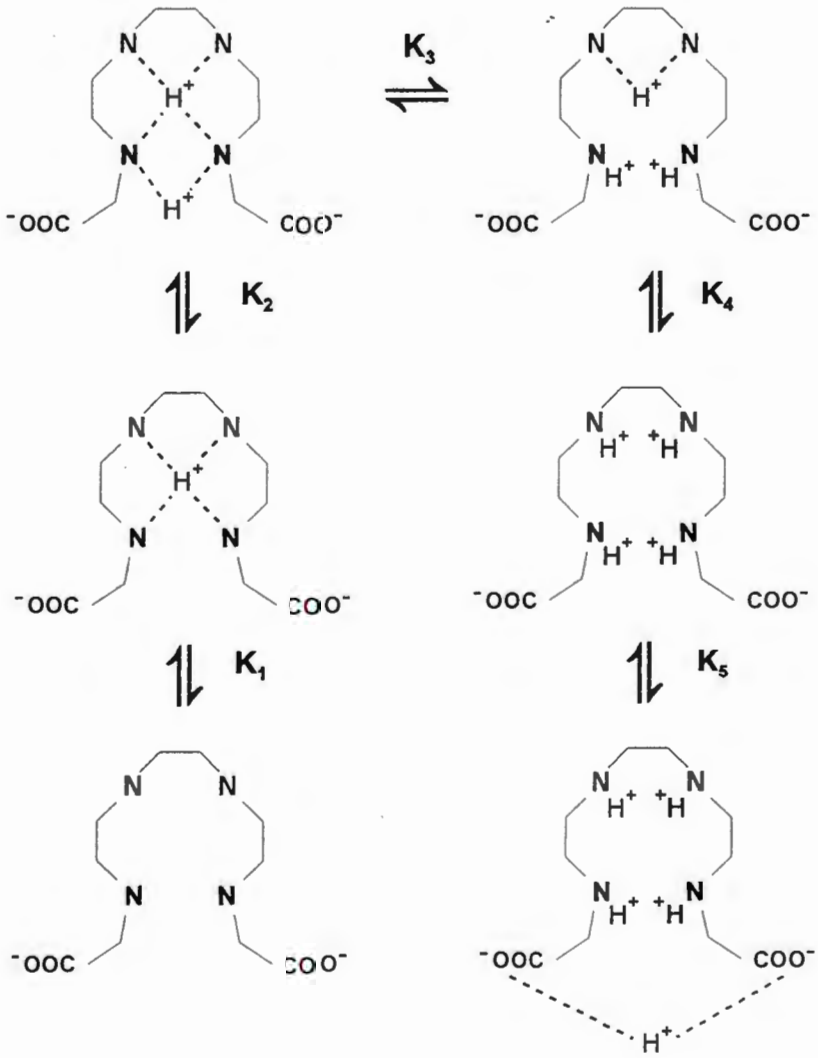

Figure 5.4.5: Protonation scheme for ttda.

By analogy, the protonation sequence for dtda is at all three nitrogen sites on addition of the first proton, at the terminal nitrogens for the second and at the central nitrogen for the third. Subsequent protonation occurs at the acetate residues.

Assignment of the ^{13}C spectra of ttda followed from the assignment of the ^{1}H n.m.r. spectra (Jackson and Kelly, 1989) via a two-dimensional heteronuclear correlation (HETCOR) experiment (Bax, 1983), Figure 5.4.6 This showed that the ^{13}C chemical shifts were not in the same order as the ^{1}H chemical shifts, C^{7} being shifted to lower field.

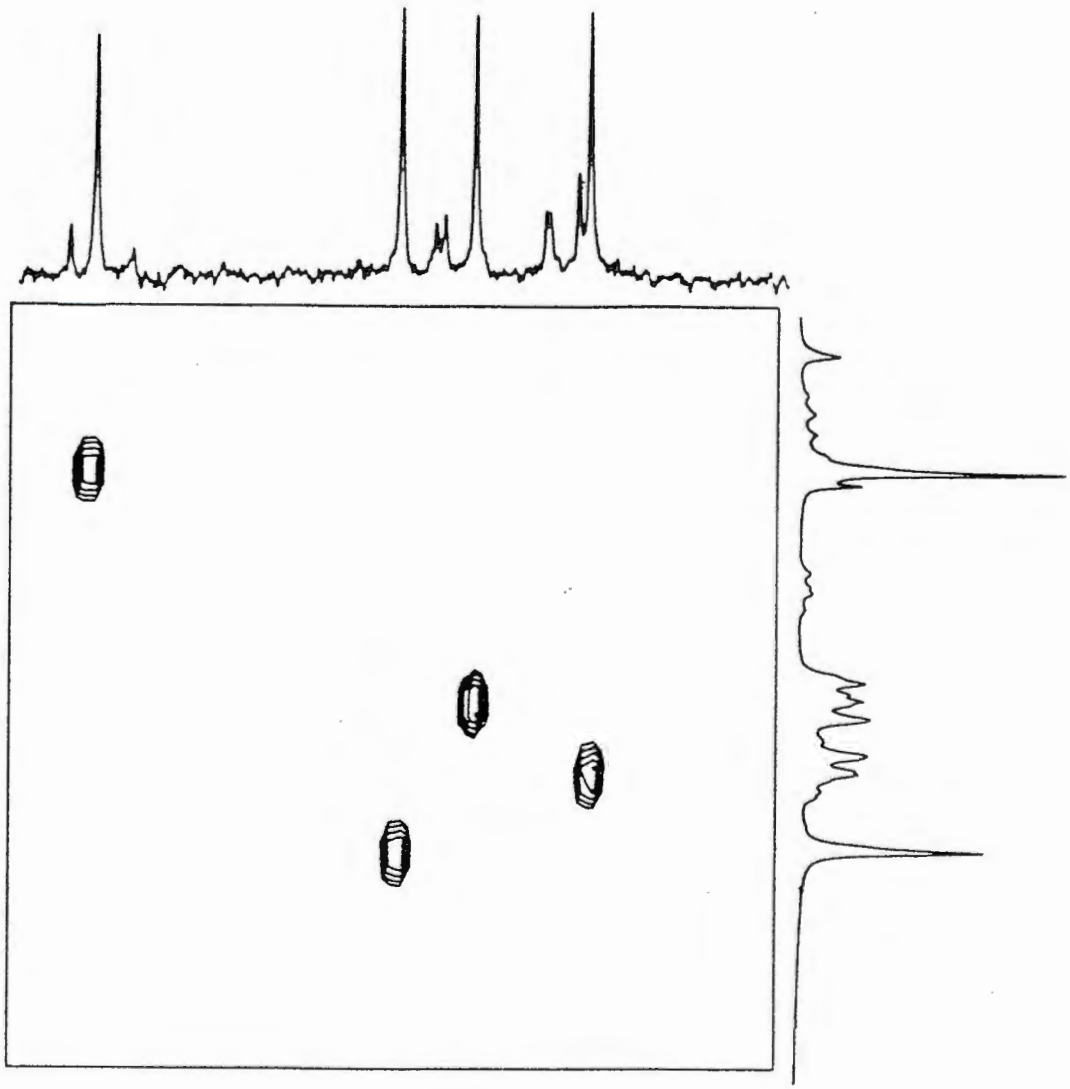

Figure 5.4.6: N.m.r. spectrum of ttda at pD 6.0 obtained using the HETCOR pulse sequence with J_{CH} = 140 Hz.

5.4.2.2 Ca-ttda and Ca-dtda

The ^{13}C chemical shifts of the Ca-dtda system as a function of pD for are shown in Figure 5.4.8. Over the entire pD range only single resonances are observed for non-equivalent carbon atoms, indicating that the ligand is in rapid exchange between the various possible isomers. Both the ^{1}H, Figure 5.4.9, and ^{13}C n.m.r. titration curves level off at pD 10 indicating that the formation of the [Ca(dtda)] complex is complete. This is reflected in the species distribution diagram of this system, Figure 4.42 (see appendix II). However, beyond pD 10 the potentiometric study indicated that substantial formation of the $[Ca(dtda)(OH)]^-$ complex occurs. This is not reflected in the n.m.r. titration curve, presumably because the ligand chemical shifts are insensitive to hydrolysis of the metal ion.

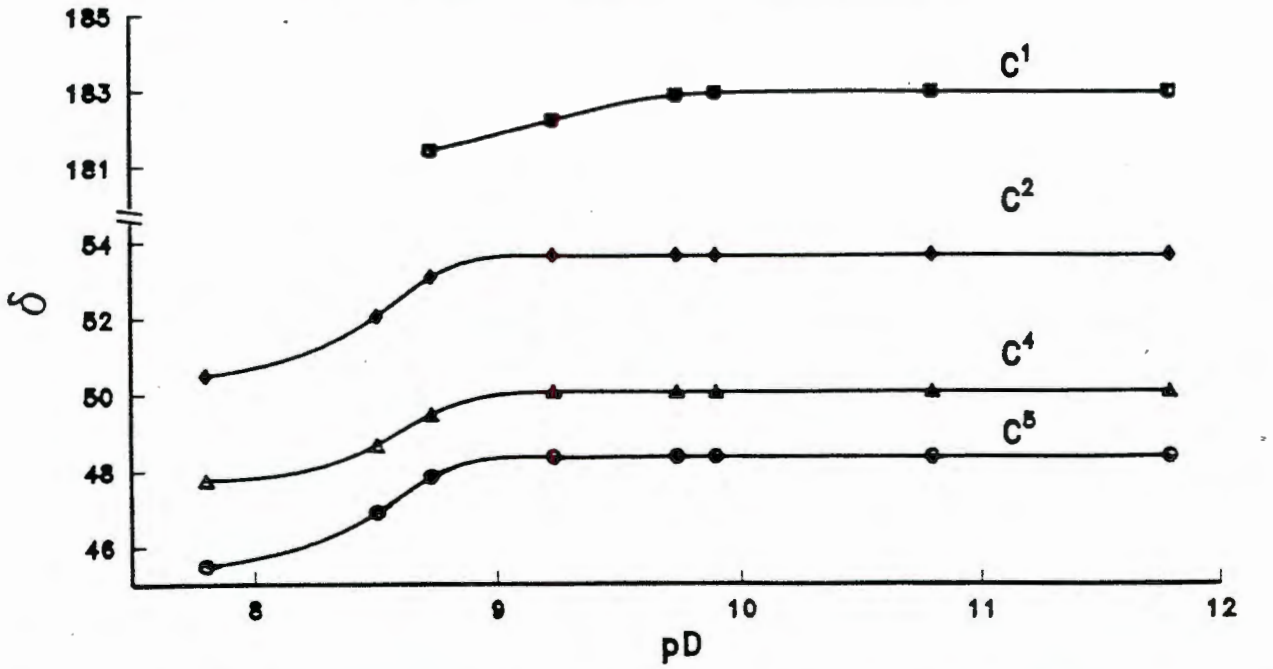

Figure 5.4.8. pD Dependence of the ^{13}C n.m.r. chemical shifts of dtda in the presence of Calcium(II). [dtda] = 0.24, [Ca(II)] = 0.48 mol dm^{-3}.

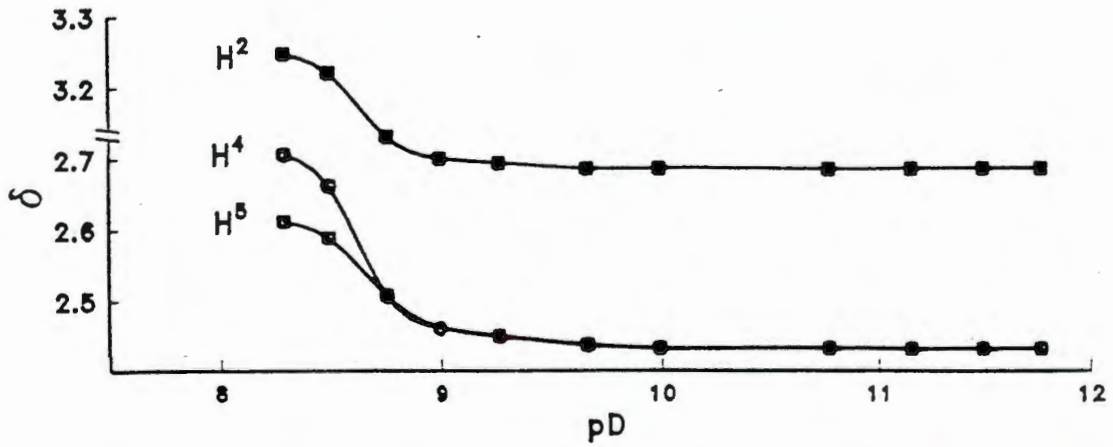

Figure 5.4.9. pD Dependence of the ^{1}H n.m.r. chemical shifts of dtda in the presence of Calcium(II). [dtda] = 0.24, [Ca(II)] = 0.48 mol dm^{-3}.

The variation in ^{13}C n.m.r. chemical shift of ttda as a function of calcium concentration is shown in Figure 5.4.10, and of dtda in Figure 5.4.11.

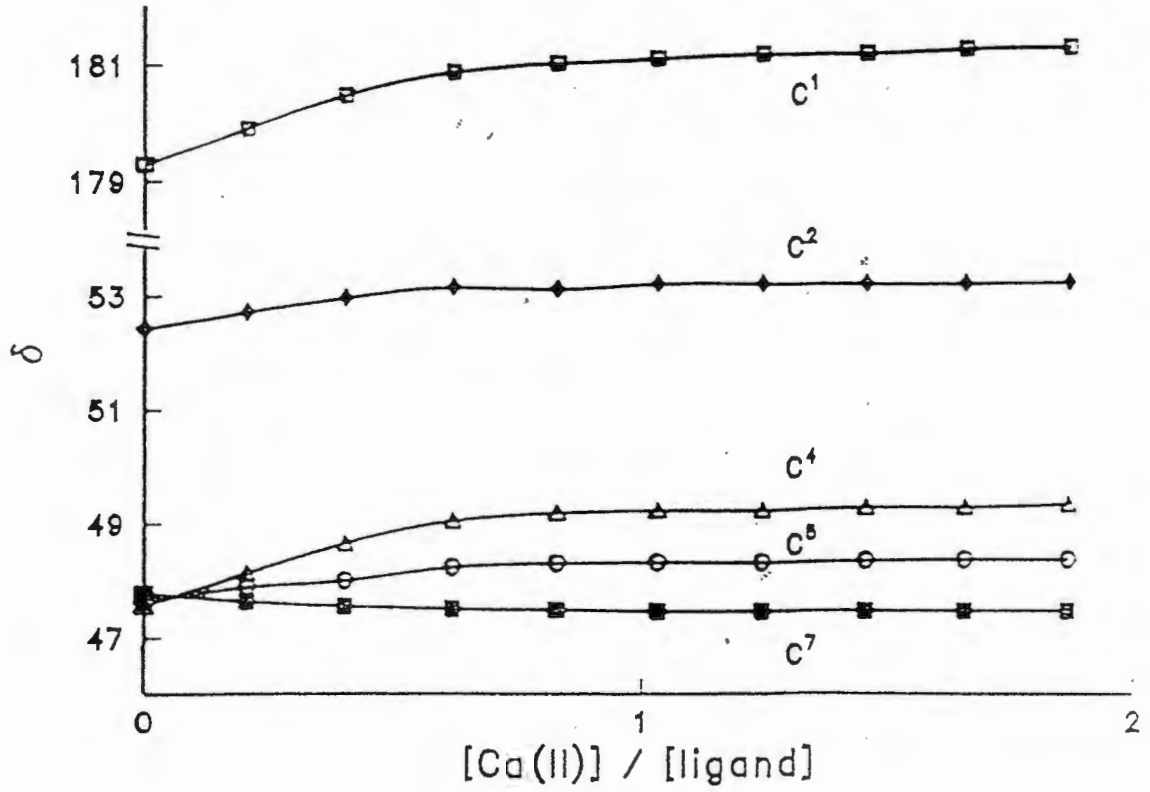

Figure 5.4.10. Carbon-13 n.m.r. chemical shifts as a function of Ca(II) concentration for ttda

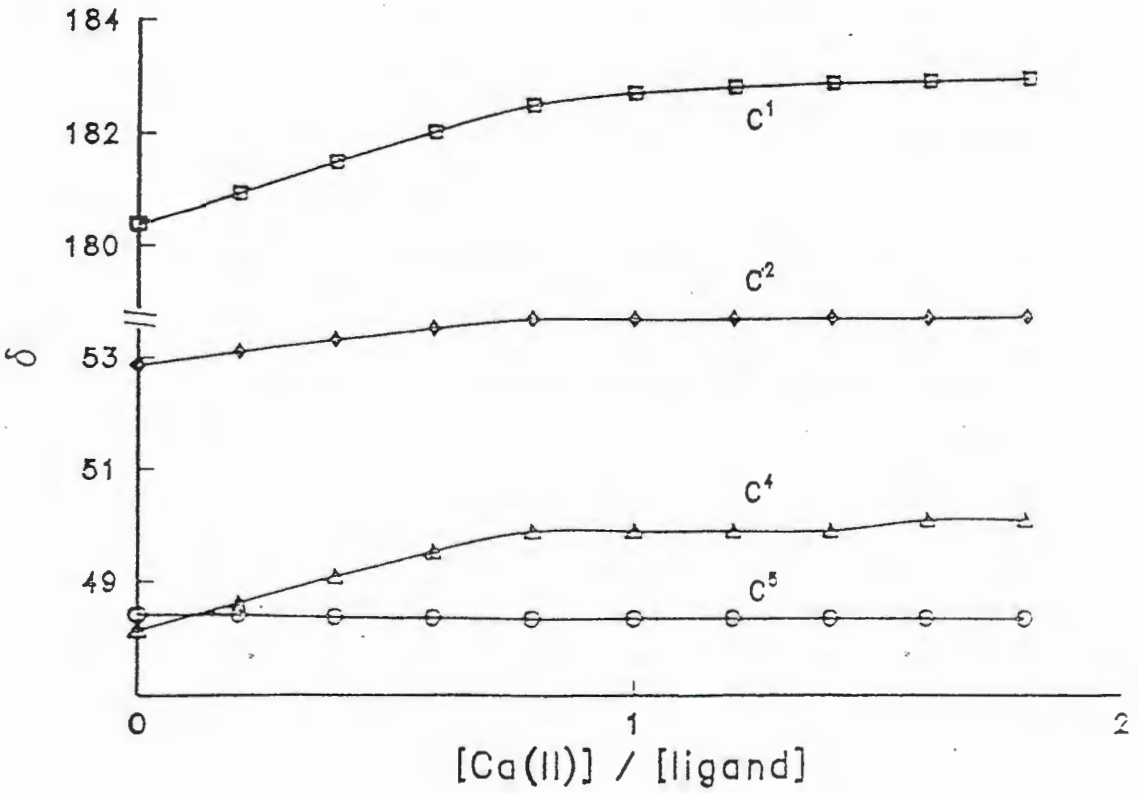

Figure 5.4.11. Carbon-13 n.m.r. chemical shifts as a function of Ca(II) concentration for dtda

In both systems the curves reach a plateau after the addition of one equivalent of metal ion. This indicates that complexation is complete after this addition. The addition of excess metal does not result in further complexation. Using the method given in Section 5.2, it is possible to analyse the titration curve for the stability of the complexes formed. Values of $10^{2.2}$ and $10^{3.2}$ were obtained for β_{110} of dtda and ttda respectively. Considering the variation of ionic strength between this system and that used for the potentiometry, this value agrees well with that determined in the potentiometry study. From the figure it can be seen that the chemical shift of C^5 is insensitive to complexation, as was the chemical shift of C^7 of ttda, suggesting that the central nitrogens are not involved in complexation. A careful examination of the n.m.r. titration curves revealed a crossover of the C^4 and C^5 resonances of dtda and the C^7, C^4, and C^5 resonances of ttda. A similar crossover is seen in the chemical shifts of 3,7-diazanonane-1,9-diamine.(Dougal, Hague and Moreton, 1987).

5.4.2.3 Zn-ttda

The study of the solution structure of the [Zn(ttda)] was complicated by the formation of several isomers in solution, and by the line broadening associated with exchange between these isomers. While a complete assignment of the spectra could not be made, conclusions about several aspects of the structure of the [Zn(ttda)] and $[Zn(Httda)]^+$ complexes in solution could be drawn.

At low pD, signals attributable to the free ligand can be seen. These are marked as such in Figure 5.4.12.

Two very broad signals are seen for H^2 and H^4, H^5, H^7. This spectrum is typical of protonated polyaminopolycarboxylate complexes, with protonation at the terminal nitrogen (Letkeman and Westmore, 1971). Since separate signals are seen for both the free and complexed ttda, exchange between these two forms must be slow on the n.m.r. time scale

As the pD is raised the ^1H n.m.r. signals move to higher field and gain fine structure. The major spectral changes occur between pD 3 and 5 which corresponds to the potentiometrically measured pK_a for the $[Zn(Httda)]^+$ complex of 3.5. At pD 8 the [Zn(ttda)] complex is completely formed. At this pD the signals arising from the acetate groups (H^2) consist of several broad peaks and a number of AB quartets (J_{AB} = 7 Hz). The non-equivalence of these geminal protons and hence the AB pattern is a clear indication that the acetate group is co-ordinated to the metal and that exchange of these acetate groups amongst the various possible isomers is slow on the n.m.r. time scale. The ABCD nature

of H^4 and H^5, together with the slow interconversion between different geometric isomers, results in the broad signals seen between δ 2.4 and 3.2. The existence of several geometric isomers in solution is confirmed by the ^{13}C n.m.r. spectrum. Here again signals attributable to the free ligand are seen, Figure 5.4.13.

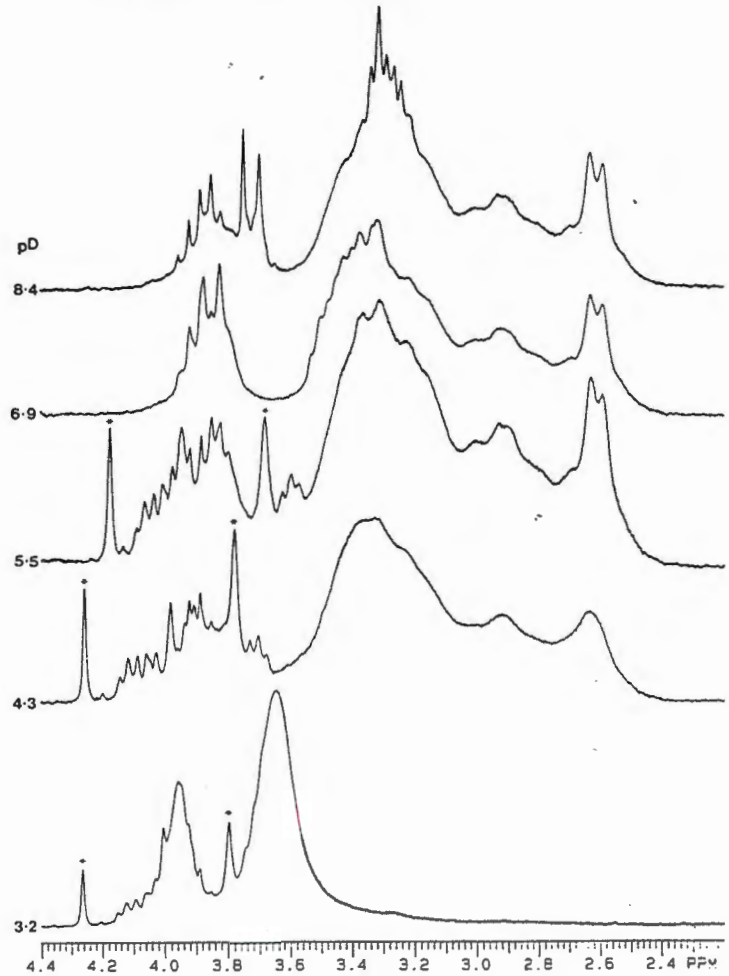

Figure 5.4.12. Proton n.m.r. spectra of Zn-ttda as a function of pD. [ttda] = [Zn] = 0.1 mol dm^{-3}. Starred peaks are assigned to free ligand.

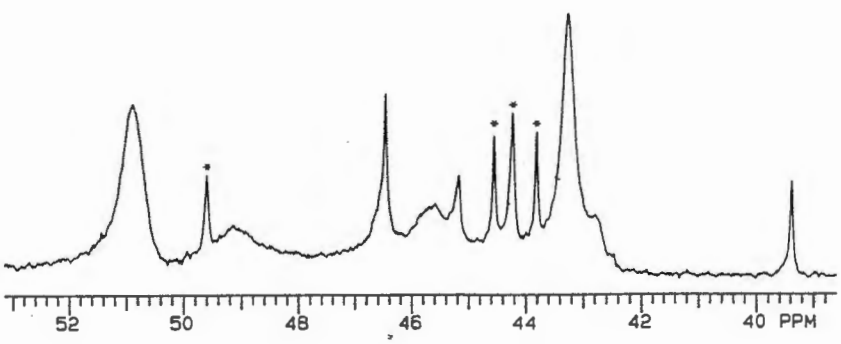

Figure 5.4.13. Carbon-13 n.m.r. spectrum of Zn-ttda. [ttda] = [Zn] = 0.1 mol dm^{-3}. Starred peaks are assigned to free ligand.

5.4.3 Experimental

For the pD scans of the ligands ttda and dtda solutions of appropriate concentration to give reasonable spectra were prepared. No attempt was made to use any specific concentration.

For the calcium/ttda scans an approximately 0.2 mol dm^{-3} solution of ttda was prepared in D_2O, and adjusted to a pD of approximately 10. A 2.9 mol dm^{-3} solution of $CaCl_2$ was made up in D_2O, and adjusted to a pD of approximately 10. No precipitate was seen. For each scan a 10 $\mu\ell$ aliquot of the calcium solution was added until a two fold excess of calcium had been added.

For the calcium/dtda pD scan a 1:2 molar ratio of the metal and ligand were dissolved in D_2O and adjusted to approximately pD 12. The pD was decreased by the addition of small quantities of DCl, and ^{1}H and ^{13}C spectra recorded at each pD. The initial concentrations were 0.48 Calcium and 0.24 mol drn^{-3} dtda.

To obtain the zinc spectra a 1:1 molar ratio of the metal and ligand were dissolved in D_2O and adjusted to approximately pD 9. The pD was decreased by the addition of small quantities of DCl. The initial concentrations were 0.1 mol dm^{-3} for ttda and zinc.

In all cases the pD was determined using a combination micro electrode calibrated with standard pH buffers. The pD was obtained from the relationship

$$pD = pH + 0.4$$

5.5 Ultra filtration

5.5.1 Introduction

The study of metal ion chemistry in biofluids has several facets. The metal ions are intimately associated with many enzyme control processes. However, their transport through and between body compartments is often mediated by low molecular weight ligands. Examples of this are given by Leigh and Miller, and Forth and Nell (Leigh and Miller, 1983; Forth and Nell, 1981).

Jackson et al have postulated that an increase in the l.m.w. pool of copper stimulates an anti-inflammatory response (Jackson, May and Williams, 1978). It is for this reason that we have attempted to manipulate this fraction of copper using exogenous ligands. It is of interest to assess experimentally the effect of the ligands on the blood plasma speciation of copper. Although the actual copper-protein binding constants are not of particular interest in this study, some of the techniques used to determine them are. The actual l.m.w. distribution is also of little importance, and in any case is extremely difficult to measure (Jackson, May and Williams, 1978). It may be assumed, however, that the predominant l.m.w. species will be the M-ttda or M-dtda complexes, as the concentration of these ligands is considerably higher than that of competing ligands.

The objectives of this study were two-fold:

1. To determine experimentally whether the ligands mobilised copper as the l.m.w. species, and

2. To compare the experimental mobilisation curves with those calculated using the blood model.

Also of interest is the effect of the ligands on the zinc and calcium equilibria. Computer calculations suggested that interference of the ligands in the Zn^{+2} and Ca^{+2} equilibria would be significant. Attempts were therefore made, using ultrafiltration, to quantify the *in vitro* mobilisation of copper from protein.

5.5.2 Theory

The reversible interaction between small molecules and macromolecules is fundamentally important in biology, and binding experiments have played a major role in elucidating biological control mechanisms and reactions (Sophianopoulos et al, 1978). The traditional

method of determining the binding between protein and small molecules has been dialysis with gel filtration, chromatography or electrophoresis. These methods can be used to identify which proteins bind a specific metal, in what proportions, to what extent, as well as how many metal ions bind to each protein and the number of classes of binding site. In this study, however, our interest is in determining the extent to which the metal-protein ⇌ metal-l.m.w. equilibrium is perturbed by our ligands, ttda and dtda.

With the introduction of semi-permeable membranes which prevent the passage of macromolecules, ultrafiltration methods became possible, (Sophianopoulos et al, 1978). Two main approaches have been used. In one method the volume of the ultrafiltered sample is kept constant by continually adding a solution containing the ligand, for example wash in and wash out procedures. In the second method nothing is added to the sample being filtered and a small aliquot of filtrate is collected. Generally the second method is considered to be approximate, as $V_0 \approx V_0 - dv$ is assumed, and it is felt that the removal of the ultrafiltered liquid, dv, disturbs the equilibrium. Only small quantities, about 10 %, (Staub and Buffle, 1984) are normally removed.

Sophianopoulos et al (Sophianopoulos et al, 1978) and Gamble et al, (Gamble, Haniff and Zienius, 1986) both showed that theoretically the concentration of free ligand (or metal) in the ultrafiltrate is the same as that in the initial sample, and is independent of the volume of the ultrafiltrate. The method may thus be used to give exact results in binding studies. It is assumed that both the ligand and solvent pass unimpeded through the membrane and that the macromolecule is completely retained by the membrane.

At equilibrium the free energy change of a system is given by

$$\partial G = \sum_i \mu_i \, \partial n_i$$

Where μ_i = The chemical potential, and

n_i = the number of moles of component *i*

The reaction at equilibrium is thus completely defined. The effect of removing quantities of one of the components, plus solvent, from the reaction mixture can be illustrated by the following simple reaction of a single ligand binding to a protein.

$$P + A \rightleftharpoons PA \qquad (5.5.1)$$

The dissociation constant can be expressed in terms of concentrations as

$$K = \frac{[P]\,[A]}{[PA]} \tag{5.5.2}$$

$$= \frac{([P_T] - [A_T] + [A])\,[A]}{([A_T] - [A])} \tag{5.5.3}$$

$[P_T]$, $[A_T]$, $[P]$, $[A]$ and $[PA]$ are the molar concentrations of total protein, total ligand, free protein, free ligand and protein-ligand complex, respectively.

If the moles of the constituents are denoted by *m*, and the states before and after removal of free ligand by (0) and (1) respectively. Let a small amount of freely diffusible ligand, *dm*, be removed at equilibrium such that $dm/dv = A_0$, *dv* being the accompanying small volume change. The equilibrium constants for each state may then be written as

$$K_0 = \frac{[m_{PTo} - m_{ATo} + (dm/dv)\cdot V_0]}{[m_{ATo} - (dm/dv)\cdot V_0]}\cdot(dm/dv) = K \tag{5.5.4}$$

$$K_1 = \frac{[m_{PTo} - m_{ATo} + dm + (A_1)\cdot(V_0 - dv)]}{[m_{ATo} - dm - (A_1)\cdot(V_0 - dv)]}\cdot(A_1) = K \tag{5.5.5}$$

As K_0 must equal K_1, equations 4 and 5 must be equal. Thus

$$A_1 = dm/dv = A_0.$$

The removal of solution is thus not limited to small amounts of filtrate, as required by the assumption

$$V_0 \approx V_0 - dv$$

and the concentration of the ligand in the ultrafiltrate is equal to that in the initial solution. Although the above illustration was for the simple case of one ligand binding to the protein molecule, it may be extended to the general case for n_j ligand molecules binding to sites of equal affinity and *i* sites of different affinities. The parameter *v*, defined as the number of moles of ligand bound per mole of protein, is given by

$$v = \frac{(A_T) - (A)}{(P_T)} = \sum_{i,j} \frac{n_j(A)}{K_i + (A)} \qquad (6)$$

In the simple case considered above, $i = j = n_j = 1$. However, (A) is the only variable, and if (A) is constant, then v is also constant, and the theory applies to the general case.

5.5.3 Results and discussion

The calculated and experimental P.M.I. curves for copper, obtained by plotting log P.M.I. against the log of the ligand concentration , are given in Figures 5.5.1 and 5.5.2 respectively.

There is a considerable difference between the two sets of curves. The most obvious difference is the slope of the lines, with the calculated curves having a much steeper slope. Experimental limitations did not allow very low concentrations to be used in the ultrafiltration, but if the experimental lines are extrapolated, then the concentration at which the mobilisation starts is of similar order of magnitude to the calculated value. The accuracy of the extrapolated value from this data is likely to be low, however. The order of the mobilising ability of the ligands is similar in both the calculated and experimental curves. The fact that the experimental curves have different slopes makes the determination of the order somewhat subjective, but the following order seems reasonable.

ttda > dtda > edda > dtpa > edta ≈ trien

The calculated order is:

trien > ttda > dtda > edda > dtpa > edta

The low mobilising ability of edta and dtpa can be understood in terms of competition from zinc and calcium, both of which are present in high concentrations in blood plasma. Compared to the other ligands studied, edta and dtpa have relatively large Ca(II) and Zn(II) formation constants, and this in effect limits the availability of these ligands for interaction with copper(II). The converse applies to trien, which has very little affinity for Calcium. The low result for trien mobilisation in the experimental study is unexpected.

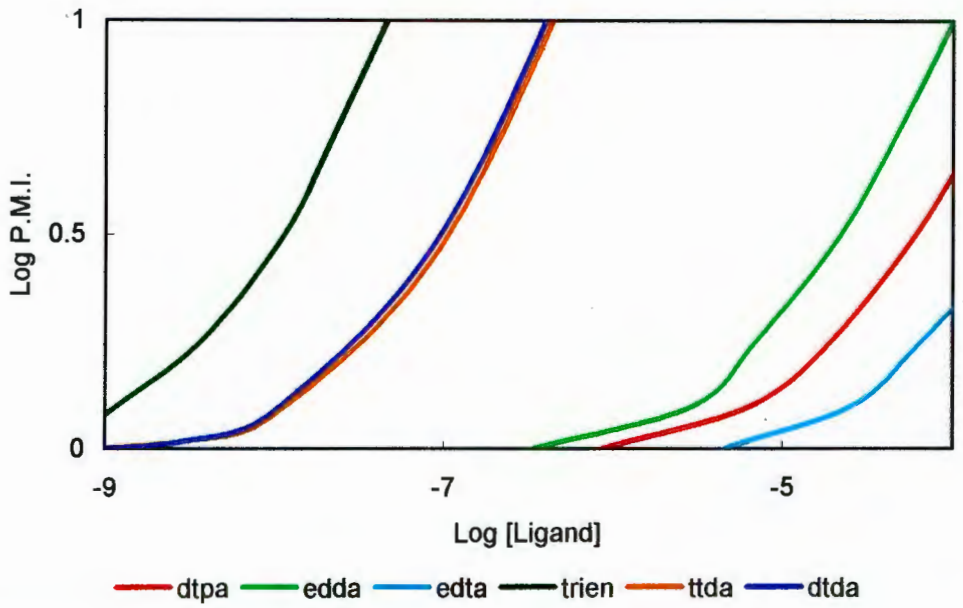

Figure 5.5.1: Calculated copper P.M.I. curves for ttda, dtda, edda, dtpa, edta and trien.

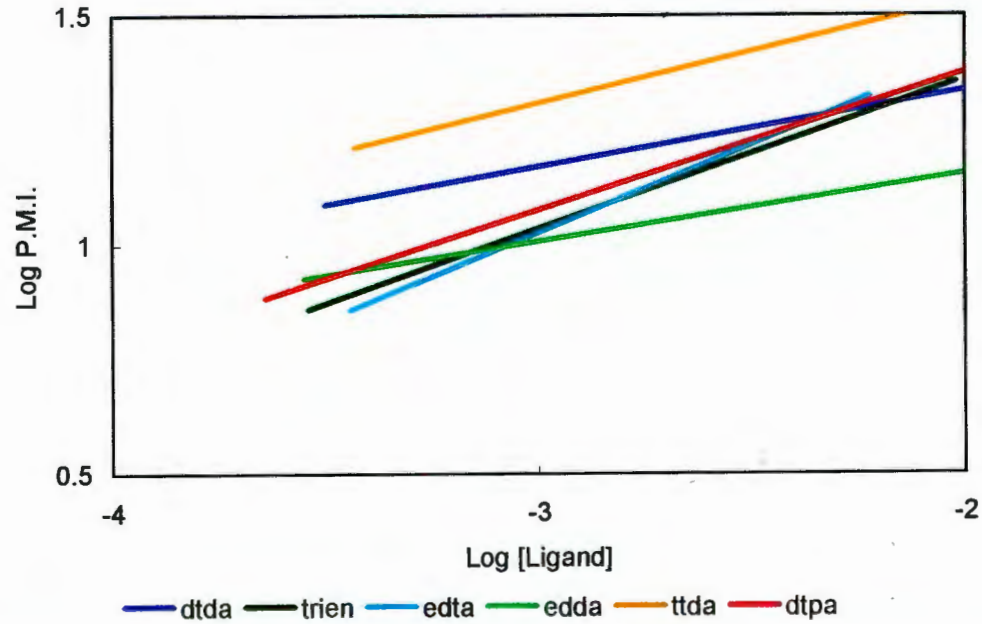

Figure 5.5.2: Experimental copper P.M.I. curves for ttda, dtda, edda, dtpa, edta and trien.

The calculated and experimental zinc P.M.I. curves for the ligands are given in Figures 5.5.3 and 5.5.4 respectively.

As with the results of the copper studies, it is difficult to unequivocally determine the order of mobilising ability of the ligands from the experimental results, but extrapolating and using the intercept where log P.M.I. is zero, the following order was established.

dtpa > ttda > dtda > edta > edda > trien

The calculated order is

ttda ≈ dtda ≈ dtpa > edda > edta > trien

Experimentally dtpa was found to be more effective than predicted from the blood model simulation. The order for edda and edta was reversed and there seems no ready explanation for this observation, but has been report previously (Jackson and Singh,1990). trien, which has a relatively low affinity for the hard zinc(II) ion, mobilised zinc poorly, as was predicted.

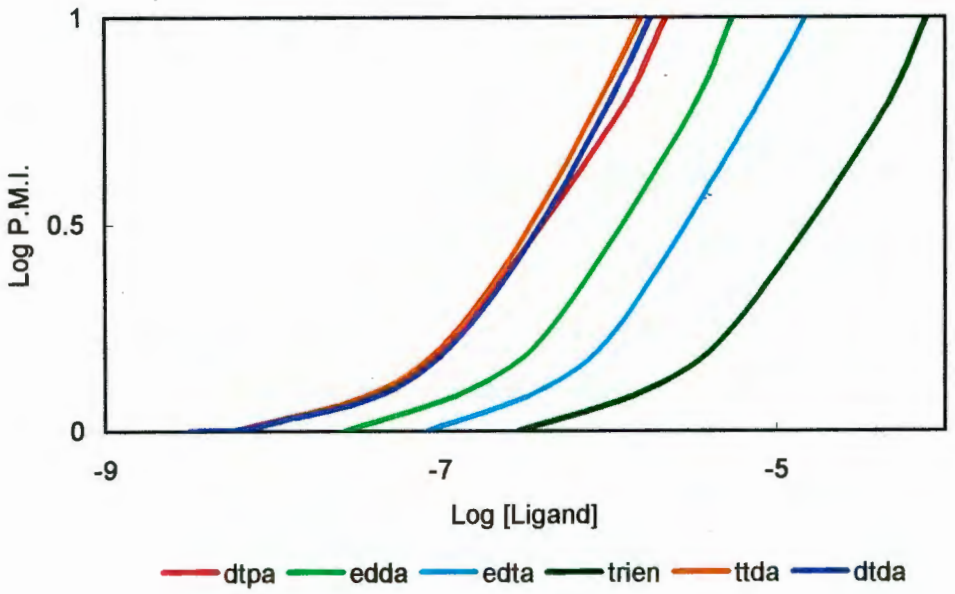

Figure 5.5.3: Calculated zinc P.M.I. curves for ttda, dtda, edda, dtpa, edta and trien.

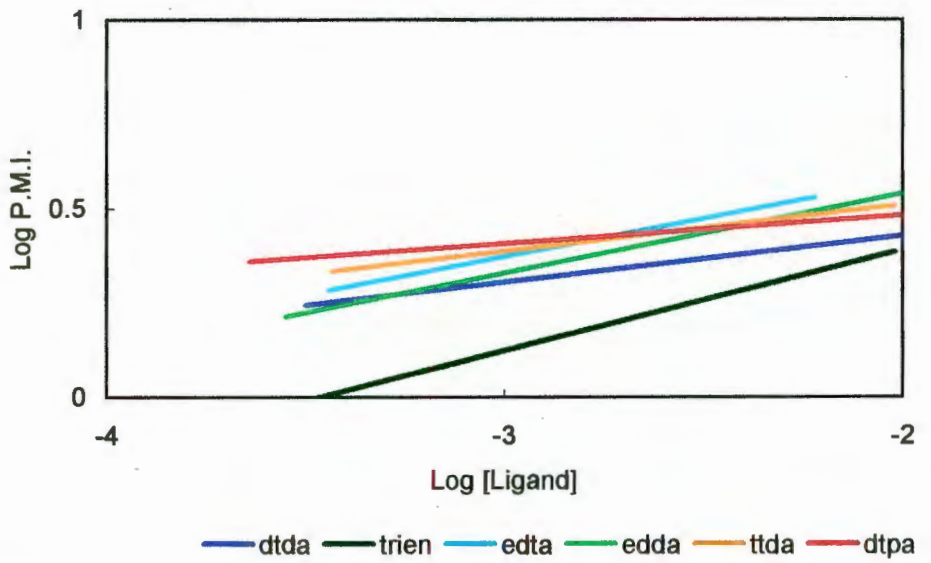

Figure 5.5.4: Experimental zinc P.M.I. curves for ttda, dtda, edda, dtpa, edta and trien.

While the model fails to predict some of the finer details of the experimental results, several aspects were successfully modelled. The general order of mobilisation is predicted, as is the approximate onset of mobilisation.

5.5.4 Experimental

Human blood serum was obtained from the Western Province Blood Transfusion Service and stored at -4°C. Dtpa (Merck), edta (NTA) and edda(Sigma) were used without further purification. Trien (Merck) was purified by distillation under reduced pressure and fractional crystallisation of the hydrochloride (Sacconi, Paolletti and Ciampolini, 1961). Accurately weighed masses of ligand were added to 10 ml aliquots of serum at pH 7.4. The solutions were incubated for 15 minutes at 37°C to allow them to reach equilibrium and then ultrafiltered. Centrifugal pressure at 300 rpm (~900 g) allowed a filtration rate of 10μm min^{-1} through YMT (Amicon) membranes to be achieved. The ultrafiltrates were analysed for copper, zinc and calcium by atomic absorption spectrometry. Calcium was measured using a N_2O/C_2H_2 flame at 422,7 nm. A 100 fold excess of lanthanum nitrate was added to each of the samples to suppress ionisation of the analyte. Zinc was measured at 213,9 nm using an oxidising air/C_2H_2 flame. Copper was measured on a Perkin Elmer 5000 AA spectrophotometer using a graphite furnace coupled to a HGA 500 programmer.

The theoretical plasma mobilisation indexes were obtained using the blood simulation program, ECCLES, as described in Chapter 2.

5.6 Animal Studies

5.6.1 Introduction

In the initial development of any drug, the use of *in vitro* methods can be advantageous. Not only is this approach more convenient, but the experimentation is generally more reproducible and does not have the moral considerations inherent in animal screens. Ultimately though, if the *in vitro* experiments indicate potential, *in vivo* testing, using animal screens, is unavoidable.

The aim of this study was to design, using computer simulation (Jackson and Kelly, 1988), a ligand which would be an effective mobilizer of copper (May and Williams, 1981). To assess whether this ligand was in reality a good copper mobilizer, the solution thermodynamics of the ligand and several biologically important metal ions, including copper, were studied using potentiometric techniques. This data allowed the mobilizing efficiency of the ligands to be assessed, using the plasma simulation model. The results of this simulation predicted that (a) the copper would be strongly mobilized and (b) that the perturbation of the other metals present would not be unacceptably high *in vivo*. These conclusions were supported by ultra filtration studies, Section 5.5. Further, the pH dependent species distribution plot, Figure 5.6.1, shows that at the physiological pH of 7.4, the Cu-ttda complex is the only important species.

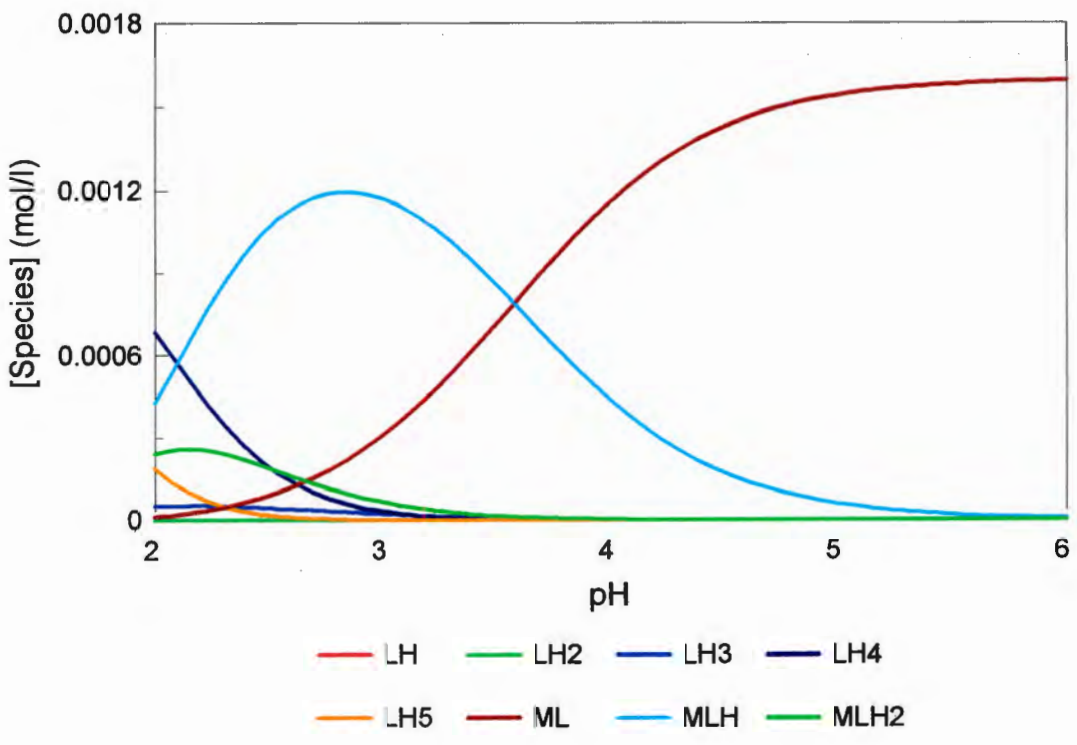

Figure 5.6.1: Species distribution plot for the copper(II)-ttda system

As this species is nominally neutral, it should be effectively transported through the cell membrane. This property is required for transport of the copper from one body compartment to another. (Sarkar, 1981). Lipophilicity would undoubtedly be enhanced if the two carboxylate residues on the ttda molecule were coordinated. The variable pH UV/VIS study indicated that the carboxylate residues were complexed to the copper.

In summary, the following positive *in vitro* results were obtained.

a) Ttda is an effective Copper(II) mobilizer.
b) Ttda is relatively selective for Copper(II).
c) The major species at physiological pH is neutral.
d) This complex appears to be six coordinate, which will increase its lipophilicity, and thus be more membrane soluble.

These results, together with the reported success of copper complexes as anti-inflammatory agents in animal tests, indicated that animal screens were warranted.

The questions of interest were :

a) Is the Cu(II)-ttda complex active as an anti-inflammatory?
b) How effective is it?
c) Is membrane transport efficient ?
d) What is the toxicity of the complex ?

Rat adjuvant arthritis was chosen as the most appropriate model of inflammation (Meyers, 1988). This model is considered to closely resemble rheumatoid arthritis in humans and allows administration of the compound during the established phase of the disease (Lewis and West, 1981).

Initial dosages were based on earlier studies (Jackson, May and Williams, 1978; Lewis and West, 1981; Lewis A.J., 1978) and are given in the experimental section.

5.6.2 Results and Discussion

Although some aspects of these animal screens were unsatisfactory, some of the information gained allows important conclusions to be drawn regarding the *in vivo* behaviour of the test complex. Figure 5.6.2 shows the comparative paw sizes of the inflamed and uninflamed paws.

Figure 5.6.2: Comparative sizes of inflamed and uninflamed paws.

The average paw volume of the rats which received the complex, group 1, is presented in Figure 5.6.3 and of the animals receiving the copper chloride, group 2, in Figure 5.6.4.

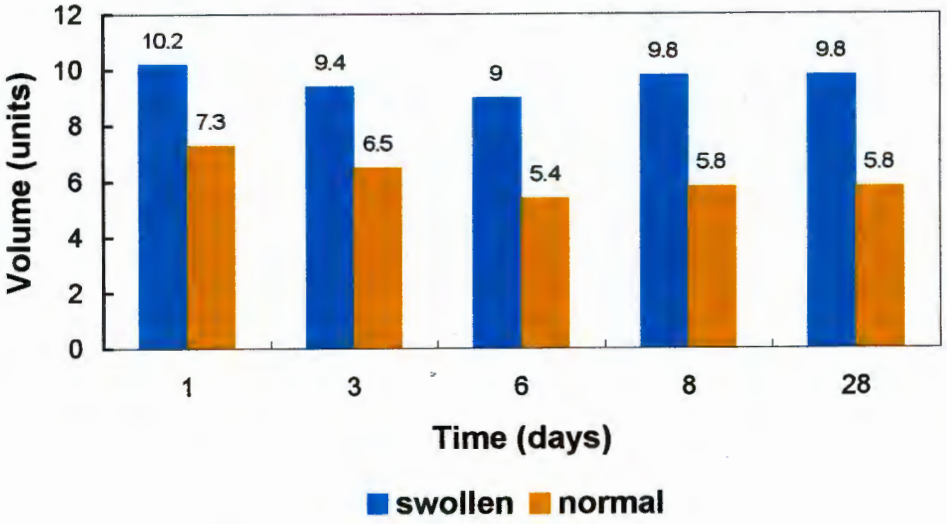

Figure 5.6.3. Average paw volume, group 1

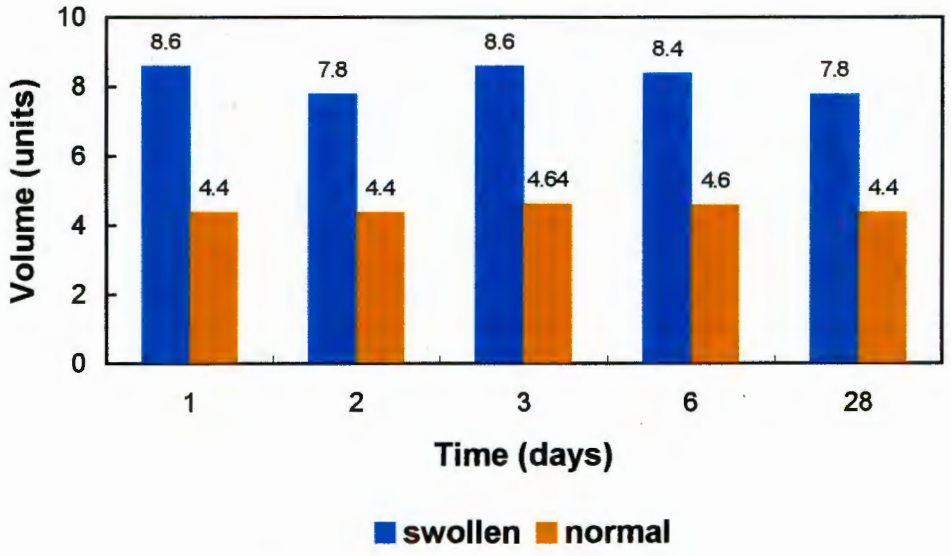

Figure 5.6.4. Average paw volume, group 2

The condition of the animals which received the copper chloride, group 2, started to deteriorate on the second day, thus it was not realistic to administer further doses. The animals started to die on the third day after injection and by the seventh day, all five were dead. There was no sign of reduction in the volume of the paw. By the time they died, the longest surviving animals had developed lesions at the site of injection. This copper induced irritation has been noted by other workers (Lewis, 1978; Lewis, Smith, and Brown, 1978). The animals in group 1 showed no sign of ill health. There was no noticeable reduction in the inflammation. Unlike the group 2 animals, these rats did not show any sign of irritation at the site of injection.

It has been reported (Lewis A.J., 1978; Sorenson,1976; Lewis and West, 1981) that copper aspirinate possesses anti-inflammatory activity when tested with this model, so this complex was used as the control instead of copper chloride. Copper aspirinate was therefore administered at the same copper concentration as the test complex (group 5). Once again the condition of the animals immediately started to deteriorate. Within 3 days, four of the animals had died. The surviving animal's condition did not return to normal with time. This animal developed a lesion at the site of injection similar to those of the group 2 animals.

The group 4 animals, those receiving the test complex, also showed signs of discomfort the day after the high dose of 15 $mgkg^{-1}$ was given. For this reason, a further dose was not given on the second day. Increased dosing was achieved by giving 10$mgkg^{-1}$ every day.

After 4 weeks there was no reduction of inflammation.

Previously it has been noted (Whitehouse, 1976; Rainsford, and Whitehouse, 1979; Lewis, Smith and Brown, 1978) that subcutaneous injection of copper complexes often produces a local irritant response. Rainsford and Whitehouse (Rainsford and Whitehouse, 1979) have suggested that the observed anti-inflammatory activity of the complexes is the result of a counter irritant mechanism, as these compounds were not active when administered orally. However, Bonta and Nordhoek (Bonta and Nordhoek, 1973) have demonstrated that irritation does not always reduce inflammation in an induced model. In this study, those animals which developed lesions, did not show any signs of inflammation reduction.

A J Lewis (Lewis, 1978), Sorenson (Sorenson, 1976) and E J Lewis (Lewis, 1981) report anti-inflammatory activity of copper aspirinate with various models of inflammation. The death of the animals after copper chloride and copper aspirinate administration was unexpected, as Sorenson gives an LD_{50} for copper aspirinate of 750mgkg^{-1} and 350mgkg^{-1} for copper acetate, administered subcutaneously. Jackson et al (Jackson, May and Williams, 1978) reported that a dose of 9.3mgkg^{-1} copper, as the chloride, was effective in the inhibition of a Carrageenan-induced oedema model of inflammation. No mention was made of animal mortality. Lewis et al (Lewis, Smith and Brown, 1981) report that after receiving a single dose of 238mgkg^{-1} copper aspirinate, all the animals injected died. The doses used in this study are substantially lower than those reported above. It has been suggested (Brown and Smith, 1980; Pharo,1988) that the strain used may be sensitive to high levels of exogenous copper. The animals which received the test complex did not generally show any signs of discomfort. The only exception was group 4, after receiving a 15mgkg-1 dose. These animals did not show any discomfort or stress when the dosage was reduced to 10mgkg^{-1} every day for 3 days. A possible explanation for this is that the toxic effects of the copper are reduced by complexation (Lauffer, 1987) although it is also a possibility that the ligand merely promotes the excretion of the copper.

The route of excretion from the body is in some measure dependent on the complex itself. Charged complexes are readily excreted in the urine, *via* the kidneys, while uncharged species are often metabolized by the liver, and excreted in the faeces. In order to test for the excretion of our test compound, urine samples were collected, at different times, from the group 4 animals. The urine was analysed for total copper by graphite furnace atomic absorption spectrometry and for the [Cu(ttda)] complex spectrophotometrically. The results are presented in Table 5.6.1.

Table 5.6.1.: Quantities of copper determined in the rat urine.

Sample	Cu_c by UV		Cu_T by AA		Cu_a p.animal mg per animal
	mg per animal	% of Cu_a	mg per animal	% of Cu_a	
0-1 hr	1.4	27%	1.83	36%	5
0-24 hrs	2.27	32%	2.7	38%	7
24-48 hrs	0		0.006		

Cu_c = Cu^{2+} present as the complex

Cu_T = total Cu^{2+} present in all forms

Cu_a = Cu^{2+} administered to the animal

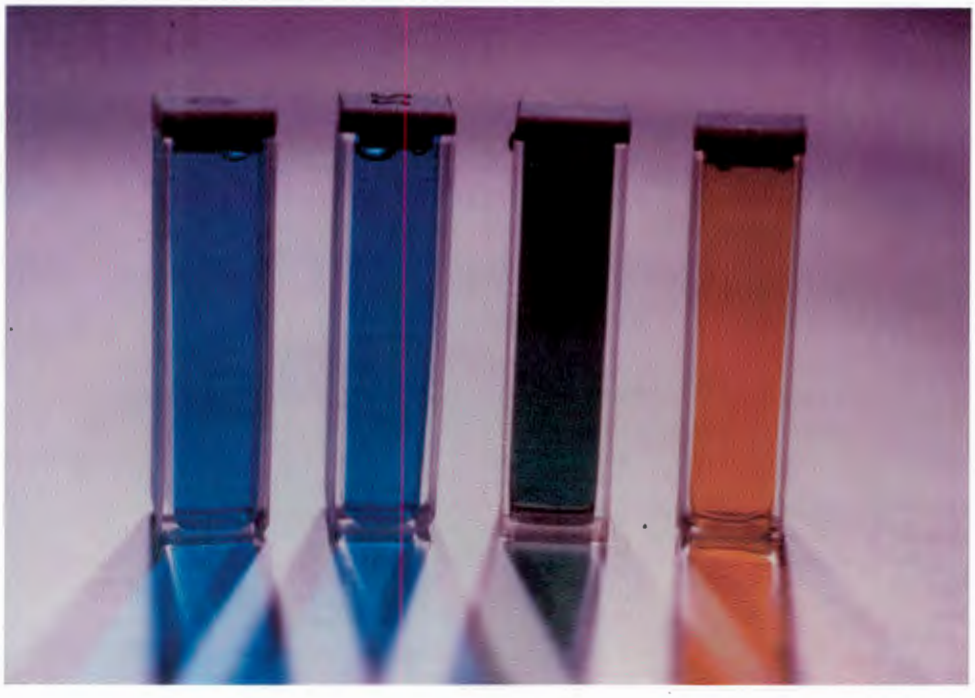

Figure 5.6.5: Colours of the injected solution and 3 urine samples. From left to right, injected solution, 0-1 hour urine sample, 0-24 hour urine sample and 24-48 hour urine sample.

Note the intense colour of the sample collected after 1 hour and its similarity to the injected sample. The concentrations of copper detected by UV were approximately 6% lower than that obtained by AA. Since the UV determination only measures the concentration of the

complex while atomic absorption measures the total copper concentration, this 6% difference represents the other forms of copper present in the urine. These other forms of copper may be inherent to the urine or be a result of contamination by faeces, food particles or dust. In both cases though, the analysis showed that the same % of administered copper was excreted in the first hour as in the first 24 hours. It is unlikely that this is a coincidence, and indicates that the compound is excreted through the urine only when there is a very high complex concentration in the blood. That is, immediately after the injection. Only an extremely low concentration of copper was detected in the 24-48 hour sample. Analysis of the faeces could have shown conclusively whether the copper was being excreted or retained in the body, but this analysis was not possible.

It has been suggested, from histological evidence, that the model developed in the animals was inadequate (Wainwright, 1988). Sharma et al (Sharma, Chandra and Basu, 1987) indicate destruction of tissue due to the release of lysosomal enzyme, as well as destructive lesions in the tarsals or metatarsals. Although the animals in this study did show extensive tissue damage, the effect on the bone and joint tissue was minimal. Difficulty was experienced in initiating the model. It is also well known that animal tests are sensitive to factors such as the species used, route of administration and time scale. All these variables may have contributed to the largely inconclusive results obtained for the anti-inflammatory activity.

5.6.3 Conclusion

The results of these experiments indicate that for this strain of rat the presence of the ligand appreciably decreases the toxicity of the copper. The rapid appearance of the copper complex in the urine suggests that while the complex is able to pass into the blood stream from the site of injection, it is too hydrophilic to be completely reabsorbed into the blood stream from the kidneys. For transport of the copper from one body compartment to another, neutral complexes, (Jackson, May and Williams, 1978; Sarker, 1981) will enhance metal ion diffusion across the cell membrane as they are relatively lipophilic.

The detection of 36% of the total administered copper in the urine also suggests that the complex is not excreted preferentially via the urine, and may well be present in a bio-available state.

There is a need to further develop the animal model used, as well as to try to duplicate other published results. The indications are, however, that this approach to anti-inflammatory drug design is well worth pursuing.

5.6.4 Experimental

Two sets of screens were conducted.

1. A dose of 10 $mgkg^{-1}$ copper was administered, as the complex, to one group, group 1, and as the chloride to another, group 2. A placebo (saline) was administered to a third group, group 3. The administration of the complex was repeated every second day for 2 doses. Only one dose of copper chloride was administered as the condition of the animals had deteriorated by the second day. The paw size was measured after each injection and inspected every day for signs of inflammation reduction.

2. The dose profile of the complex was increased to an initial dose of 15 $mgkg^{-1}$ copper (group 4). A day was skipped as the animals showed signs of discomfort, and dosing at 10 $mgkg^{-1}$ per day was then continued for 3 days. 15 $mgkg^{-1}$ copper, as the aspirinate mixture, was given to a second group (group 5). Nothing further was given as the condition of the animals started deteriorating immediately. Paw volume was monitored as above.

Exact quantities for the various doses are given in Table 5.6.1 below.

Table 5.6.1: Doses of copper compounds administered to the rats.

Masses taken			Dose		Volume	
ligand (g(mmol))		$CuCl_2.2H_2O$ (g(mmol))	complex ($mgkg^{-1}$)	copper(II) ($mgkg^{-1}$)	total (ml)	per rat (ml)
ttda (group 1)	0.232(0.568)	0.096(0.567)	52	10	22.68	3.2
Cl (group 2)	-	0.096(0.567)	-	10	22.68	3.2
ttda (group 4)	0.348(0.353)	0.144(0.844)	73	14	34.02	4.5
Asp (group 5)	0.144(0.844)	-	-	14	34.02	4.5

Paw volumes were measured using an instrument designed and constructed in this laboratory, and is shown in Figure 5.6.6.

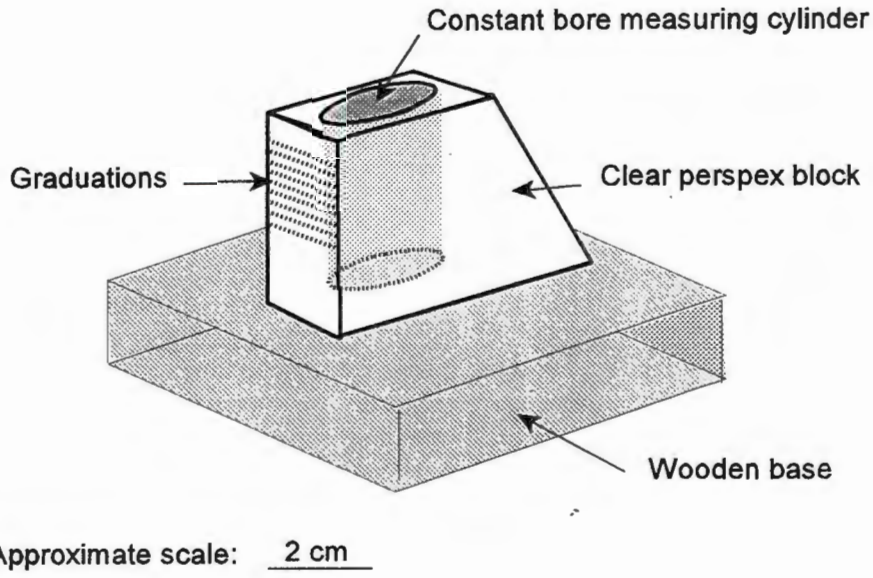

Figure 5.6.6: Apparatus used to measure paw volumes.

The graduations are constant, but the units are arbitrary. No attempt was made to calibrate the instrument as the error in the graduation was small relative to other sources of error. The "cylinder" was filled to a convenient level with a very dilute solution of ink. The colour aided in the determination of the position of the meniscus. The rat's hind ankles were ringed, using an indelible dye. The paws were measured sequentially, and the position of the meniscus noted before immersion and when the meniscus just touched the ring. Determining when the meniscus touched the mark was the largest source of error in the measurement, and was of the order of 5%. It was necessary to anaesthetize the animal both for the injection and the measurement. The compounds were administered subcutaneously.

The urine from the animals receiving the test complex was collected using metabolic cages as follows :

a) For 24 hrs immediately following the first injection of 15 $mgkg^{-1}$ copper, i.e. day 1 of the experiment.

b) The following 24 hours, i.e. day 2 of the experiment.

c) The first hour after the final dose was administered, i.e. day 5 of the experiment.

The urine was frozen as soon as possible after the samples were collected. Precipitate formed in samples (a) and (b) on storage. The samples were analysed by UV spectroscopy, for complex concentration on a Philips PU8700 UV/vis spectrophotometer. A base line adjustment was made to accommodate for the absorption due to normal urine components. AA analysis by graphite furnace on a Pye Unicam was performed to determine total copper. The samples containing precipitate were first digested with concentrated HNO_3 (Aristar, spectroscopically pure) to solubilize the solid.

Post mortems were performed on groups 1 - 4, immediately after they died or were culled at the end of the screen.

Copper(II) chloride dihydrate, sodium chloride and sodium hydroxide were obtained from SAARCHEM Ltd and were of analytical grade. Acetyl salicylic acid (aspirin) was obtained from BDH and was of reagent grade. Ttda tetrahydrochloride was synthesized in this laboratory. Solutions were made up in glass distilled water and then passed through a millipore microfilter (cat. No. SLGS 0250S) to remove microorganisms. Male Sprague-Dawley rats, from an inbred colony, weighing between 450 and 500 grams were used. The animals were divided into groups of 5, and were fed on standard rat cubes.

Adjuvant arthritis was induced by injecting Freud's complete adjuvant (0.5 ml) into the right hind paw pod. Attempts to induce the arthritis by injecting into the base of the tail failed. The inflammation was allowed to develop for 14 days at which time the experiment was started. Paw volume was monitored daily, with the animal's uninflamed left rear paw being used as a control for that animal.

Solutions of Cu(II)-ttda for injection were prepared by dissolving an appropriate quantity of ttda and $CuCl_2$ in a volume of water calculated to give a solution with a total NaCl concentration of 0.15M. The pH of the solution was adjusted to 7.4 using concentrated sodium hydroxide. The selected dose was administered by injecting a specific volume of solution, calculated on the mass of the animal. The copper chloride solutions were prepared by dissolving the required amount of copper(II) chloride, plus sufficient NaCl to give a final concentration of 0.15M, in the correct volume of distilled water. The pH was left unadjusted at about 5.5. The copper aspirinate solution was made by preparing separate solutions of copper(II)chloride and aspirinate. The pH of the aspirinate solution was raised to approximately 5 to dissolve the compound. The solutions were mixed just prior to injection, and the pH lowered again to prevent precipitation of the copper complex.

References

Akitt, J.W. (1983). *N.m.r. and Chemistry: An introduction to the Fourier transform-multinuclear era*. Chapman and Hall, London.

Bax, A. (1983). *J. Magn. Reson.*, **53**, 517.

Bonta, I.L. and Nordhoek, J. (1973). *Agents and Actions*, **3**, 348.

Brown D.H., Smith, W.E. (1980). *J. Med. Chem.*, **23**, 729.

Dougal, S., Hague, D. and Moreton, A. (1987). *J. Chem. Soc., Dalton Trans.*, 2897.

Forth, W. and Nell, G. (1981). *Agents and Actions Supplement*, **8**, 23.

Gamble, D.S., Haniff, M.I. and Zienius, R.H. (1986). *Anal Chem*, **58**, 732.

Hague, D.N., and Moreton, A.D. (1987). *J.Chem. Soc., Dalton Trans.*, 2889.

Hedwig, G.R., Love, J.L. and Powell, H.J.K. (1970). *Aust. J. Chem.*, **23**, 981.

Jackson, G.E. and Kelly M.J. (1988). *Inorg. Chim. Acta*, **152**, 215.

Jackson, G.E. and Kelly, M.J. (1989). *J. Chem. Soc., Dalton Trans.*, 2429.

Jackson, G.E., May, P.M. and Williams, D.R. (1978). *J. Inorg Nucl Chem*, **40**, 1189.

Jackson, G.E. and Singh, M. (1990). *Polyhedron*, **9(4)**, 505.

Lauffer, R.B. (1987). *Chem. Rev.*, **87**, 901.

Lengfelder, E. and Weser, U. (1981). *Bull. Eur. Physiopathol. Resp.*, **17(supp)**, 73.

Letkeman, P. (1979). *Journal of Chemical Education*, **56**, 348.

Letkeman, P. and Westmore, J. (1971). *Can. J. Chem.*, **49**, 2073.

Lever, A.B.P. (1985). *Inorganic Electronic Spectra*, 2nd edition, Elsevier, New York.

Lewis, E.J. and West, G.B. (1981). *Agents and Actions*, **8**, 339.

Lewis A.J., Smith, W.E. and Brown, D.H. (1978). *Agents and Actions*, **8**, 413.

Lewis, A.J. (1978). *Agents and Actions*, **8**, 244.

M Leigh, M. and Miller, D.D. (1983). *American journal of Clin Nutr.*, **38**, 202.

May, P.M. and Williams, D.R. (1981). *Metal ions in Biological systems*, **12**, (Sigel, H. ed), Marcel Dekker, New York, 283.

Meyers, O.L. (1988). Department of Rheumatology, University of Cape Town. Private communication.

Nicholls, D. (1974). *Complexes and First-row transition elements*, MacMillan, London.

Pharo, R. (1988). University of Cape Town, Animal unit, private communication.

Rainsford, K.D. and Whitehouse, M.W. (1979). *J. Pharm. Pharmac.*, **28**, 83.

Roberts, N.A. and Robinson, P.A. (1985). *British Journal of Rheumatology*, **24**, 128.

Sacconi, L., Paoletti, P. and Ciampolini. M. (1961). *J. Chem. Soc.*, 5115.

Sarkar, B. (1981). *Metal ions in Biological systems*, **12**, (Sigel, H. ed), Marcel Dekker, New York, 233.

The urine was frozen as soon as possible after the samples were collected. Precipitate formed in samples (a) and (b) on storage. The samples were analysed by UV spectroscopy, for complex concentration on a Philips PU8700 UV/vis spectrophotometer. A base line adjustment was made to accommodate for the absorption due to normal urine components. AA analysis by graphite furnace on a Pye Unicam was performed to determine total copper. The samples containing precipitate were first digested with concentrated HNO_3 (Aristar, spectroscopically pure) to solubilize the solid.

Post mortems were performed on groups 1 - 4, immediately after they died or were culled at the end of the screen.

Copper(II) chloride dihydrate, sodium chloride and sodium hydroxide were obtained from SAARCHEM Ltd and were of analytical grade. Acetyl salicylic acid (aspirin) was obtained from BDH and was of reagent grade. Ttda tetrahydrochloride was synthesized in this laboratory. Solutions were made up in glass distilled water and then passed through a millipore microfilter (cat. No. SLGS 0250S) to remove microorganisms. Male Sprague-Dawley rats, from an inbred colony, weighing between 450 and 500 grams were used. The animals were divided into groups of 5, and were fed on standard rat cubes.

Adjuvant arthritis was induced by injecting Freud's complete adjuvant (0.5 ml) into the right hind paw pod. Attempts to induce the arthritis by injecting into the base of the tail failed. The inflammation was allowed to develop for 14 days at which time the experiment was started. Paw volume was monitored daily, with the animal's uninflamed left rear paw being used as a control for that animal.

Solutions of Cu(II)-ttda for injection were prepared by dissolving an appropriate quantity of ttda and $CuCl_2$ in a volume of water calculated to give a solution with a total NaCl concentration of 0.15M. The pH of the solution was adjusted to 7.4 using concentrated sodium hydroxide. The selected dose was administered by injecting a specific volume of solution, calculated on the mass of the animal. The copper chloride solutions were prepared by dissolving the required amount of copper(II) chloride, plus sufficient NaCl to give a final concentration of 0.15M, in the correct volume of distilled water. The pH was left unadjusted at about 5.5. The copper aspirinate solution was made by preparing separate solutions of copper(II)chloride and aspirinate. The pH of the aspirinate solution was raised to approximately 5 to dissolve the compound. The solutions were mixed just prior to injection, and the pH lowered again to prevent precipitation of the copper complex.

Sharma, K.K., Chandra, S. and Basu, D.K. (1987). *Inorg. Chim. Acta*, **135**, 47.

Sophianopoulos, J.A., Durham, S.J., Sophianopoulos, A.J., Ragsdale, H.L. and Cropper, W.P. (1978). *Archives Biochem & Biophys*, **187**, 132.

Sorenson, J.R.J. (1976). *J. Med. Chem.*, **19**, 135.

Staub, C. and Buffle, J.J. (1984). *Anal Chem*, **56**, 2843.

Wainwright, H. (1988). University of Cape Town, Pathology Department, private communication.

Whitehouse, M.W. (1976). *Agents and Actions*, **6**, 201.

CHAPTER 6

General Discussion

The stability constants determined for the two ligands (Chapter 4) were used as input into the simulation program, and the copper P.M.I. curves for the two ligands generated. These curves are given in Figure 6.1, together with curves for trien, edda and dtpa.

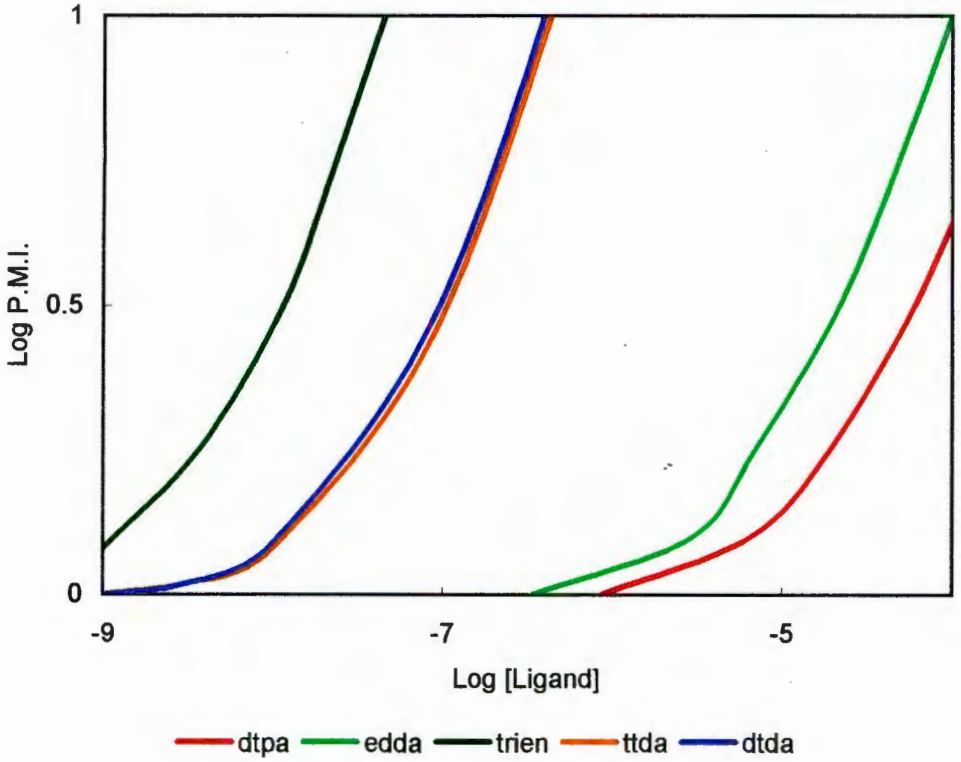

Figure 6.1: Copper(II) P.M.I. curves for ttda, dtda, trien, edda and dtpa

The simulation indicates that although ttda forms more stable complexes with copper than trien, it is less efficient than trien at mobilising copper. This demonstrates the importance of the other complex equilibria in plasma in determining the copper P.M.I. The reason for greater copper mobilisation by trien is high concentration of zinc in the blood, and the relative stability of the zinc and copper complexes. For edta the higher concentrations of zinc and calcium and the relatively strong complexes formed render this ligand an ineffective copper plasma mobiliser.

P.M.I. curves were computed for ttda and dtda with copper(II), nickel(II) and zinc(II). These curves are presented in Figure 6.2 and indicate that the ligands will cause some redistribution of zinc(II).

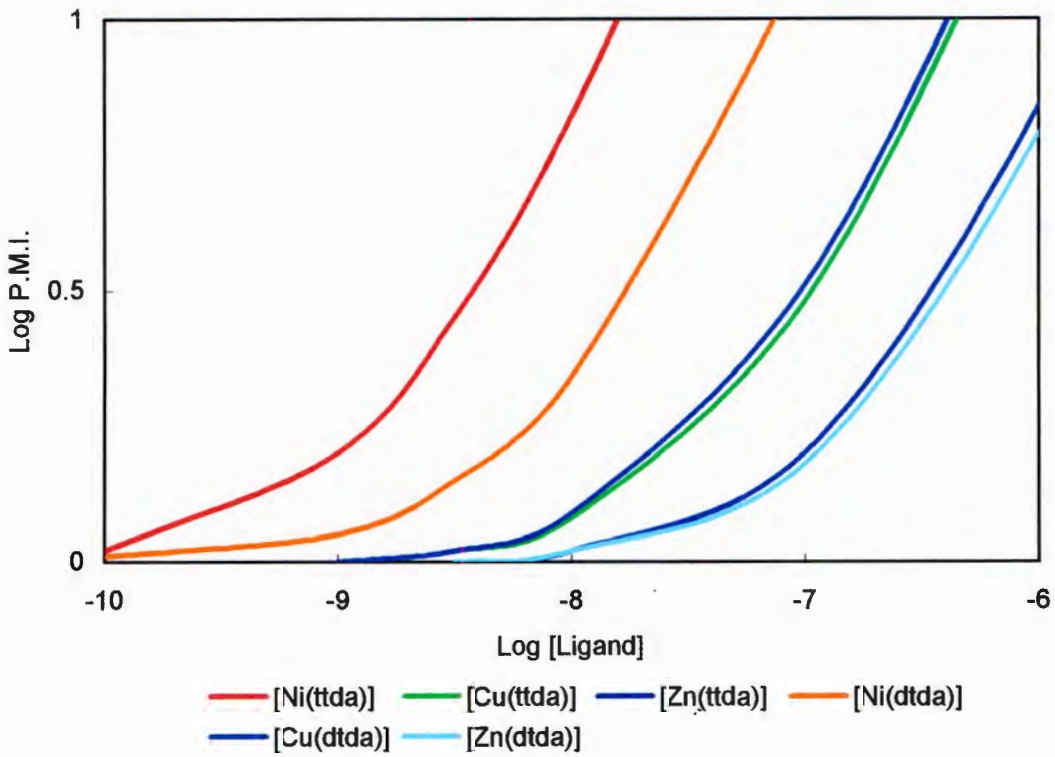

Figure 6.2: Computed P.M.I. curves for ttda and dtda with copper(II), nickel(II) and zinc(II)

At a ligand concentration of 10^{-3} the calcium(II) P.M.I. is less than 0.01, and should thus have little effect on the *in vivo* calcium (II) distribution. The results of this simulation show that ttda and dtda should be good mobilizers of copper in blood plasma. The prediction of the relative effectiveness of the two ligands by the model is interesting, in that dtda is shown to be slightly more effective than the more stable ttda complex.

The mobilisation calculations are in general supported by the results of the plasma ultrafiltration studies and confirm the validity of the model, although there are some limitations associated with the model, particularly concerning protein interactions. The predicted higher copper mobilisation by dtda is not seen experimentally. It is possible that this is due to interactions of the ligands with the protein. The success of the ultrafiltration confirms that the ligands survive in the conditions prevailing in plasma.

The species distribution of ttda, as calculated in the simulation for a total concentration of 1×10^{-5}, in plasma is mainly between the zinc complex, and the monoprotonated free ligand. The percentage distribution amongst the complexes placed in the model is given in Table 6.1 for ttda and Table 6.2 for dtda. The calculated concentrations depend on the total concentration of the ligand as supplied by the user.

Table 2.1: Distribution of ttda amongst the input complexes as predicted by the blood plasma model. The complexes are given in decreasing order of concentration, calculated for a total ligand concentration of 10^{-5}M.

Complex	Concentration	Percent Formation
Znttda	9.982×10^{-6}	99.8
ttdaH_2	1.423×10^{-8}	0.1
ttdaH_3	1.275×10^{-9}	0.0
[ZnttdaH]$^+$	1.234×10^{-9}	0.0
ttdaH	5.264×10^{-10}	0.0
Nittda	8.694×10^{-11}	0.0
Cuttda	4.889×10^{-11}	0.0
Cattda	3.735×10^{-12}	0.0
Mgttda	2.542×10^{-13}	0.0
ttdaH_4	7.038×10^{-14}	0.0
[CuttdaH]$^+$	7.435×10^{-15}	0.0
Mnttda	6.595×10^{-15}	0.0
[CattdaOH$^-$]	4.095×10^{-16}	0.0
[MgttdaOH$^-$]	8.574×10^{-17}	0.0
ttdaH_5	7.754×10^{-20}	0.0
[CuttdaH_2]$^{2+}$	1.672×10^{-20}	0.0

Table 6.2: Distribution of dtda amongst the input complexes as predicted by the blood plasma model. The complexes are given in decreasing order of concentration, calculated for a total ligand concentration of 10^{-5}M.

Complex	Concentration	Percent Formation
Zndtda	8.755×10^{-6}	87.6
dtdaH_2	1.139×10^{-6}	11.4
dtdaH	1.034×10^{-7}	1.0
[ZndtdaH]$^+$	1.187×10^{-9}	0.0

Complex	Concentration	Percent Formation
$dtdaH_3$	8.099×10^{-10}	0.0
Cadtda	2.788×10^{-10}	0.0
Mgdtda	1.225×10^{-10}	0.0
Cudtda	5.398×10^{-11}	0.0
Nidtda	1.829×10^{-11}	0.0
$[CadtdaOH]^-$	4.713×10^{-14}	0.0
Mndtda	2.411×10^{-14}	0.0
$[CudtdaOH]^-$	1.175×10^{-14}	0.0
$dtdaH_4$	4.271×10^{-15}	0.0
$[CudtdaH]^+$	4.114×10^{-16}	0.0
$[NidtdaH]^+$	6.828×10^{-17}	0.0

The order given for the various complexes demonstrates their relative stability under the concentration parameters given in the blood model. Although the concentrations calculated are dependent on the total concentration given for the ligand, they do serve to illustrate the large differences in concentration of the resulting complexes. Of note is the large difference in the concentrations of the zinc and copper complexes for both the ligands. Due to the large differences in free metal concentrations, these figures indicate that a therapeutic using either of these ligands would require some countermeasures to be taken to reduce the effect on the zinc balance. A possible counter to the zinc disturbance would be to administer the ligand as the zinc complex, which is the approach used with dtpa which is administered as the calcium complex (Jackson and Jarvis, 1995).

A second aspect that needs to be considered with the distribution of the metal, is the specific complex with which it is associated. The concentrations given in Tables 6.1 and 6.2 above are calculated at the pH of blood, approximately 7.4, and the major complexes for copper and zinc are found to be neutral species. This form is most likely to be transported into tissue (Neumann and Silverberg, 1966). Very little of either metal is present as charged complexes, in which form it would be excreted through the kidneys.

Confirmation of the bonding of the negative carboxylic groups is thus important. The ultrafiltration measurements determined total l.m.w. copper only, with no information concerning the species present. The indication from the UV/VIS study is that above pH 6

the six co-ordinated Cu-ttda complex is the major species present in solution. The Zn-ttda n.m.r. results also indicate that the acetate residues are co-ordinated to the metal. On this evidence it is to be expected that the copper complex should possess a relatively high degree of lipophilicity, which should facilitate transport across the biological membrane.

The species concentration distribution curves for the ttda-Cu^{2+} and dtda-Cu^{2+} systems are given in Figures 6.3 and 6.4.

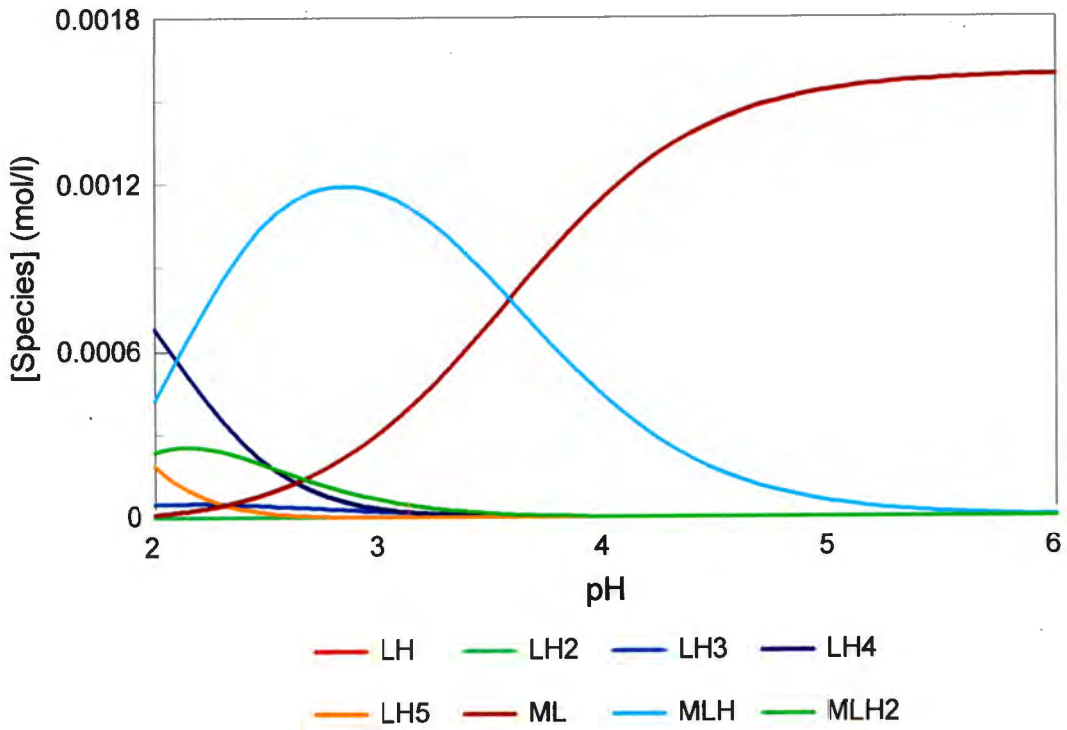

Figure 6.3: Species concentration distribution for the Cu(II)-ttda system, with a ligand to metal concentration ratio of 1. Total [Cu(II)] = 1.6 mM = Total [ttda]

At the pH of the stomach, approximately 2, the proportion of the neutral [Cu(ttda)] formed is very small. With dtda the neutral complex forms a much higher proportion, but it is still very low. From this data it can be expected that most of the absorption will take place in the intestine, rather than the stomach. At the stomach pH the mono- and diprotonated copper complex species predominate, but most of the ligand is present as a copper complex of some form. A large proportion of the ligand is present in the LH_3 and LH_4 form, and may not be available for complexation in the intestine, either from losses to other metal ions, or

through conversion to the lactam, which is a known degradation reaction with these ligands at low pH.

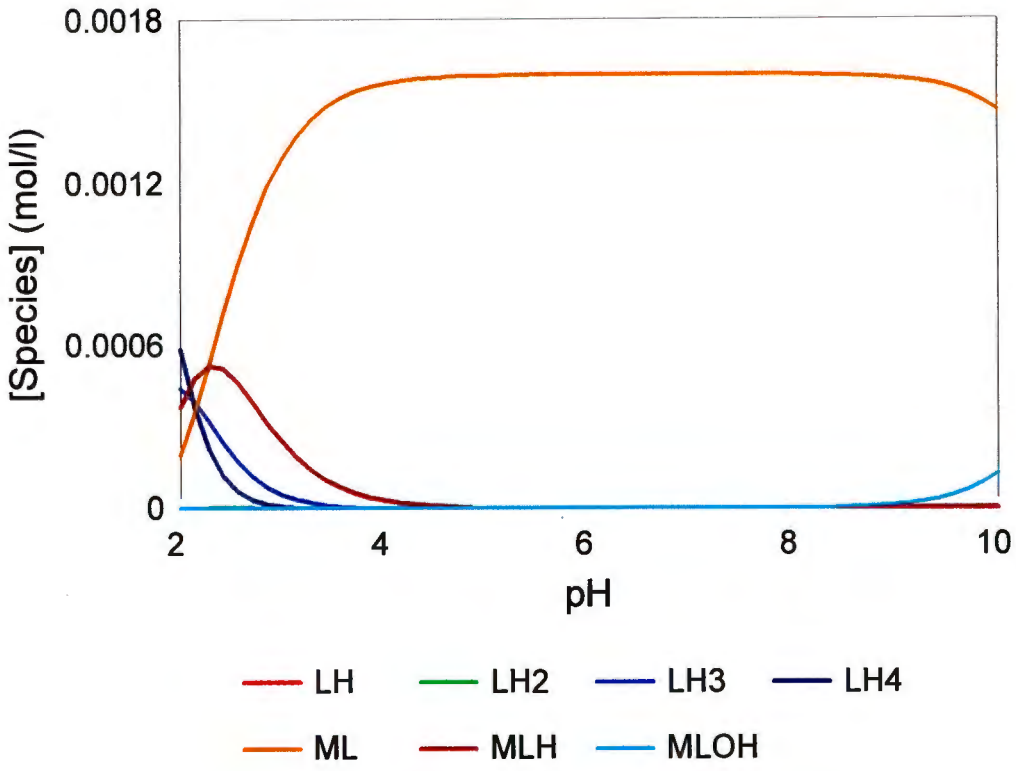

Figure 6.4: Species concentration distribution for the Cu-dtda system, with a ligand to metal concentration ratio of 1. Total [Cu(II)] = 1.6 mM = Total [dtda]

The nickel(II) P.M.I. curve, Figure 6.2, suggests that these ligands could be useful as drugs in chelation therapy for nickel(II) poisoning. The indication given by the model is that ttda is 10 times more effective at mobilising nickel(II) than copper(II). There is a marked decrease in the relative mobilising ability of the Ni-dtda complex when compared to the Ni-ttda complex.

The conclusions derived from the computer simulation support the use of the two target ligands as copper mobilisation drugs, and suggest that they have potential as anti-inflammatory therapeutics. Studies of a more biological nature were undertaken to supplement the modelling and chemical work.

The results of the SOD activity simulation test demonstrated minimal superoxide dismutase like activity. The implication of these results is not clear, as some SAARDs, such as

chloroquine and azathioprine (Roberts and Robinson, 1985) are also inactive. An explanation for this is that alternative mechanisms of relief may also be present. Roberts *et al* (Roberts and Robinson, 1985) note that ethylenediamine diacetic acid (edda) is active in this test. As dtda and ttda are very close structurally to edda, it is surprising that ttda has such a low activity level.

In undertaking animal screens it was hoped that clear indication of any anti-inflammatory action would be obtained. The failure to successfully develop the adjuvant arthritis model leaves this question unanswered, but does provide some information on how the complex responds in animal systems.

When the irritation caused by the copper chloride and copper aspirinate injections is considered, it is certain that the complex survives *in vivo* as this explains the absence of irritation at the site of the injection. The high concentration of copper in the one hour urine sample could be an indication that the complex is charged, and hence has a high degree of hydrophilicity. Although the complex is nominally neutral, it could also be polar, with the carboxylate groups uncoordinated. One aspect of the data gathered which does not support this hypothesis is the absence of a marked increase in the copper concentration in the 24 hour urine sample.

In subsequent work (Voyé, 1993), ^{67}Cu was used to study the bio-distribution of several ligands, including ttda and dtda, in mice. The results confirmed the high excretion via the urine, 72% of the dose in the first 24 hours in the case of ttda. The bio-distribution showed small quantities of copper retained in the liver, blood and kidneys. When compared to the $CuCl_2$ control, it was apparent that the ttda and dtda copper(II) complexes were stable *in vivo*.

In summary, the ligands designed by use of the blood plasma model, ECCLES, were successfully synthesised. The formation constants measured using potentiometric techniques were added to the ECCLES data base and the copper (II) mobilisation calculated. The calculated P.M.I. curves were compared to experimental curves obtained by ultrafiltration techniques. The trends demonstrated by the calculated and experimental curves were largely in agreement. Animal screens using the adjuvant arthritis model were unsuccessful, as the model was not correctly induced. The results of bio-distribution studies using these ligands, and the high concentration of copper measured in the urine, it is unlikely that these ligands will be effective anti-inflammatory agents, as they are apparently too hydrophilic.

References

Jackson G.E. and Jarvis, N. (1995). In *'Handbook on Metal-Ligand interactions in Biological Fluids'*, Berthon, G. (ed), Vol2, 1206.

Neumann, P.Z. and Silverberg, M. (1966). *Nature*, **210**, 414.

Roberts, N.A. and Robinson, P.A. (1985). *British Journal of Rheumatology*, **24**, 128.

Voyé, A. (1993). *PhD thesis*, University of Cape Town.

APPENDIX I

Adjusted formation constants used in the ligand design in Chapter 2. The subscripts pqr refer the metal, ligand and proton stoichiometries, respectively.

Ligand	Metal	Formation constant (β_{pqr})	
4-oxa-1,7,diazaheptane	H^+	β_{011}	9.45
		β_{012}	18.18
	Mg^{+2}	β_{110}	0.30
	Ca^{+2}	β_{110}	0.20
	Mn^{+2}	β_{110}	2.00
		β_{120}	3.40
	Ni^{+2}	β_{110}	5.50
		β_{120}	8.77
	Cu^{+2}	β_{110}	8.50
		β_{120}	12.59
		β_{11-1}	18.65
	Zn^{+2}	β_{110}	5.57
		β_{120}	9.43
		β_{11-1}	18.57
4-thia-1,7-diazaheptane	H^+	β_{011}	9.29
		β_{012}	17.78
	Mg^{+2}	β_{110}	0.20
	Ca^{+2}	β_{110}	0.20
	Mn^{+2}	β_{110}	2.00
		β_{120}	3.40
	Ni^{+2}	β_{110}	7.39
		β_{120}	12.98
	Cu^{+2}	β_{110}	8.83
		β_{120}	13.83
		β_{11-1}	19.22
	Zn^{+2}	β_{110}	5.38
		β_{120}	9.50

Ligand	Metal	Formation constant (β_{pqr})	
iminobis(2-ethylamine)	H^+	β_{011}	9.52
		β_{012}	18.22
		β_{013}	22.29
	Mg^{+2}	β_{110}	0.60
	Ca^{+2}	β_{110}	0.50
	Mn^{+2}	β_{110}	3.94
		β_{120}	6.71
	Ni^{+2}	β_{110}	10.15
		β_{120}	17.86
	Cu^{+2}	β_{110}	15.37
		β_{120}	20.14
		β_{111}	3.25
		β_{112}	13.30
		β_{11-1}	17.80
	Zn^{+2}	β_{110}	8.61
		β_{120}	13.82
N,N'-bis(2-aminobenzyl)ethylenediamine	H^+	β_{011}	8.80
		β_{012}	14.55
		β_{013}	16.86
		β_{014}	18.85
	Mg^{+2}	β_{110}	0.40
	Ca^{+2}	β_{110}	0.30
	Mn^{+2}	β_{110}	3.50
	Ni^{+2}	β_{110}	9.70
	Cu^{+2}	β_{110}	12.64
	Zn^{+2}	β_{110}	7.00

Ligand	Metal	Formation constant (β_{pqr})	
N,N'-bis(2-imidazolylmethyl)ethylenediamine	H^+	β_{011}	9.52
		β_{012}	18.22
		β_{013}	22.29
	Mg^{+2}	β_{110}	0.60
	Ca^{+2}	β_{110}	0.50
	Mn^{+2}	β_{110}	3.94
		β_{120}	6.71
	Ni^{+2}	β_{110}	10.15
		β_{120}	17.86
	Cu^{+2}	β_{110}	15.37
		β_{120}	20.14
		β_{111}	3.25
		β_{112}	13.30
		β_{11-1}	17.80
	Zn^{+2}	β_{110}	8.61
		β_{120}	13.82
N,N'-bis(4-imidazolylmethyl)ethylenediamine	H^+	β_{011}	9.52
		β_{012}	18.22
		β_{013}	22.29
	Mg^{+2}	β_{110}	0.60
	Ca^{+2}	β_{110}	0.50
	Mn^{+2}	β_{110}	3.94
		β_{120}	6.71
	Ni^{+2}	β_{110}	10.15
		β_{120}	17.86
	Cu^{+2}	β_{110}	15.37
		β_{120}	20.14
		β_{111}	3.25
		β_{112}	13.30
		β_{11-1}	17.80
	Zn^{+2}	β_{110}	8.61
		β_{120}	13.82

Ligand	Metal	Formation constant (β_{pqr})	
N,N'bis(2-pyridylmethyl)-1,2-diaminoethane	H^+	β_{011}	7.94
		β_{012}	13.10
	Mg^{+2}	β_{110}	0.80
	Ca^{+2}	β_{110}	0.60
	Mn^{+2}	β_{110}	5.48
	Ni^{+2}	β_{110}	13.98
	Cu^{+2}	β_{110}	16.49
	Zn^{+2}	β_{110}	10.80
1,4,7,10-tetraazadecane	H^+	β_{011}	9.43
		β_{012}	18.21
		β_{013}	24.55
		β_{014}	27.67
	Mg^{+2}	β_{110}	0.80
	Ca^{+2}	β_{110}	0.60
	Mn^{+2}	β_{110}	4.86
	Ni^{+2}	β_{110}	13.46
		β_{120}	17.87
		β_{230}	36.09
	Cu^{+2}	β_{110}	19.51
		β_{111}	22.99
		β_{11-1}	24.02
	Zn^{+2}	β_{110}	11.77
		β_{111}	16.86

Ligand	Metal	Formation constant (β_{pqr})	
2,6-bis(5(1,4diazahexyl))pyridine	H^+	β_{011}	9.75
		β_{012}	18.80
		β_{013}	25.12
		β_{014}	30.59
	Mg^{+2}	β_{110}	0.80
	Ca^{+2}	β_{110}	0.70
	Mn^{+2}	β_{110}	6.87
	Ni^{+2}	β_{110}	17.78
		β_{111}	21.28
	Cu^{+2}	β_{110}	21.22
		β_{111}	26.17
	Zn^{+2}	β_{110}	15.73
		β_{111}	18.47
1,4,7,10,13-pentaazatridecane	H^+	β_{011}	9.38
		β_{012}	18.19
		β_{013}	25.92
		β_{014}	30.39
		β_{015}	33.16
	Mg^{+2}	β_{110}	1.05
	Ca^{+2}	β_{110}	0.90
	Mn^{+2}	β_{110}	6.44
	Ni^{+2}	β_{110}	16.84
		β_{111}	20.84
		β_{112}	23.74
	Cu^{+2}	β_{110}	22.06
		β_{111}	27.16
		β_{112}	30.89
	Zn^{+2}	β_{110}	14.96

Ligand	Metal	Formation constant (β_{pqr})	
1,9-bis(2-pyridyl)-2,5,8triazanonane	H^+	β_{011}	8.88
		β_{012}	15.92
		β_{013}	19.74
		β_{014}	21.18
	Mg^{+2}	β_{110}	0.80
	Ca^{+2}	β_{110}	0.70
	Mn^{+2}	β_{110}	6.30
	Ni^{+2}	β_{110}	19.20
	Cu^{+2}	β_{110}	20.85
	Zn^{+2}	β_{110}	13.71
		β_{111}	15.71
Ammonia	H^+	β_{011}	9.52
		β_{012}	18.22
		β_{013}	22.29
	Mg^{+2}	β_{110}	0.60
	Ca^{+2}	β_{110}	0.50
	Mn^{+2}	β_{110}	3.94
		β_{120}	6.71
	Ni^{+2}	β_{110}	10.15
		β_{120}	17.86
	Cu^{+2}	β_{110}	15.37
		β_{120}	20.14
		β_{111}	3.25
		β_{112}	13.30
		β_{11-1}	17.80
	Zn^{+2}	β_{110}	8.61
		β_{120}	13.82

Ligand	Metal	Formation constant (β_{pqr})	
ethylenediamine	H^+	β_{011}	9.51
		β_{012}	16.31
	Mg^{+2}	β_{110}	0.25
	Ca^{+2}	β_{110}	0.20
	Mn^{+2}	β_{110}	2.66
		β_{120}	4.62
	Ni^{+2}	β_{110}	7.05
		β_{120}	12.90
		β_{130}	16.73
	Cu^{+2}	β_{110}	10.14
		β_{120}	18.90
	Zn^{+2}	β_{110}	5.50
		β_{120}	10.28
		β_{130}	12.12
N,N'-bis(3-aminopropyl)trimethylenediamine	H^+	β_{011}	10.11
		β_{012}	19.59
		β_{013}	27.84
		β_{014}	34.78
	Mg^{+2}	β_{110}	0.65
	Ca^{+2}	β_{110}	0.55
	Mn^{+2}	β_{110}	4.51
	Ni^{+2}	β_{110}	10.10
	Cu^{+2}	β_{110}	16.47
	Zn^{+2}	β_{110}	9.11

Ligand	Metal	Formation constant (β_{pqr})	
N,N'-bis(3-aminopropane)ethylenediamine	H^+	β_{011}	10.18
		β_{012}	19.62
		β_{013}	27.67
		β_{014}	33.08
	Mg^{+2}	β_{110}	0.70
	Ca^{+2}	β_{110}	0.60
	Mn^{+2}	β_{110}	3.94
	Ni^{+2}	β_{110}	14.09
		β_{111}	19.51
	Cu^{+2}	β_{110}	20.98
		β_{111}	24.42
	Zn^{+2}	β_{110}	10.91
		β_{111}	17.07
		β_{11-1}	17.39
Ethylenebis(iminomethylenephosphorous acid)	H^+	β_{011}	7.80
		β_{012}	12.64
	Mg^{+2}	β_{110}	0.70
	Ca^{+2}	β_{110}	0.50
	Mn^{+2}	β_{110}	2.70
	Ni^{+2}	β_{110}	7.24
	Cu^{+2}	β_{110}	10.32
	Zn^{+2}	β_{110}	5.91

Ligand	Metal	Formation constant (β_{pqr})	
Ethylenebis(iminomethylenephosphonic acid)	H^+	β_{011}	10.18
		β_{012}	17.50
		β_{013}	23.05
		β_{014}	27.48
	Mg^{+2}	β_{110}	3.50
	Ca^{+2}	β_{110}	3.00
	Mn^{+2}	β_{110}	6.92
	Ni^{+2}	β_{110}	11.19
		β_{111}	16.56
		β_{112}	21.41
	Cu^{+2}	β_{110}	16.77
		β_{111}	21.30
		β_{112}	24.99
	Zn^{+2}	β_{110}	10.00
		β_{111}	15.50
		β_{112}	20.50
edda	H^+	β_{011}	9.34
		β_{012}	15.65
		β_{013}	18.01
		β_{014}	19.35
	Mg^{+2}	β_{110}	3.95
	Ca^{+2}	β_{110}	2.85
	Mn^{+2}	β_{110}	6.87
	Ni^{+2}	β_{110}	13.52
	Cu^{+2}	β_{110}	15.66
	Zn^{+2}	β_{110}	10.11

APPENDIX II

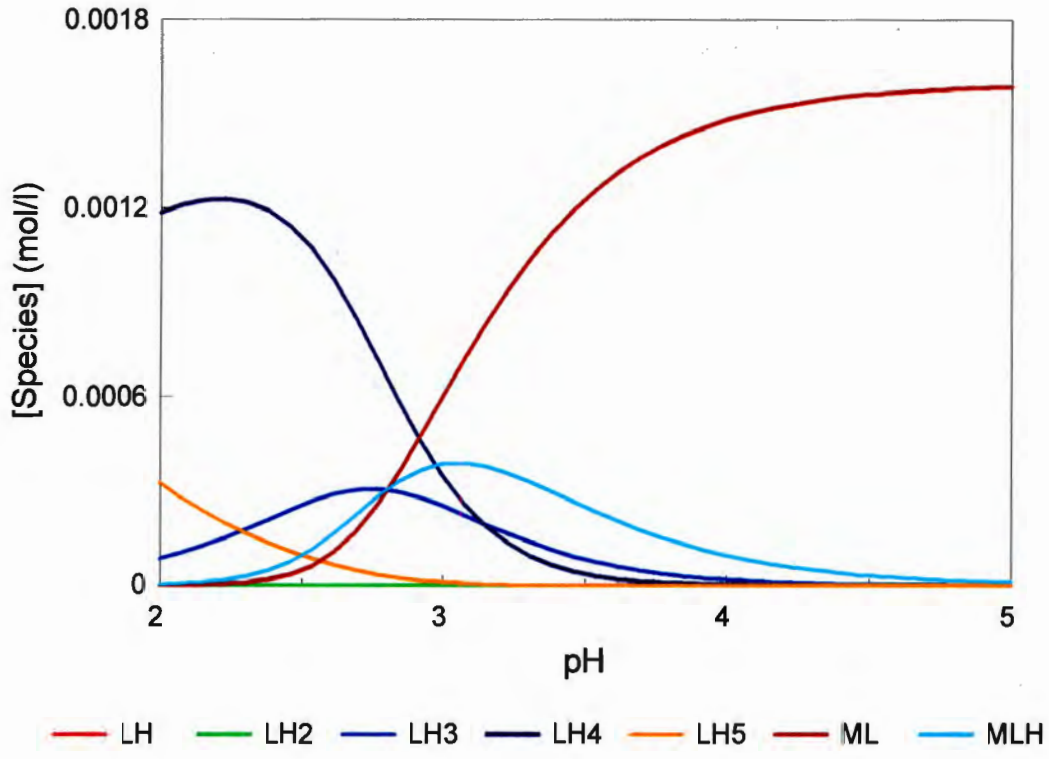

Figure 4.23: Species distribution curves for [Ni(ttda)]; Total [Ni(II)] = 1.6 mM = Total [ttda]

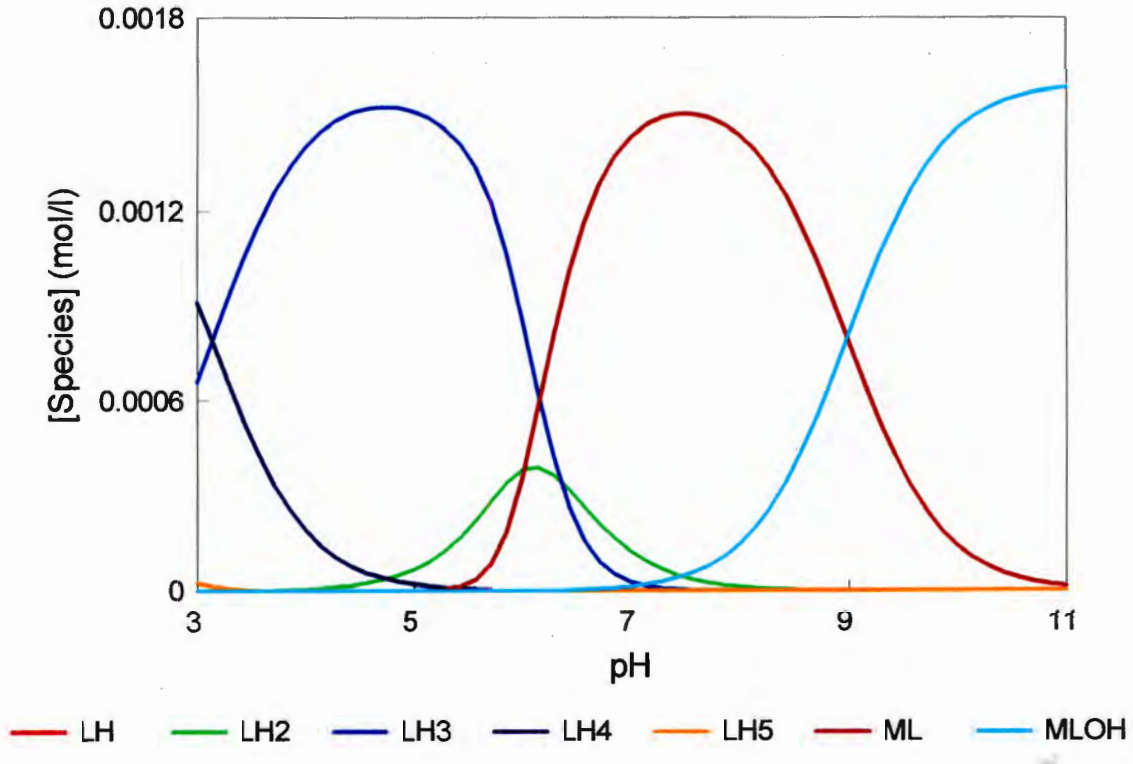

Figure 4.24: Species distribution curves for [Mn(ttda)]; Total [Mn(II)] = 1.6 mM = Total [ttda]

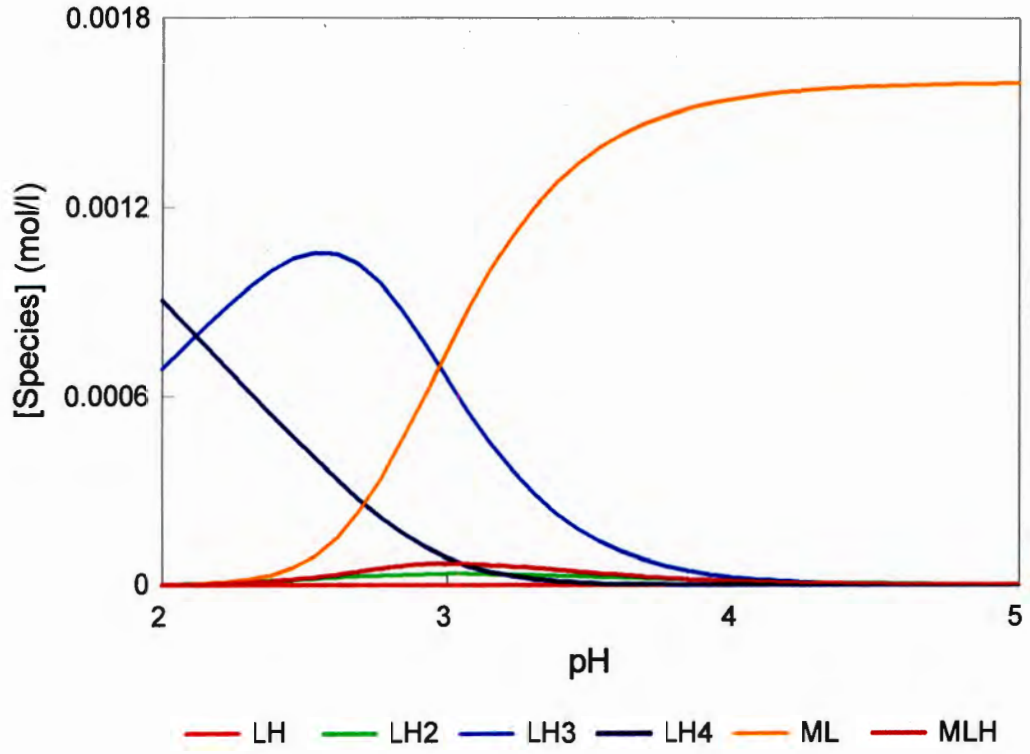

Figure 4.25: Species distribution curves for [Ni(dtda)]; Total [Ni(II)] = 1.6 mM = Total [dtda]

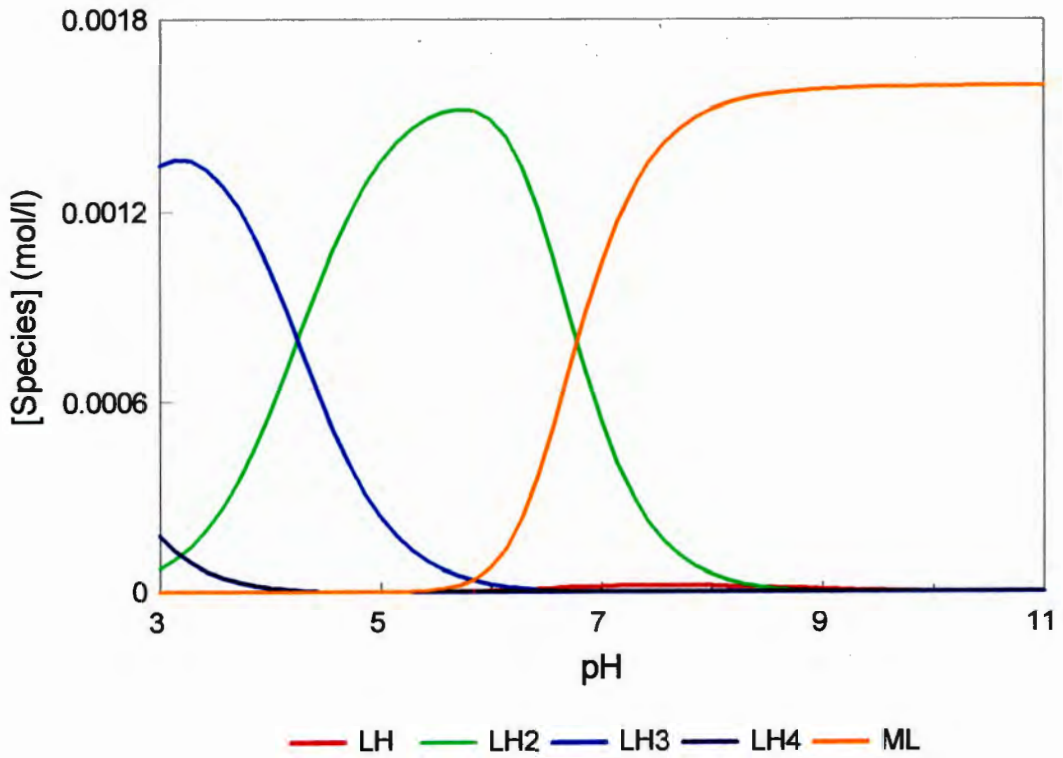

Figure 4.26: Species distribution curves for [Mn(dtda)]; Total [Mn(II)] = 1.6 mM = Total [dtda]

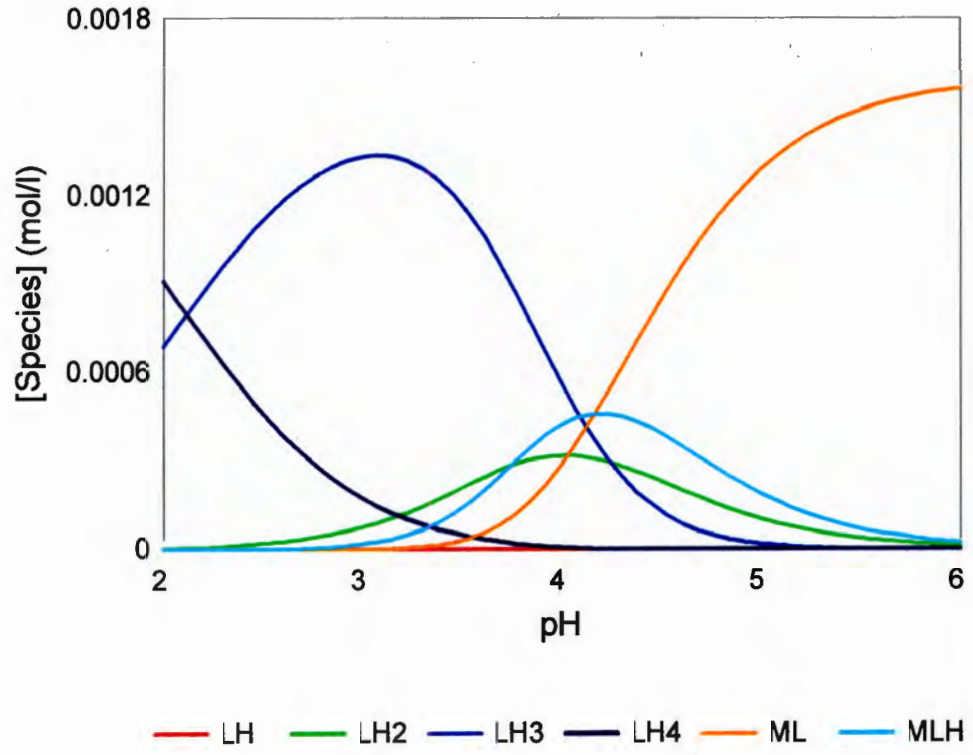

Figure 4.32: Species distribution curves for [Co(dtda)]; Total [Co(II)] = 1.6 mM = Total [dtda]

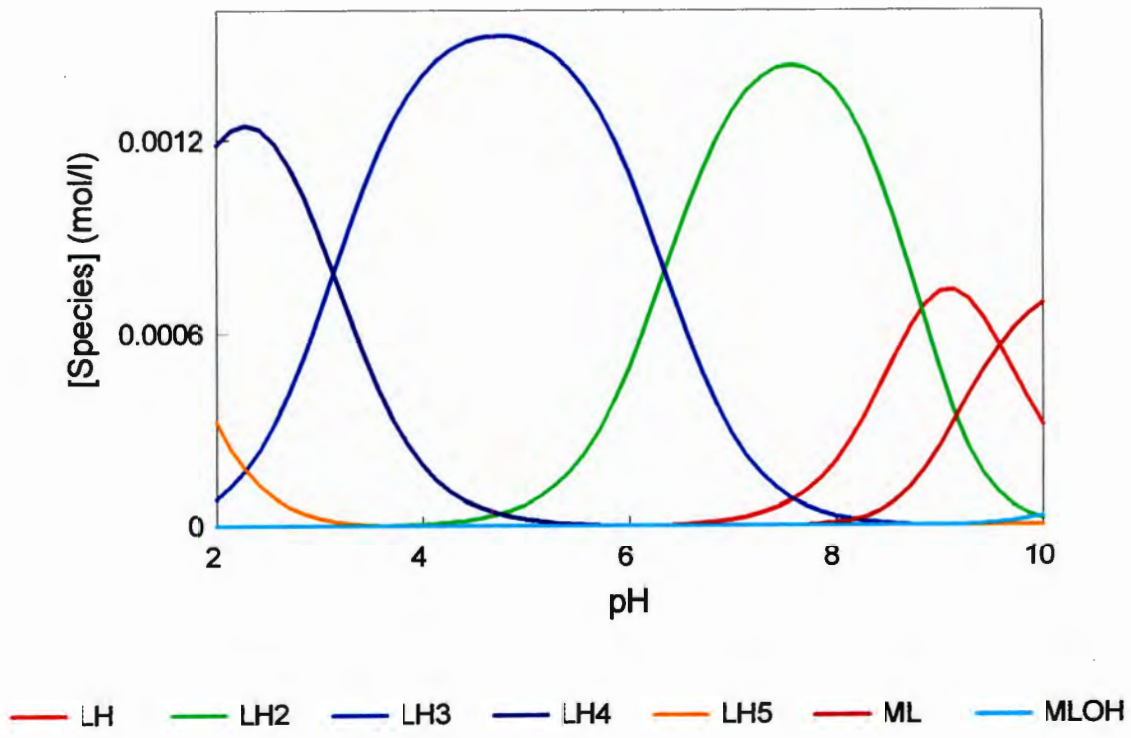

Figure 4.41: Species distribution curves for [Ca(ttda)]; Total [Ca(II)] = 1.6 mM = Total [ttda]

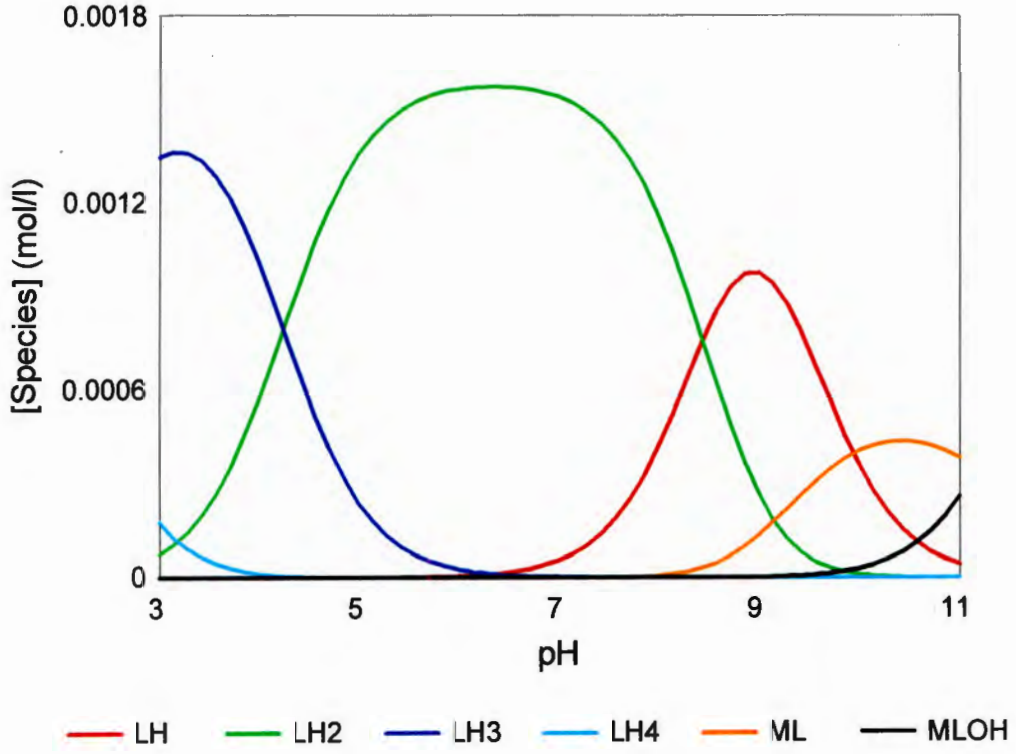

Figure 4.42: Species distribution curves for [Ca(dtda)]; Total [Ca(II)] = 1.6 mM = Total [dtda]

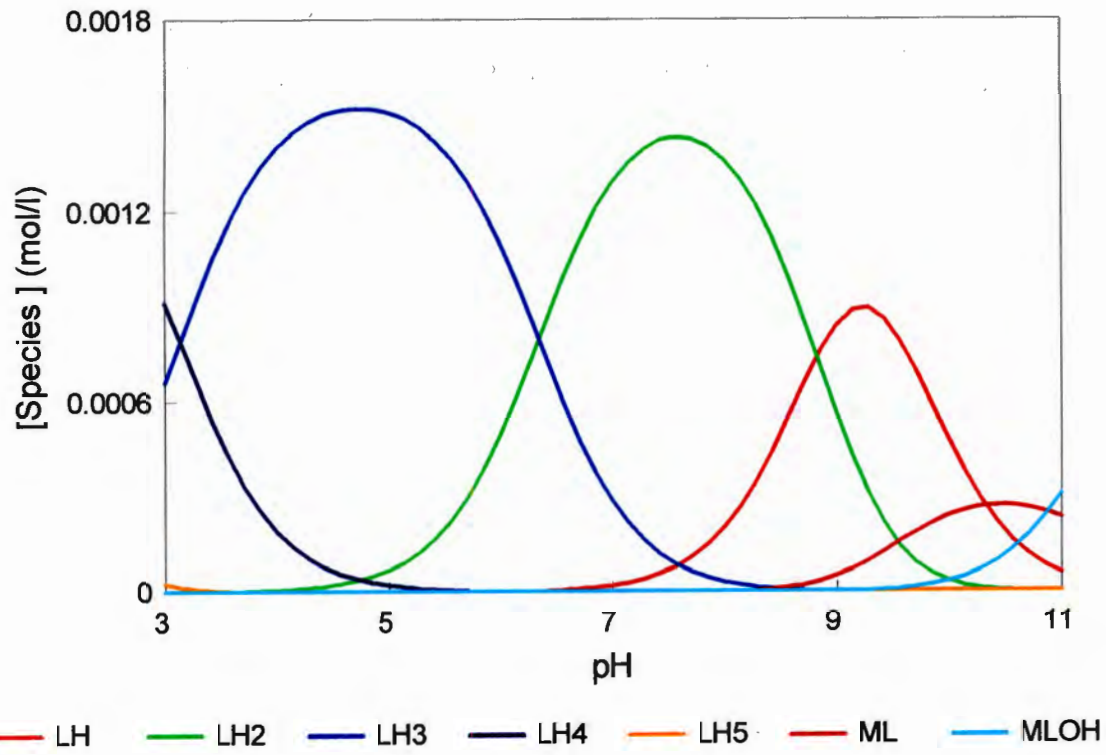

Figure 4.43: Species distribution curves for [Mg(ttda)]; Total [Mg(II)] = 1.6 mM = Total [ttda]

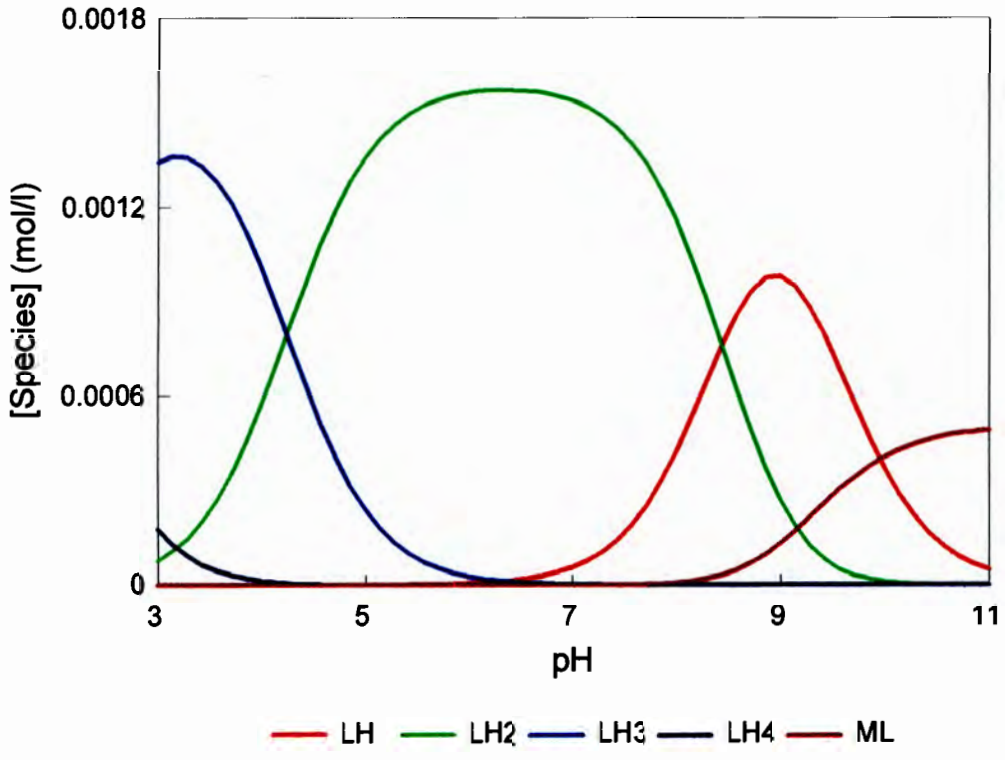

Figure 4.44: Species distribution curves for [Mg(dtda)];Total [Mg(II)] = 1.6 mM = Total [dtda]